J. Fluid Mech. (2024), *vol.* 1000, A11, doi:10.1017/jfm.2024.651

JFM PAPERS

On the theory of body motion in confined Stokesian fluids

Giuseppe Procopio[1] **and Massimiliano Giona**[1,†]

[1]Dipartimento di Ingegneria Chimica Materiali Ambiente, Sapienza Università di Roma, via Eudossiana 18, Rome 00184, Italy

(Received 29 July 2023; revised 18 April 2024; accepted 29 May 2024)

We propose a theoretical method to decompose the solution of a Stokes flow past a body immersed in a confined fluid into two simpler problems, related separately to the two geometrical elements of these systems: (i) the body immersed in the unbounded fluid (represented by its Faxén operators); and (ii) the domain of the confinement (represented by its Stokesian multipoles). Specifically, by using a reflection method, and assuming linear and reciprocal boundary conditions (Procopio & Giona, *Phys. Fluids*, vol. 36, issue 3, 2024, 032016), we provide the expression for the velocity field, the forces, torques and higher-order moments acting on the body in terms of: (i) the volume moments of the body in the unbounded ambient flow; (ii) the multipoles in the domain of the confinement; (iii) the collection of all the volumetric moments on the body immersed in all the regular parts of the multipoles considered as ambient flows. A detailed convergence analysis of the reflection method is developed. In light of the practical applications, we estimate the truncation error committed by considering only the lower-order moments (thus, truncating the matrices) and the errors associated with the approximated expressions available in the literature for force and torques. We apply the theoretical results to the archetypal hydrodynamic system of a sphere with Navier-slip boundary conditions near a plane wall with no-slip boundary conditions, to determine forces and torques on a translating and rotating sphere as a function of the slip length and of the distance of the sphere from the plane. The hydromechanics of a spheroid is also addressed.

Key words: Stokesian dynamics, particle/fluid flows

† Email address for correspondence: massimiliano.giona@uniroma1.it

1. Introduction

The behaviour of particles immersed in a viscous fluid in the low-Reynolds-number regime is inevitably affected by hydrodynamic interactions with other nearby bodies, such as other particles, fluid interfaces and solid walls confining the fluid. These interactions, that are the origin of fundamental phenomena, including the enhanced resistance on bodies (Hill & Power 1956), the intrinsic convection of suspensions (Beenakker & Mazur 1985), the Segre–Silberberg effect (Segre & Silberberg 1961), to quote just few of them, become significant whenever the characteristic particle length ℓ_b is comparable with the characteristic separation distance ℓ_d from the nearest boundary. Therefore, the accurate description of fluid–particle interactions is of paramount relevance in several areas of microfluidics, such as separation devices (Huang *et al.* 2004; Striegel & Brewer 2012; Cerbelli, Giona & Garofalo 2013), capillary transport (Goldsmith & Skalak 1975; Popel & Johnson 2005; Undvall *et al.* 2022), dynamics of micro-swimmers (Lauga 2020) and active particles (Michelin 2023), where, by definition, the micrometric (or even sub-micrometric) characteristic dimension of the fluid domain may be of the same order of magnitude of the particle size.

Microfluidics is typically characterised by low Reynolds numbers (apart from the specific applications referred to as *inertial microfluidics* Di Carlo 2009; Zhang *et al.* 2016) so that, in most of the cases, the fluid can be considered in the Stokes regime and, when the inertia of the fluid becomes significant ($Re \sim 1$) but not too large, it can be treated by perturbative methods with respect to the Stokes-flow solution (Cox & Brenner 1968; Ho & Leal 1974). Although hydrodynamic problems related to particles in confined fluids can be approached by means of typical numerical methods for solving the Stokes equation (such as the finite-element method (FEM) (De Corato *et al.* 2015; Venditti *et al.* 2022) and boundary-element method (BEM) (Pozrikidis 1992), a deeper mathematical understanding of fluid–particle interactions can be beneficial in order to overcome, by means of explicit analytical solutions, the limits and shortcomings of the numerical approaches, to improve the current numerical methods (such as Stokesian dynamics Brady & Bossis 1988) and develop new ones, and to explain and predict the non-intuitive flow and transport phenomena that may occur at the microscale.

One of the main difficulties in the analytical approaches to multibody systems is the intrinsic geometric complexity induced by the presence of bodies and surfaces of different shapes where to impose the boundary conditions (BCs). This difficulty holds even when dealing with the most regular bodies (such as spheres or ellipsoids) and the simplest confinement geometries (for example, planar or cylindrical walls), since the union of many bodies, in most of the cases, breaks down the original symmetries making impossible to find a coordinate system which permit to express simultaneously all the BCs in a simple mathematical way. This is the reason why the only exact solutions available in the literature regard axisymmetric geometries of the hydrodynamic problem (where the symmetry is defined with respect to a suitable orthogonal system of curvilinear coordinates). This is the case of the resistance of a rigid sphere close to a plane considering no-slip BCs (Jeffery 1915; Brenner 1961; Dean & O'Neill 1963; O'Neill 1964), Navier-slip BCs (Goren 1979) and phoretic slip BCs (Desai & Michelin 2021), the resistance between two spheres moving relative to each other (O'Neill & Majumdar 1970) and of the resistance of a sphere at the centre of a cylindrical channel, translating parallelly to the symmetry axis assuming no-slip BCs (Haberman & Sayre 1958). Only in few cases an ambient flow has been also considered, such as in (Haberman & Sayre 1958), for a sphere immersed in a Poiseuille flow and in Pasol *et al.* (2005), where a sphere immersed in an axisymmetric polynomial flow bounded by a plane wall has been analysed.

Whereas, for the majority of the confined systems considered in the literature, approximate analytical solutions have been obtained under the assumption of asymptotic approximations, by using mainly a lubrication method for short-range interactions ($\ell_d \ll \ell_b$) and a reflection method for long-range interactions ($\ell_d \gg \ell_b$). In some cases, such as that of the resistance of two rigid moving spheres with no-slip BCs (Jeffrey & Onishi 1984), the solution has been approximated by matching the asymptotic solutions.

In the case of short-range interactions, many specific solutions are available in the literature, such as the resistance on a sphere near a plane by considering both no-slip (Cox & Brenner 1967*b*; Goldman, Cox & Brenner 1967) and Navier-slip (Hocking 1973) BCs, and a general lubrication theory, regardless of the shape of the surfaces in close contact, has been developed by Cox (1974) assuming no-slip BCs.

On the other hand, in the case of long-range interactions, the reflection method (in its multifaceted variations (Happel & Brenner 1983)) is commonly employed to obtain the leading-order terms for the series expansion in powers of ℓ_b/ℓ_d of the particle transport parameters, such as resistance, mobility and diffusivity. The reflection method, developed by Smoluchowski (1911) (see Happel & Brenner 1983, p. 236) in order to match the BCs of Stokes flows on a system of n spheres, consists of expressing the total flow (i.e. the solution of the Stokes equations with BCs assigned simultaneously on each sphere) as a series of an infinite number of flows satisfying Stokes equations with BCs assigned separately on each body considered in a unbounded domain. For example, a simple version of this method, to obtain the exact flow in the case of two moving spheres, can be summarised as follows: the first term of the series is the flow due to the motion of the first sphere considered in the unbounded fluid, which generates, in turn, a flow on the domain occupied by the second sphere; the second term of the series corrects the flow on the surface of the second sphere generating a flow on the domain of the first sphere and so on. A similar ping-pong correction at the boundaries of the two spheres proceeds iteratively. Although the Stokes equations and the BCs of the global problem are formally satisfied, this procedure is affected by two main limitations: (i) it is not easy to obtain analytical expressions for the solutions of the infinite system of Stokes problems involved even for the simplest geometries; (ii) the convergence of the series can be ensured only for some specific problems, and it is still an open question in the general case.

For example, as regards the second limitation, convergence has been proved heuristically for two equal spheres moving with the same velocity for all the separation distances (Happel & Brenner 1983, p. 259), but in the case of three equally separated spheres it has been shown that the reflection method does not converge if the distance between the centres of the spheres is smaller than 2.16 times the radius of the spheres (Ichiki & Brady 2001). In fact, as shown by Höfer & Velázquez (2018), if particle velocities are imposed by Dirichlet BCs, the method converges only for diluted systems enclosed in an finite volume; whereas, as proved by Luke (1989) using a variational method, in the case of suspensions with n particles enclosed in a finite volume, the convergence of the reflection method is ensured regardless of the particles concentration, if particle velocities are not assigned, i.e. if they move under the action of an external force as in the case of sedimentation phenomena.

Therefore, given that the convergence is ensured only for $\ell_d \gg \ell_b$ and that the exact evaluation of the terms in the series is feasible only for the first ones, i.e. the first corrections to the unbounded approximation, reflection methods are widely employed to model very long range interactions between particles. The main fields of application are in the analysis of suspensions, indirectly applied in Stokesian dynamics (Durlofsky, Brady & Bossis 1987; Brady & Bossis 1988) under the form of inverting the particle–particle interaction mobility matrix (Ichiki & Brady 2001), and in the analysis of confined systems, mainly considering the interaction between a single particle with the walls of the confinement, such as a sphere or a spheroid near planar (Swan & Brady 2007, 2010; Mitchell & Spagnolie 2015) or cylindrical (Goldsmith & Mason 1962; Sonshine, Cox & Brenner 1966; Hasimoto 1976) walls.

However, the convergence of the method even for touching bodies, such as in the case of two translating spheres or in the case of the Luke's suspensions, and the relative small breakdown gap ($\sim 0.16\,\ell_b$), computed by Ichiki & Brady (2001) for three translating spheres, suggest that, if all the terms of the series were evaluated exactly, reflection method should be a valid approach to provide exact solutions not only in the asymptotic limit $\ell_d \gg \ell_b$, but also in a closer region $\ell_d \sim \ell_b$, albeit external to the lubrication range $\ell_d \ll \ell_b$. A general theory, furnishing the reflection solution regardless of the geometry of the bodies involved, has been developed by Brenner (1962, 1964*a*) and Cox & Brenner (1967*a*) for obtaining the resistance on an arbitrary body immersed in an arbitrarily confined Stokesian fluid, that can be also regarded as confined by a second fixed body. In Brenner (1962, 1964*a*), the first-order correction with respect to the unbounded approximation of the hydrodynamic resistance (force and torque) on a body rigidly moving (translating and rotating) is provided in terms of the resistance matrix of the body in the unbounded fluid and the Stokes's Green function of the domain of the confined fluid without the body inclusion; whereas in Cox & Brenner (1967*a*) a formal expression for the resistance in the large-distance limit is derived, considering also an arbitrary ambient flow, in terms of unspecified tensors depending separately on the geometry of the body and on the geometry of the confinement. The formal approach by Cox & Brenner (1967*a*) is not easily amenable to a simple practical implementation as regards the higher-order terms in the expansion, and for this reason it has remained as a beautiful formal development disjoint from practical implementation in confined flows.

In this work we develop a novel approach, amenable to practical implementation, in the theory of the hydrodynamic interactions between a body in a confined fluid and the confinement walls, by providing exact reflection solutions for the fluid flow in the system and for the grand-resistance matrix on the body (force, torque and higher moments). We express the global solution in terms of well-defined tensors depending separately on the geometry of the body and on the geometry of the confinement: moments on the body in the unbounded fluid (or the Faxén operators of the body), and multipoles of the domain of the confinement (hence, derivatives of the confined Green function). Unlike the tensors appearing in the expressions for the resistance on the body provided by Cox & Brenner (1967*a*), these tensors, when not yet available in the literature, can be directly evaluated by classical analytical or numerical methods in all the practical cases of interest. Furthermore, we consider BCs on the body more general than the no-slip case, requiring only that these BCs satisfy the principle of BC reciprocity as defined in Procopio & Giona (2024). For instance, Navier-slip and many other fluid–fluid boundary conditions of common hydrodynamic practice fall in this class.

To this aim, we enforce the bitensorial formulation (Poisson, Pound & Vega 2011) of the Stokes singularities developed by Procopio & Giona (2023) in dealing with the entries of the two-point-dependent tensorial field (in hydrodynamics these fields depend simultaneously on the position of fluid element and on the position of the body in the confinement). Furthermore, we make use of the results derived in Procopio & Giona (2024) in order to express the hydrodynamics of a body with arbitrary BCs (requiring solely BC reciprocity) in ambient flows generated by the walls of the confinement, which turn out to be highly non-trivial flows even in the simplest case of translation motion.

The article is organised as follows. Section 2 states the problem and provides the definition of the two simpler sub-problems, the solution of which permits to obtain the analytic expression for the global confined hydrodynamics: (i) the Faxén operators of the body and (ii) the multipoles in the domain of the confinement. In § 3, we derive the exact expression for the terms entering in the reflection expansion, showing that they can be expressed as the product of suitable tensorial quantities depending on the volume moments on the body immersed in the ambient flows associated with the regular parts of the bounded multipoles. In § 4 we introduce a generalised matrix notation for tensorial systems more compact than the componentwise representation in terms of the entries of each individual tensor, and we obtain a simple expression for the global velocity field. Moreover, by using the properties of infinite matrices (Cooke 1950), we show in Appendix A that the convergence of the method is ensured for $\ell_d \gtrsim 2.65\ell_b$. This does not mean that the series expansion could not converge under more general conditions, although it is reasonable to hypothesise that there exist a constant $\Gamma = O(1) > 0$, depending on the geometry of the problem, such that the reflection solution converges for $\ell_d > \Gamma \ell_b$. In § 5, we provide the exact reflection formulae for force, torque and higher-order moments on the body. The estimate of the error resulting in truncating the exact solutions by considering only lower-order multi-pole (or Faxén operators) is addressed in § 6. We also analyse the truncation error made in classical literature works in the field, specifically in Brenner (1962, 1964*a*) and in Swan & Brady (2007, 2010), and we extend these approximate approaches to more general hydrodynamic problems than those for which they were originally developed. In § 7 we compare and contrast the reflection solution obtained with the present theory (using Faxén operators and bounded multi-pole available in the literature), approximated to the order $O(\ell_b/\ell_d)^5$, with the exact solution of a sphere translating and rotating near a planar wall, and we provide the expressions for forces and torques considering the more general situation of Navier-slip BCs assumed at the surface of the body. Finally, in § 8, we investigate the effect of the shape and of the orientation on the hydrodynamic interactions between the body and the confinement. Specifically, by using the approximated expressions obtained in § 6, we estimate the resistance matrix truncated to the order $O(\ell_b/\ell_d)^4$ of a prolate spheroid near a plane wall by solely employing the zeroth-order Faxén operator available in the literature (Hasimoto 1983; Kim 1985) for no-slip BCs. This case study shows how it is possible to obtain accurate hydromechanical effects using lower-order approximations for complex geometries of the system. In fact, by comparing the results obtained with numerical FEM simulation, we show that approximated solutions provide correctly the far-field hydrodynamic interaction independently of the orientation and the shape of the body. We also address the effect of the confinement on the lift force experienced by the spheroid.

2. Statement of the problem

Consider a rigid body immersed in a Newtonian fluid with viscosity μ at vanishing Reynolds number. Let $V_b \subset \mathbb{R}^3$ be the domain representing the space occupied by the body and V_f the space occupied by the fluid domain. The surface bounding the body is S_b, whereas the surface bounding the fluid is $S_b \cup S_w \cup S_\infty$, where S_w is the surface bounding externally the fluid and considered in the proximity of the body, and S_∞ the boundary at infinity, i.e. any surface considered infinitely far from the body. See the schematic representation of the system geometry in figure 1.

The body is immersed in an *ambient flow* $(\boldsymbol{u}(\boldsymbol{x}), \boldsymbol{\pi}(\boldsymbol{x}))$, which is defined as any flow, regular at the surface of the body S_b, satisfying the Stokes equations (Kim & Karrila

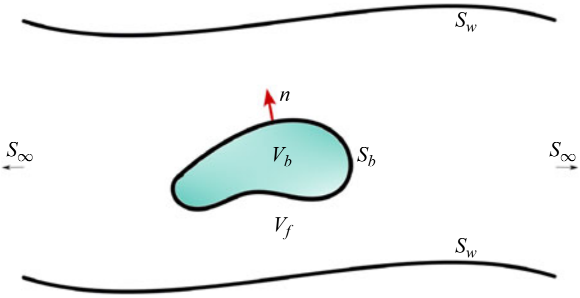

Figure 1. Schematic representation of geometry of the system.

2005). Considering no-slip BCs on S_w, the Stokes equations for the ambient flow read

$$\left.\begin{array}{c} -\nabla \cdot \boldsymbol{\pi}(\boldsymbol{x}) = \mu \Delta \boldsymbol{u}(\boldsymbol{x}) - \nabla p(\boldsymbol{x}) = 0, \\ \nabla \cdot \boldsymbol{u}(\boldsymbol{x}) = 0, \quad \boldsymbol{x} \in V_f \cup V_b, \\ \boldsymbol{u}(\boldsymbol{x}) = 0, \quad \boldsymbol{x} \in S_w, \end{array}\right\} \tag{2.1}$$

where $\boldsymbol{u}(\boldsymbol{x})$ represents the velocity field, $p(\boldsymbol{x})$ the pressure field and

$$\boldsymbol{\pi}(\boldsymbol{x}) = p(\boldsymbol{x})I - \mu(\nabla \boldsymbol{u}(\boldsymbol{x}) + \nabla \boldsymbol{u}(\boldsymbol{x})^t) \tag{2.2}$$

is the stress tensor. In (2.2) I represents the identity matrix and the superscript 't' denotes the transposition operation for a matrix.

Assuming linear homogeneous BCs at the surface of the body S_b, expressed by a generic linear operator $\mathcal{L}[\,]$ acting on the velocity at the surface of the body (this implies that $\mathcal{L}[\boldsymbol{v}(\boldsymbol{x})]$ at the point $\boldsymbol{x} \in S_b$ may depend not only on the velocity $\boldsymbol{v}(\boldsymbol{x})$ but also on its derivatives at that point), and no-slip BCs at the surface of the confinement S_w, the *total (or disturbed) flow* $(\boldsymbol{v}(\boldsymbol{x}), \boldsymbol{\sigma}(\boldsymbol{x}))$ is

$$\left.\begin{array}{c} -\nabla \cdot \boldsymbol{\sigma}(\boldsymbol{x}) = \mu \Delta \boldsymbol{v}(\boldsymbol{x}) - \nabla s(\boldsymbol{x}) = 0, \\ \nabla \cdot \boldsymbol{v}(\boldsymbol{x}) = 0, \quad \boldsymbol{x} \in V_f, \\ \mathcal{L}[\boldsymbol{v}(\boldsymbol{x})] = 0, \quad \boldsymbol{x} \in S_b, \\ \boldsymbol{v}(\boldsymbol{x}) = 0, \quad \boldsymbol{x} \in S_w, \end{array}\right\} \tag{2.3}$$

with the obvious meaning for $\boldsymbol{v}(\boldsymbol{x})$, $s(\boldsymbol{x})$, and $\boldsymbol{\sigma}(\boldsymbol{x})$, representing velocity, pressure and stress tensor fields of the total flow, respectively. Henceforth, we require that the BCs expressed by the linear operator $\mathcal{L}[\,]$, satisfy the following condition at the surface of the body: for any couple of flows $(\boldsymbol{v}'(\boldsymbol{x}), \boldsymbol{\sigma}'(\boldsymbol{x}))$ and $(\boldsymbol{v}''(\boldsymbol{x}), \boldsymbol{\sigma}''(\boldsymbol{x}))$ solution of (2.3), the following identity holds:

$$\int_{S_b} (\boldsymbol{v}'(\boldsymbol{x}) \cdot \boldsymbol{\sigma}''(\boldsymbol{x}) - \boldsymbol{v}(\boldsymbol{x}) \cdot \boldsymbol{\sigma}'(\boldsymbol{x})) \cdot \boldsymbol{n}(\boldsymbol{x}) \, \mathrm{d}S = 0, \tag{2.4}$$

where $\boldsymbol{n}(\boldsymbol{x})$ is the unitary normal vector outwardly oriented with respect to the body as shown in figure 1. This condition has been introduced and thoroughly discussed in Procopio & Giona (2024) in connection to the concept of the Hinch–Kim dualism, and it is referred to as the condition of *BC reciprocity*. BCs satisfying (2.4), are therefore called *reciprocal BCs*. As it will become clear in the remainder, the assumption of BC reciprocity, coupled with the linearity of the BCs expressed by the operator $\mathcal{L}[\,]$, are the

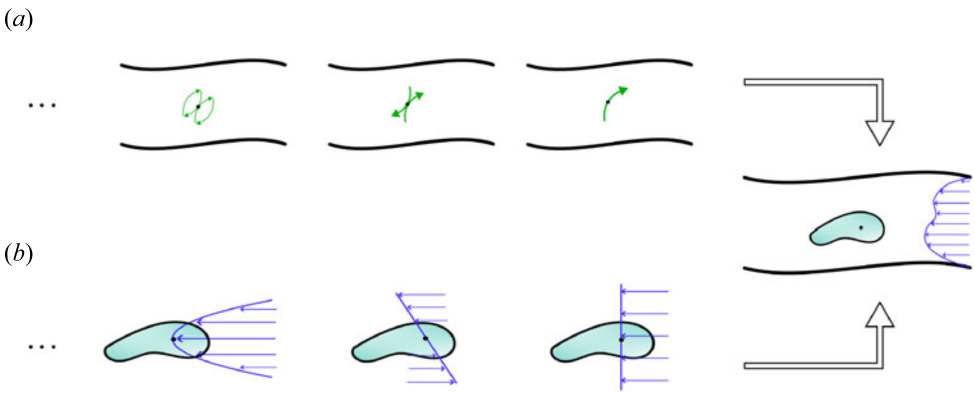

Figure 2. Schematic representation of the decomposition of the main problem (a body in a confined fluid with an ambient flow) in problems separately related to the geometry of the confinement and of the particle: (i) multipoles of the confinement (at the top) centred at the position point (e.g. the barycentric coordinate) in the volume the body; (ii) flows around the body in *n*th-order ambient flows centred at the position of the body provided by the Faxén operators (at the bottom). Green arrows in (*a*) represent concentrated forces whereas blue arrows in (*b*) represent velocity fields. The black dot is the position point of the body.

necessary prerequisites in the development of the present theory. Linear reciprocal BCs are, for example, no-slip $\boldsymbol{v}(\boldsymbol{x}) = 0$, complete slip $\boldsymbol{\sigma}(\boldsymbol{x}) = 0$ and Navier-slip BCs

$$\boldsymbol{v}(\boldsymbol{x}) + \frac{\lambda}{\mu}\boldsymbol{n}(\boldsymbol{x}) \cdot \boldsymbol{\sigma}(\boldsymbol{x}) \cdot \boldsymbol{t}(\boldsymbol{x}) = 0 \tag{2.5}$$

with λ being the slip length and $\boldsymbol{t}(\boldsymbol{x})$ an unitary base vectors tangents to the surface of the body. On the other hand, BCs representing the interaction of the Stokes fluid with a non-Newtonian fluid, for example, are not reciprocal because the reciprocity theorem does not hold in the body domain.

In the next paragraph, the solution of the problem (2.3) is expressed in terms of the hydrodynamic solutions of two simpler problems related separately to the confinement of the fluid and to the body: (i) the Green function of the Stokes equations in the domain of the confinement $V_f \cup V_b$ and (ii) the geometrical moments of the body in the unbounded fluid. See the schematic representation in figure 2. For this reason, it is useful to define these solutions and discuss briefly their formal properties, introducing and clarifying in this way the notation that we use throughout this article.

2.1. *Green function of the confinement*

As discussed in Procopio & Giona (2023), the Green function in the confined domain $V_f \cup V_b$ is a bitensorial field, hence a field depending on two points (called *field* and *source points*) with entries at both points expressed, in principle, in different coordinate systems.

The Green function $G_{a\beta}(\boldsymbol{x}, \boldsymbol{\xi})$ of the confined flow is the solution of the equations

$$\left.\begin{aligned} -\nabla_b \Sigma_{ab\beta}(\boldsymbol{x}, \boldsymbol{\xi}) = \Delta G_{a\beta}(\boldsymbol{x}, \boldsymbol{\xi}) - \nabla_a P_\beta(\boldsymbol{x}, \boldsymbol{\xi}) = -8\pi\delta_{a\beta}\delta(\boldsymbol{x} - \boldsymbol{\xi}), \\ \nabla_a G_{a\beta}(\boldsymbol{x}, \boldsymbol{\xi}) = 0, \quad \boldsymbol{x}, \boldsymbol{\xi} \in V_f \cup V_b, \\ G_{a\beta}(\boldsymbol{x}, \boldsymbol{\xi}) = 0, \quad \boldsymbol{x} \in S_w \cup S_\infty, \end{aligned}\right\} \tag{2.6}$$

where $G_{a\beta}(\boldsymbol{x}, \boldsymbol{\xi})$, $P_\beta(\boldsymbol{x}, \boldsymbol{\xi})$, $\Sigma_{ab\beta}(\boldsymbol{x}, \boldsymbol{\xi})$ are the associated velocity, pressure and stress tensor field. In (2.6) and in the remainder, the notation of the bitensor calculus is applied:

(i) Latin letters $a, b, \ldots = 1, 2, 3$ are used for indices referred to the entries of the tensorial entities at the field point $\boldsymbol{x}$, with Greek letters $\alpha, \beta, \ldots = 1, 2, 3$ for indices referred to the entries of the tensorial entities at the source points (i.e. the poles of the singularity) $\boldsymbol{\xi}$; (ii) Einstein's summation convention is adopted; and (iii) ∇_a, with the Latin index, is the gradient with respect to the field point $\boldsymbol{x}$, while ∇_β, with the Greek index, is the gradient with respect to the source point $\boldsymbol{\xi}$.

It is useful to define also the *regular part of the Green function* $(W_{a\beta}(\boldsymbol{x}, \boldsymbol{\xi}), Q_\beta(\boldsymbol{x}, \boldsymbol{\xi}))$ as the bitensorial fields solving the problem

$$\left.\begin{aligned} -\nabla_b T_{ab\beta}(\boldsymbol{x}, \boldsymbol{\xi}) = \Delta W_{a\beta}(\boldsymbol{x}, \boldsymbol{\xi}) - \nabla_a Q_\beta(\boldsymbol{x}, \boldsymbol{\xi}) = 0, \\ \nabla_a W_{a\beta}(\boldsymbol{x}, \boldsymbol{\xi}) = 0, \quad \boldsymbol{x}, \boldsymbol{\xi} \in V_f \cup V_b, \\ W_{a\beta}(\boldsymbol{x}, \boldsymbol{\xi}) = -S_{a\beta}(\boldsymbol{x} - \boldsymbol{\xi}), \quad \boldsymbol{x} \in S_w \cup S_\infty, \end{aligned}\right\} \tag{2.7}$$

where $S_{a\beta}(\boldsymbol{x} - \boldsymbol{\xi})$ is the *Stokeslet* (Pozrikidis 1992; Kim & Karrila 2005), i.e. the bitensorial velocity field of the unbounded Green function

$$S_{a\beta}(\boldsymbol{x} - \boldsymbol{\xi}) = \frac{\delta_{a\beta}}{|(\boldsymbol{x} - \boldsymbol{\xi})|} + \frac{(\boldsymbol{x} - \boldsymbol{\xi})_a (\boldsymbol{x} - \boldsymbol{\xi})_\beta}{|(\boldsymbol{x} - \boldsymbol{\xi})|^3}. \tag{2.8}$$

Therefore, the bounded Green function can be written as the superposition of a regular field $W_{a\beta}(\boldsymbol{x}, \boldsymbol{\xi})$ and a singular contribution given by the Stokeslet

$$G_{a\beta}(\boldsymbol{x}, \boldsymbol{\xi}) = S_{a\beta}(\boldsymbol{x} - \boldsymbol{\xi}) + W_{a\beta}(\boldsymbol{x}, \boldsymbol{\xi}). \tag{2.9}$$

By differentiating (2.9) at the pole, higher-order singularities in the domain $V_b \cup V_f$ are obtained. For example, the nth-order multipole, with $n = 1, 2, \ldots$, is obtained by

$$\nabla_{\boldsymbol{\beta}_n} G_{a\beta}(\boldsymbol{x}, \boldsymbol{\xi}) = \nabla_{\boldsymbol{\beta}_n} S_{a\beta}(\boldsymbol{x} - \boldsymbol{\xi}) + \nabla_{\boldsymbol{\beta}_n} W_{a\beta}(\boldsymbol{x}, \boldsymbol{\xi}), \tag{2.10}$$

where bold index $\boldsymbol{\beta}_n = \beta_1 \ldots \beta_n$ denotes a multi-index and $\nabla_{\boldsymbol{\beta}_n} = \nabla_{\beta_1} \ldots \nabla_{\beta_n}$ is a compact notation for nth-order differentiation.

2.2. *Moments on the body and Faxén operators*

Let us briefly define the *nth-order moments*, the (m, n)*th-order geometrical moments* and the *nth-order Faxén operators* of a body, addressed in more detail in Procopio & Giona (2024).

Consider the same body immersed in an ambient flow $(\boldsymbol{u}(\boldsymbol{x}), \boldsymbol{\pi}(\boldsymbol{x}))$ in the unbounded domain. The *disturbance flow* $(\boldsymbol{w}(\boldsymbol{x}), \boldsymbol{\tau}(\boldsymbol{x}))$ generated by the body immersed in the ambient flow is solution of

$$\left.\begin{aligned} -\nabla \cdot \boldsymbol{\tau}(\boldsymbol{x}) = \mu \Delta \boldsymbol{w}(\boldsymbol{x}) - \nabla q(\boldsymbol{x}) = 0, \\ \nabla \cdot \boldsymbol{w}(\boldsymbol{x}) = 0, \quad \boldsymbol{x} \in V_f, \\ \mathcal{L}[\boldsymbol{w}(\boldsymbol{x})] = -\mathcal{L}[\boldsymbol{u}(\boldsymbol{x})], \quad \boldsymbol{x} \in S_b, \\ \boldsymbol{w}(\boldsymbol{x}) = 0, \quad \boldsymbol{x} \to \infty, \end{aligned}\right\} \tag{2.11}$$

where $\boldsymbol{w}(\boldsymbol{x})$, $q(\boldsymbol{x})$ and $\boldsymbol{\tau}(\boldsymbol{x})$ are the associated disturbance velocity, pressure and stress tensor fields accounting for the hydrodynamics at the surface S_b of the rigid body due to the interaction with the ambient flow $\boldsymbol{u}(\boldsymbol{x})$.

To begin with, consider the entries $\psi_a(\boldsymbol{x})$ of any force field distribution, with compact support belonging to V_b, such that the Ladyzhenskaya (2014) volume potential reads

$$\frac{1}{8\pi\mu}\int_{V_b}\psi_\beta(\boldsymbol{\xi})S_{a\beta}(\boldsymbol{x}-\boldsymbol{\xi})\,\mathrm{d}V(\boldsymbol{\xi}) = w_a(\boldsymbol{x}) \quad \boldsymbol{x}\in S_b. \tag{2.12}$$

Next, the nth-order moments on the body immersed in a generic ambient flow $\boldsymbol{u}(\boldsymbol{x})$, generating a disturbance field at the surface of the body $\boldsymbol{w}(\boldsymbol{x})$, are defined as

$$M_{\beta\boldsymbol{\beta}_n}(\boldsymbol{\xi}) = \int_{V_b}(\boldsymbol{x}-\boldsymbol{\xi})_{\boldsymbol{\beta}_n}\psi_\beta(\boldsymbol{x})\,\mathrm{d}V(\boldsymbol{x}) \quad \boldsymbol{\xi}\in V_b, \tag{2.13}$$

where $(\boldsymbol{x}-\boldsymbol{\xi})_{\boldsymbol{\beta}_n} = (\boldsymbol{x}-\boldsymbol{\xi})_{\beta_1}\ldots(\boldsymbol{x}-\boldsymbol{\xi})_{\beta_n}$ and where $(\boldsymbol{x}-\boldsymbol{\xi})_\beta = g_{\beta a}(\boldsymbol{\xi},\boldsymbol{x})(\boldsymbol{x}-\boldsymbol{\xi})_a$ and $\psi_\beta(\boldsymbol{x}) = g_{\beta a}(\boldsymbol{\xi},\boldsymbol{x})\psi_a(\boldsymbol{x})$, $g_{\beta a}(\boldsymbol{\xi},\boldsymbol{x})$ being the transformation matrix between the coordinate systems at the pole and field point (or, more generically, the parallel propagator (Poisson *et al.* 2011), i.e. the bitensor transforming the entries of a vector at the point $\boldsymbol{x}$ into the entries at the point $\boldsymbol{\xi}$).

Consider an nth-order polynomial ambient flow $\boldsymbol{u}^{(n)}(\boldsymbol{x},\boldsymbol{\xi})$, centred at a point $\boldsymbol{\xi}'\in V_b$ within the domain of the body, with entries

$$u_a(\boldsymbol{x}) = A_{a\boldsymbol{a}_n}(\boldsymbol{x}-\boldsymbol{\xi}')_{\boldsymbol{a}_n}, \quad \boldsymbol{\xi}'\in V_b \tag{2.14}$$

($A_{a\boldsymbol{a}_n}$ being an $(n+1)$-dimensional constant tensor) and its associated disturbance field $w_a^{(n)}(\boldsymbol{x},\boldsymbol{\xi}')$, obtained from (2.13) by a force field distribution $\boldsymbol{\psi}^{(n)}(\boldsymbol{\xi},\boldsymbol{\xi}')$. According to the definition (2.13), the mth-order moments on the body immersed in the nth-order ambient flow can be expressed as

$$M^{(n)}_{\beta\boldsymbol{\beta}_m}(\boldsymbol{\xi},\boldsymbol{\xi}') = \int(\boldsymbol{x}-\boldsymbol{\xi})_{\boldsymbol{\beta}_m}\psi^{(n)}_\beta(\boldsymbol{x},\boldsymbol{\xi}')\,\mathrm{d}V(\boldsymbol{x}) \quad \boldsymbol{\xi},\boldsymbol{\xi}'\in V_b. \tag{2.15}$$

By the linearity of the Stokes equations with respect to the constant tensor $A_{a\boldsymbol{a}_n}$, we can define the (m,n)th-order geometrical moments $m_{\beta\boldsymbol{\beta}_m\gamma'\boldsymbol{\gamma}'_n}(\boldsymbol{\xi},\boldsymbol{\xi}')$ by the relation

$$M^{(n)}_{\beta\boldsymbol{\beta}_m}(\boldsymbol{\xi},\boldsymbol{\xi}') = 8\pi\mu A_{\gamma\boldsymbol{\gamma}_n}m_{\beta\boldsymbol{\beta}_m\gamma'\boldsymbol{\gamma}'_n}(\boldsymbol{\xi},\boldsymbol{\xi}'), \tag{2.16}$$

where the multi-index $\gamma'\boldsymbol{\gamma}'_n$ is referred to the entries of the field at the point $\boldsymbol{\xi}'$.

Based on the hierarchy of the geometrical moments, the operator

$$\mathcal{F}_{\beta\gamma'\boldsymbol{\gamma}'_n} = \sum_{m=0}^{\infty}\frac{m_{\beta\boldsymbol{\beta}_m\gamma'\boldsymbol{\gamma}'_n}(\boldsymbol{\xi},\boldsymbol{\xi}')\nabla_{\boldsymbol{\beta}_m}}{m!} \tag{2.17}$$

can be introduced. As shown in Procopio & Giona (2024), if BC reciprocity holds, $\mathcal{F}_{\beta\gamma'\boldsymbol{\gamma}'_n}$ represents the nth-order Faxén operator of the body. By the assumption that the operator $\mathcal{L}[\boldsymbol{v}(\boldsymbol{x})]$ in the total Stokes system (2.3) belongs to the class of linear homogeneous reciprocal BCs satisfying (2.4), the following relations for the body in the unbounded domain hold (Procopio & Giona 2023, 2024):

$$M_{\beta\boldsymbol{\beta}_n}(\boldsymbol{\xi}) = 8\pi\mu\mathcal{F}_{\gamma'\beta\boldsymbol{\beta}_n}u_{\gamma'}(\boldsymbol{\xi}') \tag{2.18}$$

and

$$w_a(\boldsymbol{x}) = \sum_{n=0}^{\infty}\frac{\nabla_{\boldsymbol{\gamma}'_n}u_{\gamma'}(\boldsymbol{\xi}')}{n!}\mathcal{F}_{\beta\gamma'\boldsymbol{\gamma}'_n}S_{a\beta}(\boldsymbol{x}-\boldsymbol{\xi}). \tag{2.19}$$

Furthermore, owing to the property that $\mathcal{F}_{\beta\gamma'\boldsymbol{\gamma}'_n}$ is a Faxén operator, the disturbance field can be expressed by

$$\begin{aligned} w_a(\boldsymbol{x}) &= \sum_{m=0}^{\infty}\frac{\mathcal{F}_{\gamma'\beta\boldsymbol{\beta}_m}u_{\gamma'}(\boldsymbol{\xi}')}{m!}\nabla_{\boldsymbol{\beta}_m}S_{a\beta}(\boldsymbol{x}-\boldsymbol{\xi}) \\ &= \frac{1}{8\pi\mu}\sum_{m=0}^{\infty}\frac{M_{\beta\boldsymbol{\beta}_m}(\boldsymbol{\xi})}{m!}\nabla_{\boldsymbol{\beta}_m}S_{a\beta}(\boldsymbol{x}-\boldsymbol{\xi}). \end{aligned} \tag{2.20}$$

Finally, it is useful in the remainder to remark that the force exerted by the fluid on the body is $F_\beta = -M_\beta(\boldsymbol{\xi})$, thus, by (2.18),

$$F_\beta = -8\pi\mu\mathcal{F}_{\gamma\beta}u_\gamma(\boldsymbol{\xi}) \tag{2.21}$$

whereas the torque $T_\beta = \varepsilon_{\beta\gamma\gamma_1}M_{\gamma\gamma_1}(\boldsymbol{\xi})$, is given by

$$T_\beta = 8\pi\mu\mathcal{T}_{\gamma\beta}\,u_\gamma(\boldsymbol{\xi}), \tag{2.22}$$

where $\mathcal{T}_{\delta\beta} = \varepsilon_{\beta\gamma\gamma_1}\mathcal{F}_{\delta\gamma\gamma_1}$ and $\varepsilon_{\beta\gamma\gamma_1}$ the Ricci–Levi Civita symbol.

3. The flow due to a body in a confined fluid

3.1. *The reflection method*

Consider the problem defined by (2.3) providing the total flow in the system in the case of no-slip conditions both on the body surface and on the confinement walls, thus considering the identity matrix as operator $\mathcal{L}[\,] = I$. Owing to the linearity of the equations and of the BCs, we can apply the reflection method (see Happel & Brenner 1983) to express the solution $(v_a(\boldsymbol{x}), \sigma_{ab}(\boldsymbol{x}))$ as the superposition of a countable system of fields $(v_a^{[k]}(\boldsymbol{x}), \sigma_{ab}^{[k]}(\boldsymbol{x}))$, with $k = 0, 1, 2, \ldots$,

$$\left.\begin{aligned} v_a(\boldsymbol{x}) &= v_a^{[0]}(\boldsymbol{x}) + v_a^{[1]}(\boldsymbol{x}) + \cdots + v_a^{[k]}(\boldsymbol{x}) + \cdots, \\ \sigma_{ab}(\boldsymbol{x}) &= \sigma_{ab}^{[0]}(\boldsymbol{x}) + \sigma_{ab}^{[1]}(\boldsymbol{x}) + \cdots + \sigma_{ab}^{[k]}(\boldsymbol{x}) + \cdots, \end{aligned}\right\} \tag{3.1}$$

where

$$\sigma_{ab}^{[k]}(\boldsymbol{x}) = s^{[k]}(\boldsymbol{x})\delta_{ab} - \mu(\nabla_a v_b^{[k]}(\boldsymbol{x}) + \nabla_b v_a^{[k]}(\boldsymbol{x})), \tag{3.2}$$

with $s^{[k]}(\boldsymbol{x})$ being the associated pressure, each of which is the solution of the Stokes equations equipped with the following system of BCs:

$$\left.\begin{aligned} v_a^{[2k+1]}(\boldsymbol{x}) &= -v_a^{[2k]}(\boldsymbol{x}), \quad \boldsymbol{x} \in S_b, \\ v_a^{[2k+2]}(\boldsymbol{x}) &= -v_a^{[2k+1]}(\boldsymbol{x}), \quad \boldsymbol{x} \in S_w. \end{aligned}\right\} \tag{3.3}$$

For $k = 0$,

$$v_a^{[0]}(\boldsymbol{x}) = u_a(\boldsymbol{x}), \quad \boldsymbol{x} \in V_b \cup V_f. \tag{3.4}$$

Hence, as can be observed from (3.3), for odd k the condition involves the boundary of the body, for even k the walls of the confinement.

3.2. *The velocity fields* $\boldsymbol{v}^{[1]}$ *and* $\boldsymbol{v}^{[2]}$

Let us start by expressing the first velocity fields $v_a^{[1]}(\boldsymbol{x})$ and $v_a^{[2]}(\boldsymbol{x})$ in terms of the Green function of the confinement and the Faxén operator of the body that are supposed to be given.

Comparing (3.3) with (2.11) it is easy to recognise that $\boldsymbol{v}^{[1]}(\boldsymbol{x})$ is the disturbance field of the ambient field $\boldsymbol{u}(\boldsymbol{x})$. Therefore, by using (2.19), it is possible to explicit the velocity field with $k = 1$ as

$$v_a^{[1]}(\boldsymbol{x}) = \sum_{n=0}^{\infty} \frac{\nabla_{\boldsymbol{\gamma}_n} u_\gamma(\boldsymbol{\xi})}{n!} \mathcal{F}_{\beta\gamma\boldsymbol{\gamma}_n} S_{a\beta}(\boldsymbol{x} - \boldsymbol{\xi}). \tag{3.5}$$

Alternatively, from (2.20), the first velocity field can be expressed as

$$v_a^{[1]}(\boldsymbol{x}) = \frac{1}{8\pi\mu} \sum_{m=0}^{\infty} \frac{M_{\beta\boldsymbol{\beta}_m}(\boldsymbol{\xi})}{m!} \nabla_{\boldsymbol{\beta}_m} S_{a\beta}(\boldsymbol{x} - \boldsymbol{\xi}). \tag{3.6}$$

Since, by linearity, any $\boldsymbol{v}^{[k]}(\boldsymbol{x})$ is solution of the Stokes equations, equipped with the BCs (3.3), the flow with $k = 2$ is the solution of the problem

$$\left.\begin{aligned} \mu\Delta v_a^{[2]}(\boldsymbol{x}) - \nabla_a s^{[2]}(\boldsymbol{x}) = 0, \\ \nabla_a v_a^{[2]}(\boldsymbol{x}) = 0, \quad \boldsymbol{x} \in V_b \cup V_f, \\ v_a^{[2]}(\boldsymbol{x}) = -v_a^{[1]}(\boldsymbol{x}), \quad \boldsymbol{x} \in S_w. \end{aligned}\right\} \tag{3.7}$$

By applying the operator

$$\sum_{n=0}^{\infty} \frac{\nabla_{\boldsymbol{\gamma}_n} u_\gamma(\boldsymbol{\xi})}{n!} \mathcal{F}_{\beta\gamma\boldsymbol{\gamma}_n}, \tag{3.8}$$

at a source point $\boldsymbol{\xi} \in V_b$ of the regular part of the Green function defined by the (2.7), and comparing the resulting problem with (3.7), it is easy to conclude, by the uniqueness of the solution of Stokes equations, that

$$v_a^{[2]}(\boldsymbol{x}) = \sum_{n=0}^{\infty} \frac{\nabla_{\boldsymbol{\gamma}_n} u_\gamma(\boldsymbol{\xi})}{n!} \mathcal{F}_{\beta\gamma\boldsymbol{\gamma}_n} W_{a\beta}(\boldsymbol{x}, \boldsymbol{\xi}) \tag{3.9}$$

or, alternatively, by applying the operator

$$\frac{1}{8\pi\mu} \sum_{m=0}^{\infty} \frac{M_{\beta\boldsymbol{\beta}_m}(\boldsymbol{\xi})}{m!} \nabla_{\boldsymbol{\beta}_m}, \tag{3.10}$$

we obtain the representation

$$v_a^{[2]}(\boldsymbol{x}) = \frac{1}{8\pi\mu} \sum_{m=0}^{\infty} \frac{M_{\beta\boldsymbol{\beta}_m}(\boldsymbol{\xi})}{m!} \nabla_{\boldsymbol{\beta}_m} W_{a\beta}(\boldsymbol{x}, \boldsymbol{\xi}) \tag{3.11}$$

and, thus,

$$\begin{aligned} v_a^{[1]}(\boldsymbol{x}) + v_a^{[2]}(\boldsymbol{x}) &= \sum_{n=0}^{\infty} \frac{\nabla_{\boldsymbol{\gamma}_n} u_\gamma(\boldsymbol{\xi})}{n!} \mathcal{F}_{\beta\gamma\boldsymbol{\gamma}_n} G_{a\beta}(\boldsymbol{x}, \boldsymbol{\xi}) \\ &= \frac{1}{8\pi\mu} \sum_{m=0}^{\infty} \frac{M_{\beta\boldsymbol{\beta}_m}(\boldsymbol{\xi})}{m!} \nabla_{\boldsymbol{\beta}_m} G_{a\beta}(\boldsymbol{x}, \boldsymbol{\xi}). \end{aligned} \tag{3.12}$$

3.3. *The velocity fields* $\boldsymbol{v}^{[3]}$ *and* $\boldsymbol{v}^{[4]}$

From the BCs (3.3), the velocity field for $k = 3$ is the disturbance field of $v_a^{[2]}(\boldsymbol{x})$ and, therefore, by (2.19),

$$v_a^{[3]}(\boldsymbol{x}) = \sum_{\ell=0}^{\infty} \frac{\nabla_{\boldsymbol{\delta}'_\ell} v_{\delta'}^{[2]}(\boldsymbol{\xi}')}{\ell!} \mathcal{F}_{\gamma\delta'\boldsymbol{\delta}'_\ell} S_{a\gamma}(\boldsymbol{x}-\boldsymbol{\xi}) \tag{3.13}$$

and, equivalently to (3.9),

$$v_a^{[4]}(\boldsymbol{x}) = \sum_{\ell=0}^{\infty} \frac{\nabla_{\boldsymbol{\delta}'_\ell} v_{\delta'}^{[2]}(\boldsymbol{\xi}')}{\ell!} \mathcal{F}_{\gamma\delta'\boldsymbol{\delta}'_\ell} W_{a\gamma}(\boldsymbol{x}-\boldsymbol{\xi}). \tag{3.14}$$

Substituting (3.11) into (3.13) one obtains

$$v_a^{[3]}(\boldsymbol{x}) = \frac{1}{8\pi\mu} \sum_{m=0}^{\infty} \frac{M_{\beta\boldsymbol{\beta}_m}(\boldsymbol{\xi})}{m!} \sum_{\ell=0}^{\infty} \frac{\nabla_{\boldsymbol{\delta}'_\ell} \nabla_{\boldsymbol{\beta}_m} W_{\delta'\beta}(\boldsymbol{\xi}',\boldsymbol{\xi})}{\ell!} \mathcal{F}_{\gamma\delta'\boldsymbol{\delta}'_\ell} S_{a\gamma}(\boldsymbol{x}-\boldsymbol{\xi}). \tag{3.15}$$

By the equivalence between the two expressions (2.19) and (2.20),

$$\sum_{\ell=0}^{\infty} \frac{\nabla_{\boldsymbol{\delta}'_\ell} \nabla_{\boldsymbol{\beta}_m} W_{\delta'\beta}(\boldsymbol{\xi}',\boldsymbol{\xi})}{\ell!} \mathcal{F}_{\gamma\delta'\boldsymbol{\delta}'_\ell} S_{a\gamma}(\boldsymbol{x}-\boldsymbol{\xi}) = \sum_{n=0}^{\infty} \frac{\mathcal{F}_{\delta'\gamma\boldsymbol{\gamma}_n} \nabla_{\boldsymbol{\beta}_m} W_{\delta'\beta}(\boldsymbol{\xi}',\boldsymbol{\xi})}{n!} \nabla_{\boldsymbol{\gamma}_n} S_{a\gamma}(\boldsymbol{x}-\boldsymbol{\xi}). \tag{3.16}$$

It is useful to introduce the tensor $N_{\alpha\boldsymbol{\alpha}_m\beta\boldsymbol{\beta}_n}(\boldsymbol{\xi})$ defined as

$$N_{\beta\boldsymbol{\beta}_m\gamma\boldsymbol{\gamma}_n}(\boldsymbol{\xi}) = \mathcal{F}_{\delta'\gamma\boldsymbol{\gamma}_n} \nabla_{\boldsymbol{\beta}_m} W_{\delta'\beta}(\boldsymbol{\xi}',\boldsymbol{\xi})\big|_{\boldsymbol{\xi}'=\boldsymbol{\xi}}, \tag{3.17}$$

which corresponds to the nth-order moment on the body immersed in an ambient field consisting in the regular part of the mth derivative of the Green function. The tensor defined in (3.17) is fundamental for the further development of this analysis because, as shown in the following, it completely represents the hydrodynamic interaction between the body and the confinement.

Using the identity (3.16) and the definition (3.17), (3.15) can be expressed as

$$v_a^{[3]}(\boldsymbol{x}) = \frac{1}{8\pi\mu} \sum_{m=0}^{\infty} \frac{M_{\beta\boldsymbol{\beta}_m}(\boldsymbol{\xi})}{m!} \sum_{n=0}^{\infty} \frac{N_{\beta\boldsymbol{\beta}_m\gamma\boldsymbol{\gamma}_n}(\boldsymbol{\xi})}{n!} \nabla_{\boldsymbol{\gamma}_n} S_{a\gamma}(\boldsymbol{x}-\boldsymbol{\xi}) \tag{3.18}$$

and, enforcing the same argument applied above to obtain (3.7)–(3.11), we have

$$v_a^{[4]}(\boldsymbol{x}) = \frac{1}{8\pi\mu} \sum_{m=0}^{\infty} \frac{M_{\beta\boldsymbol{\beta}_m}(\boldsymbol{\xi})}{m!} \sum_{n=0}^{\infty} \frac{N_{\beta\boldsymbol{\beta}_m\gamma\boldsymbol{\gamma}_n}(\boldsymbol{\xi})}{n!} \nabla_{\boldsymbol{\gamma}_n} W_{a\gamma}(\boldsymbol{x},\boldsymbol{\xi}) \tag{3.19}$$

so that

$$v_a^{[3]}(\boldsymbol{x}) + v_a^{[4]}(\boldsymbol{x}) = \frac{1}{8\pi\mu} \sum_{m=0}^{\infty} \frac{M_{\beta\boldsymbol{\beta}_m}(\boldsymbol{\xi})}{m!} \sum_{n=0}^{\infty} \frac{N_{\beta\boldsymbol{\beta}_m\gamma\boldsymbol{\gamma}_n}(\boldsymbol{\xi})}{n!} \nabla_{\boldsymbol{\gamma}_n} G_{a\gamma}(\boldsymbol{x},\boldsymbol{\xi}). \tag{3.20}$$

3.4. *The velocity fields* $\boldsymbol{v}^{[5]}$ *and* $\boldsymbol{v}^{[6]}$

The subsequent velocity fields can be determined following the same procedure used for $\boldsymbol{v}^{[3]}(\boldsymbol{x})$ and $\boldsymbol{v}^{[4]}(\boldsymbol{x})$. In fact, $\boldsymbol{v}^{[5]}(\boldsymbol{x})$ can be considered as the disturbance field of $\boldsymbol{v}^{[4]}(\boldsymbol{x})$ and, thus,

$$v_a^{[5]}(\boldsymbol{x}) = \sum_{\ell=0}^{\infty} \frac{\nabla_{\boldsymbol{\gamma}'_\ell} v_{\gamma'}^{[4]}(\boldsymbol{\xi}')}{\ell!} \mathcal{F}_{\delta\gamma'\boldsymbol{\gamma}'_\ell} S_{a\delta}(\boldsymbol{x}-\boldsymbol{\xi}) \tag{3.21}$$

and, equivalently to (3.9),

$$v_a^{[6]}(\boldsymbol{x}) = \sum_{\ell=0}^{\infty} \frac{\nabla_{\boldsymbol{\gamma}'_\ell} v_{\gamma'}^{[4]}(\boldsymbol{\xi}')}{\ell!} \mathcal{F}_{\delta\gamma'\boldsymbol{\gamma}'_\ell} W_{a\delta}(\boldsymbol{x}-\boldsymbol{\xi}). \tag{3.22}$$

Enforcing the same argument used previously in (3.15)–(3.20) for $v_a^{[3]}(\boldsymbol{x})$ and $v_a^{[4]}(\boldsymbol{x})$, we obtain

$$v_a^{[5]}(\boldsymbol{x}) = \frac{1}{8\pi\mu} \sum_{m=0}^{\infty} \frac{M_{\beta\boldsymbol{\beta}_m}(\boldsymbol{\xi})}{m!} \sum_{n=0}^{\infty} \frac{N_{\beta\boldsymbol{\beta}_m\gamma\boldsymbol{\gamma}_n}(\boldsymbol{\xi})}{n!} \sum_{\ell=0}^{\infty} \frac{N_{\gamma\boldsymbol{\gamma}_n\delta\boldsymbol{\delta}_\ell}(\boldsymbol{\xi})}{\ell!} \nabla_{\boldsymbol{\delta}_\ell} S_{a\delta}(\boldsymbol{x}-\boldsymbol{\xi}), \tag{3.23}$$

$$v_a^{[6]}(\boldsymbol{x}) = \frac{1}{8\pi\mu} \sum_{m=0}^{\infty} \frac{M_{\beta\boldsymbol{\beta}_m}(\boldsymbol{\xi})}{m!} \sum_{n=0}^{\infty} \frac{N_{\beta\boldsymbol{\beta}_m\gamma\boldsymbol{\gamma}_n}(\boldsymbol{\xi})}{n!} \sum_{\ell=0}^{\infty} \frac{N_{\gamma\boldsymbol{\gamma}_n\delta\boldsymbol{\delta}_\ell}(\boldsymbol{\xi})}{\ell!} \nabla_{\boldsymbol{\delta}_\ell} W_{a\delta}(\boldsymbol{x},\boldsymbol{\xi}), \tag{3.24}$$

so that

$$v_a^{[5]}(\boldsymbol{x}) + v_a^{[6]}(\boldsymbol{x}) = \frac{1}{8\pi\mu} \sum_{m=0}^{\infty} \frac{M_{\beta\boldsymbol{\beta}_m}(\boldsymbol{\xi})}{m!} \sum_{n=0}^{\infty} \frac{N_{\beta\boldsymbol{\beta}_m\gamma\boldsymbol{\gamma}_n}(\boldsymbol{\xi})}{n!} \sum_{\ell=0}^{\infty} \frac{N_{\gamma\boldsymbol{\gamma}_n\delta\boldsymbol{\delta}_\ell}(\boldsymbol{\xi})}{\ell!} \nabla_{\boldsymbol{\delta}_\ell} G_{a\delta}(\boldsymbol{x},\boldsymbol{\xi}). \tag{3.25}$$

3.5. *The total velocity field*

Iterating the same procedure for any k, it is possible to generalise the above results in the form

$$v_a^{[2k+1]}(\boldsymbol{x}) = \frac{1}{8\pi\mu} \sum_{m=0}^{\infty} \frac{M_{\beta\boldsymbol{\beta}_m}(\boldsymbol{\xi})}{m!} \sum_{m_1=0}^{\infty} \frac{N_{\beta\boldsymbol{\beta}_m\gamma\boldsymbol{\gamma}_{m_1}}(\boldsymbol{\xi})}{m_1!} \cdots \sum_{m_k=0}^{\infty} \frac{N_{\delta\boldsymbol{\delta}_{m_{k-1}}\eta\boldsymbol{\eta}_{m_k}}(\boldsymbol{\xi})}{m_k!} \nabla_{\boldsymbol{\eta}_{m_k}} S_{a\eta}(\boldsymbol{x}-\boldsymbol{\xi}) \tag{3.26}$$

and

$$v_a^{[2k+2]}(\boldsymbol{x}) = \frac{1}{8\pi\mu} \sum_{m=0}^{\infty} \frac{M_{\beta\boldsymbol{\beta}_m}(\boldsymbol{\xi})}{m!} \sum_{m_1=0}^{\infty} \frac{N_{\beta\boldsymbol{\beta}_m\gamma\boldsymbol{\gamma}_{m_1}}(\boldsymbol{\xi})}{m_1!} \cdots \sum_{m_k=0}^{\infty} \frac{N_{\delta\boldsymbol{\delta}_{m_{k-1}}\eta\boldsymbol{\eta}_{m_k}}(\boldsymbol{\xi})}{m_k!} \nabla_{\boldsymbol{\eta}_{m_k}} W_{a\eta}(\boldsymbol{x},\boldsymbol{\xi}), \tag{3.27}$$

so that

$$v_a^{[2k+1]}(\boldsymbol{x}) + v_a^{[2k+2]}(\boldsymbol{x}) = \frac{1}{8\pi\mu} \sum_{m=0}^{\infty} \frac{M_{\beta\boldsymbol{\beta}_m}(\boldsymbol{\xi})}{m!} \sum_{m_1=0}^{\infty} \frac{N_{\beta\boldsymbol{\beta}_m\gamma\boldsymbol{\gamma}_{m_1}}(\boldsymbol{\xi})}{m_1!} \cdots \sum_{m_k=0}^{\infty} \frac{N_{\delta\boldsymbol{\delta}_{m_{k-1}}\eta\boldsymbol{\eta}_{m_k}}(\boldsymbol{\xi})}{m_k!} \nabla_{\boldsymbol{\eta}_{m_k}} G_{a\eta}(\boldsymbol{x},\boldsymbol{\xi}). \tag{3.28}$$

Summing all the fields according to (3.1), the total velocity field can be expressed as

$$
\begin{aligned}
v_a(\boldsymbol{x}) - u_a(\boldsymbol{x}) &= \sum_{k=0}^{\infty} v_a^{[2k+1]}(\boldsymbol{x}) + v_a^{[2k+2]}(\boldsymbol{x}) \\
&= \frac{1}{8\pi\mu} \sum_{m=0}^{\infty} \frac{M_{\beta\boldsymbol{\beta}_m}(\boldsymbol{\xi})}{m!} \sum_{k=0}^{\infty} \sum_{m_1=0}^{\infty} \frac{N_{\beta\boldsymbol{\beta}_m\gamma\boldsymbol{\gamma}_{m_1}}(\boldsymbol{\xi})}{m_1!} \cdots \sum_{m_k=0}^{\infty} \frac{N_{\delta\boldsymbol{\delta}_{m_{k-1}}\eta\boldsymbol{\eta}_{m_k}}(\boldsymbol{\xi})}{m_k!} \nabla_{\boldsymbol{\eta}_{m_k}} G_{a\eta}(\boldsymbol{x}, \boldsymbol{\xi}).
\end{aligned}
\tag{3.29}
$$

3.6. *Extension to Linear and BC-reciprocal BCs on the body*

The extension to more general linear homogeneous reciprocal BCs is straightforward. To this purpose, the expansion (3.1) still applies, but the BCs (3.3) are substituted by the conditions

$$
\left.
\begin{aligned}
\mathcal{L}[v_a^{[2k+1]}(\boldsymbol{x})] &= -\mathcal{L}[v_a^{[2k]}(\boldsymbol{x})], \quad \boldsymbol{x} \in S_b, \\
v_a^{[2k+2]}(\boldsymbol{x}) &= -v_a^{[2k+1]}(\boldsymbol{x}), \quad \boldsymbol{x} \in S_w,
\end{aligned}
\right\}
\tag{3.30}
$$

for $k = 1, 2, \ldots$, keeping for $k = 0$

$$
v_a^{[0]}(\boldsymbol{x}) = u_a(\boldsymbol{x}), \quad \boldsymbol{x} \in V_b \cup V_f. \tag{3.31}
$$

In fact, by applying the operator $\mathcal{L}[\,]$ to the total field in (3.1) at the surface of the body, and using the linearity of $\mathcal{L}[\,]$, we have

$$
\left.
\begin{aligned}
&\mathcal{L}[v_a(\boldsymbol{x})] = \mathcal{L}[v_a^{[0]}(\boldsymbol{x}) + v_a^{[1]}(\boldsymbol{x}) + v_a^{[2]}(\boldsymbol{x}) + v_a^{[3]}(\boldsymbol{x}) + \cdots] = \\
&\mathcal{L}[v_a^{[0]}(\boldsymbol{x})] + \mathcal{L}[v_a^{[1]}(\boldsymbol{x})] + \mathcal{L}[v_a^{[2]}(\boldsymbol{x})] + \mathcal{L}[v_a^{[3]}(\boldsymbol{x})] + \cdots = 0, \quad \boldsymbol{x} \in S_b,
\end{aligned}
\right\}
\tag{3.32}
$$

where all the terms on the right-hand side cancel each other for (3.30). Therefore, the Stokes flow provided by (3.1), with BCs (3.30)–(3.31), is a solution of (2.3).

Since the procedure developed in the previous paragraph (3.5)–(3.29) is independent of the BCs at the surface of the body, with the only constraint of the BC reciprocity of $\mathcal{L}[\,]$, we can conclude that (3.29) is still valid considering the Faxén operators associated with the BCs assumed on the body surface.

4. Matrix representation of the velocity field

In this section, a compact and useful matrix representation of the equations obtained in the § 3 is developed. To this aim, collect the entries of the system of moments $M_{\beta\boldsymbol{\beta}_m}(\boldsymbol{\xi})$ in an infinite-dimensional vector (Cooke 1950)

$$
[M] = \begin{bmatrix} \boldsymbol{M}_{(0)} \\ \boldsymbol{M}_{(1)} \\ \dfrac{\boldsymbol{M}_{(2)}}{2} \\ \vdots \\ \dfrac{\boldsymbol{M}_{(m)}}{m!} \\ \vdots \end{bmatrix}, \tag{4.1}
$$

where $\boldsymbol{M}_{(m)}$ are 3^{m+1} dimensional vectors obtained by the vectorisation of the $(m+1)$th-order tensors $M_{\beta\boldsymbol{\beta}_m}(\boldsymbol{\xi})$ so that any entry $[M]_i$ corresponds to the entry $M_{\beta\boldsymbol{\beta}_m}(\boldsymbol{\xi})$

i	1	2	3	4	5	6	7	8	9	10	11	12	13	14	15	16	...
$(\beta\,\beta_1\,\beta_2\ldots\beta_m)$	(1)	(2)	(3)	(11)	(12)	(13)	(21)	(22)	(23)	(31)	(32)	(33)	(111)	(112)	(113)	(121)	...

Table 1. Conversion according to (4.2) between the index i of the entries of the vector $[M]_i$ and the multi-index $\beta\,\boldsymbol{\beta}_m$ of the entries of the $(m+1)$th-order tensors $M_{\beta\boldsymbol{\beta}_m}(\boldsymbol{\xi})$.

according the conversion $i \leftrightarrow \beta\boldsymbol{\beta}_m$

$$i = \sum_{h=0}^{m} \beta_h 3^{m-h}, \tag{4.2}$$

where $\beta_0 \equiv \beta$.

The conversion $i \leftrightarrow \beta\boldsymbol{\beta}_m$ for $m = 0, 1, 2$, according to (4.2), is presented in table 1.

We use the notation $[M_{(n:m)}]$ to indicate the part of the array (4.1) collecting the entries of the tensors with orders going from n to m $(m > n)$, i.e.

$$[M_{(n:m)}] = \begin{bmatrix} \dfrac{\boldsymbol{M}_{(n)}}{n!} \\ \vdots \\ \dfrac{\boldsymbol{M}_{(m)}}{m!} \end{bmatrix}. \tag{4.3}$$

In the same way, the entries of $\nabla_{\boldsymbol{\beta}_m} G_{\alpha\beta}(\boldsymbol{x}, \boldsymbol{\xi})$ can be collected in the $3^{m+1} \times 3$ matrices $\boldsymbol{G}_{(0)}, \boldsymbol{G}_{(1)}, \ldots, \boldsymbol{G}_{(m)}, \ldots$ (with column indices corresponding to the Latin field point indices) to build the $\infty \times 3$ matrix $[G]$ defined by

$$[G] = \begin{bmatrix} \boldsymbol{G}_{(0)} \\ \boldsymbol{G}_{(1)} \\ \vdots \\ \boldsymbol{G}_{(m)} \\ \vdots \end{bmatrix}. \tag{4.4}$$

Adopting this representation, (3.12) can be compactly expressed as

$$\boldsymbol{v}^{[1]}(\boldsymbol{x}) + \boldsymbol{v}^{[2]}(\boldsymbol{x}) = \frac{[M]^t[G]}{8\pi\mu}, \tag{4.5}$$

with $[M]^t$ being the transpose of $[M]$.

It is also possible to define the infinite matrix $[N]$ as

$$[N] = \begin{bmatrix} \boldsymbol{N}_{(0,0)} & \boldsymbol{N}_{(0,1)} & \cdots & \dfrac{\boldsymbol{N}_{(0,n)}}{n!} & \cdots \\ \boldsymbol{N}_{(1,0)} & \ddots & & \vdots & \\ \vdots & & \ddots & \vdots & \\ \boldsymbol{N}_{(m,0)} & \cdots & \cdots & \dfrac{\boldsymbol{N}_{(m,n)}}{n!} & \cdots \\ \vdots & & & \vdots & \ddots \end{bmatrix}, \tag{4.6}$$

where $\boldsymbol{N}_{(m,n)}$ are $3^{m+1} \times 3^{n+1}$ matrices obtained unfolding the $(m+n+2)$th-order tensors $N_{\beta\boldsymbol{\beta}_m\gamma\boldsymbol{\gamma}_n}(\boldsymbol{\xi})$ so that the entries $[N]_{i,j}$ are obtained by converting both $i \leftrightarrow \beta\,\boldsymbol{\beta}_m$ and $j \leftrightarrow \gamma\,\boldsymbol{\gamma}_m$ according to (4.2).

Using this representation, (3.20) becomes

$$\boldsymbol{v}^{[3]}(\boldsymbol{x}) + \boldsymbol{v}^{[4]}(\boldsymbol{x}) = \frac{[M]^t[N][G]}{8\pi\mu}, \tag{4.7}$$

whereas (3.25) takes the form

$$\boldsymbol{v}^{[5]}(\boldsymbol{x}) + \boldsymbol{v}^{[6]}(\boldsymbol{x}) = \frac{[M]^t[N]^2[G]}{8\pi\mu}, \tag{4.8}$$

where $[N]^2 = [N][N]$. Defining the power of $[N]$ by induction as $[N]^3 = [N]^2[N]$, $[N]^k = [N]^{k-1}[N]$ and $[N]^0 = [I]$, $[I]$ being the infinite identity matrix, the total velocity field expressed by (3.29) can be compactly represented as

$$\boldsymbol{v}(\boldsymbol{x}) - \boldsymbol{u}(\boldsymbol{x}) = \frac{1}{8\pi\mu}\sum_{k=0}^{\infty}[M]^t[N]^k[G]. \tag{4.9}$$

Let us consider the sum entering (4.9) truncated up to $k = K$ and multiply it by $([I] - [N])$. It is straightforward to show that

$$([I] - [N])\sum_{k=0}^{K}[N]^k = [I] - [N]^K \tag{4.10}$$

as for the truncated geometric series defined over a scalar field. As shown in Appendix A, the series in (4.10) converges for characteristic distances ℓ_d of the body from the nearest walls larger enough than the characteristic length ℓ_b of the body itself, since there exists a constant $\Gamma = O(1) > 0$, depending on the geometry of the system, such that

$$\lim_{K\to\infty}[N]^K = 0, \quad \text{for } \ell_d > \Gamma\ell_b. \tag{4.11}$$

As a consequence

$$([I] - [N])\sum_{k=0}^{\infty}[N]^k = [I], \quad \ell_d > \Gamma\ell_b \tag{4.12}$$

and, thus,

$$\sum_{k=0}^{\infty}[N]^k = ([I] - [N])^{-1}, \quad \ell_d > \Gamma\ell_b, \tag{4.13}$$

with $([I] - [N])^{-1}$ being the inverse matrix of $([I] - [N])$ (Cooke 1950).

Therefore, the velocity field attains the simple expression

$$\boldsymbol{v}(\boldsymbol{x}) - \boldsymbol{u}(\boldsymbol{x}) = \frac{[M]^t([I] - [N])^{-1}[G]}{8\pi\mu}, \quad \ell_d > \Gamma\,\ell_b \tag{4.14}$$

or, alternatively,

$$\boldsymbol{v}(\boldsymbol{x}) - \boldsymbol{u}(\boldsymbol{x}) = \frac{[M]^t[X]}{8\pi\mu}, \quad \ell_d > \Gamma\ell_b, \tag{4.15}$$

where $[X]$ is the solution of the infinite-matrix equation

$$([I] - [N])[X] = [G]. \tag{4.16}$$

In the remainder, we consider exclusively the situation $\ell_d > \Gamma\ell_b$, for which (4.14) holds. By (4.14) it is possible to conclude that, for $\ell_d > \Gamma\ell_b$, the solution of a the Stokes flow past a body immersed in a confined fluid can be expressed in terms of the vector $[M]$, depending only on the hydrodynamic interaction of the body with unbounded (external) Stokes flows, the matrix $[G]$, depending only on the hydrodynamic interaction of the confinement with unbounded (internal) Stokes flows and the matrix $[N]$ ($[N]$-matrix, for short), representing the hydrodynamic interaction between the body and the confinement.

5. Force and torque on the particle

By linearity, the force and the torque acting on the particle due to the hydrodynamic interactions with the fluid, are given by the summation of all the forces and torques associated with the terms in (3.1), i.e.

$$\left.\begin{aligned} \boldsymbol{F} &= \boldsymbol{F}^{[0]} + \boldsymbol{F}^{[1]} + \boldsymbol{F}^{[2]} + \cdots, \\ \boldsymbol{T} &= \boldsymbol{T}^{[0]} + \boldsymbol{T}^{[1]} + \boldsymbol{T}^{[2]} + \cdots, \end{aligned}\right\} \tag{5.1}$$

where

$$\left.\begin{aligned} \boldsymbol{F}^{[k]} &= -\int_{S_p} \boldsymbol{\sigma}^{[k]}(\boldsymbol{x}) \boldsymbol{\cdot} \boldsymbol{n}\, \mathrm{d}S, \quad k = 0, 1, 2, \ldots, \\ \boldsymbol{T}^{[k]} &= -\int_{S_p} (\boldsymbol{x} - \boldsymbol{\xi}) \times \boldsymbol{\sigma}^{[k]}(\boldsymbol{x}) \boldsymbol{\cdot} \boldsymbol{n}\, \mathrm{d}S, \quad k = 0, 1, 2, \ldots. \end{aligned}\right\} \tag{5.2}$$

Since $\boldsymbol{\nabla} \boldsymbol{\cdot} \boldsymbol{\sigma}^{[k]}(\boldsymbol{x}) = 0$, and due to the symmetry of the stress tensors $\boldsymbol{\sigma}^{[k]}(\boldsymbol{x})$, the forces and torques associated to even values of k (i.e. the forces due to regular fields on the boundary of the particle) vanish for the Gauss–Green theorem (Brenner 1962). The only terms contributing to the total force and torque are the terms corresponding to odd value of $k = 1, 3, 5, \ldots$

$$\left.\begin{aligned} \boldsymbol{F} &= \boldsymbol{F}^{[1]} + \boldsymbol{F}^{[3]} + \boldsymbol{F}^{[5]} + \cdots, \\ \boldsymbol{T} &= \boldsymbol{T}^{[1]} + \boldsymbol{T}^{[3]} + \boldsymbol{T}^{[5]} + \cdots. \end{aligned}\right\} \tag{5.3}$$

The first contribution $\boldsymbol{F}^{[1]}$ in the sum (5.3) is the force experienced by the body immersed in the unbounded ambient flow $\boldsymbol{u}(\boldsymbol{x})$, therefore it can be obtained by applying the zeroth-order Faxén operator according (2.21)

$$F_\beta^{[1]} = F_\beta^{[\infty]} = -M_\beta(\boldsymbol{\xi}) = -8\pi\mu \mathcal{F}_{\gamma\beta} u_\gamma(\boldsymbol{\xi}), \tag{5.4}$$

where we used the notation $F_\beta^{[\infty]}$ to remark that the force $F_\beta^{[1]}$ is exactly that experienced by the body if the fluid were unbounded.

The other contribution $\boldsymbol{F}^{[3]} + \boldsymbol{F}^{[5]} + \cdots$ in (5.3) is the force experienced by the body immersed in the ambient flow $\boldsymbol{v}^{[2]}(\boldsymbol{x}) + \boldsymbol{v}^{[4]}(\boldsymbol{x}) + \cdots$. Therefore,

$$F_\beta^{[3]} + F_\beta^{[5]} + \cdots = -8\pi\mu \mathcal{F}_{\gamma\beta}(v_\gamma^{[2]}(\boldsymbol{\xi}) + v_\gamma^{[4]}(\boldsymbol{\xi}) + \cdots). \tag{5.5}$$

Indicating with $[S]$ the $\infty \times 3$-dimensional matrix collecting all the derivatives of the Stokeslet $\nabla_{\boldsymbol{\beta}_m} S_{\alpha\beta}(\boldsymbol{x} - \boldsymbol{\xi})$ (analogously to the definition (4.4) for $[G]$) and with $[W]$ the $\infty \times 3$-dimensional matrix collecting all the derivatives of the regular part of the Green function $\nabla_{\boldsymbol{\beta}_m} W_{\alpha\beta}(\boldsymbol{x}, \boldsymbol{\xi})$, according to (2.8) and (2.9), the matrix $[G]$ can be decomposed

https://doi.org/10.1017/jfm.2024.651 Published online by Cambridge University Press

as

$$[G] = [S] + [W] \tag{5.6}$$

and the sum of the fields $v_\gamma^{[2]}(\boldsymbol{\xi}) + v_\gamma^{[4]}(\boldsymbol{\xi}) + \cdots$ with even values of k, (4.9), takes the form

$$\sum_{k=0}^{\infty} \boldsymbol{v}^{[2k+2]}(\boldsymbol{x}) = \frac{[M]^t([I] - [N])^{-1}[W]}{8\pi\mu}, \tag{5.7}$$

whereas the sum of all the fields corresponding to odd values of k, associated with the disturbance field due to the body, is given by

$$\sum_{k=0}^{\infty} \boldsymbol{v}^{[2k+1]}(\boldsymbol{x}) = \frac{[M]^t([I] - [N])^{-1}[S]}{8\pi\mu}. \tag{5.8}$$

Substituting (5.4), (5.5) and (5.7) into (5.3), a compact representation of the force is achieved

$$\boldsymbol{F} = \boldsymbol{F}^{[\infty]} - [M]^t([I] - [N])^{-1}[N_{(:,0)}], \tag{5.9}$$

where the matrix

$$[N_{(:,0)}] = \begin{bmatrix} \boldsymbol{N}_{(0,0)} \\ \boldsymbol{N}_{(1,0)} \\ \vdots \\ \boldsymbol{N}_{(m,0)} \\ \vdots \end{bmatrix} \tag{5.10}$$

collecting the entries $N_{\alpha\boldsymbol{\alpha}_m\beta\boldsymbol{\beta}_n}(\boldsymbol{\xi})$ for $n = 0$, is exactly the $\infty \times 3$ matrix corresponding to the first three columns of the matrix $[N]$.

The same procedure can be applied to obtain an analogous relation for the torque acting on the body. By (2.22), the torque $\boldsymbol{T}^{[1]} = \boldsymbol{T}^{[\infty]}$ is provided by the operator $\mathcal{T}_{\gamma\beta} = \varepsilon_{\beta\delta\delta_1}\mathcal{F}_{\gamma\delta\delta_1}$ applied at the ambient flow $\boldsymbol{u}(\boldsymbol{x})$, i.e.

$$T_\beta^{[1]} = T_\beta^{[\infty]} = \varepsilon_{\beta\delta\delta_1} M_{\delta\delta_1}(\boldsymbol{\xi}) = 8\pi\mu \mathcal{T}_{\gamma\beta} u_\gamma(\boldsymbol{\xi}) \tag{5.11}$$

and the remaining term in (5.3) is equal to

$$T_\beta^{[3]} + T_\beta^{[5]} + \cdots = 8\pi\mu\mathcal{T}_{\gamma\beta}(v_\gamma^{[2]}(\boldsymbol{\xi}) + v_\gamma^{[4]}(\boldsymbol{\xi}) + \cdots). \tag{5.12}$$

Therefore, the total torque is compactly expressed by the equation by

$$\boldsymbol{T} = \boldsymbol{T}^{[\infty]} + [M]^t([I] - [N])^{-1}[L] \tag{5.13}$$

with

$$[L] = \begin{bmatrix} \boldsymbol{L}_{(0)} \\ \boldsymbol{L}_{(1)} \\ \vdots \\ \boldsymbol{L}_{(m)} \\ \vdots \end{bmatrix}, \tag{5.14}$$

where $\boldsymbol{L}_{(m)}$ are the $3^{(m+1)} \times 3$-dimensional matrices with entries $\varepsilon_{\beta\delta\delta_1} N_{\gamma\boldsymbol{\gamma}_m\delta\delta_1}(\boldsymbol{\xi})$, thus

$$[L] = [N_{(:,1)}]\,\boldsymbol{\varepsilon}^t, \tag{5.15}$$

where

$$\boldsymbol{\varepsilon} = \begin{pmatrix} 0 & 0 & 0 & 0 & 0 & 1 & 0 & -1 & 0 \\ 0 & 0 & -1 & 0 & 0 & 0 & 1 & 0 & 0 \\ 0 & 1 & 0 & -1 & 0 & 0 & 0 & 0 & 0 \end{pmatrix} \tag{5.16}$$

corresponds to the vectorisation of the Ricci–Levi Civita tensor $\varepsilon_{\beta\delta\delta_1}$ with respect to indices $\delta\delta_1$.

This result can be generalised to the moments: the nth-order moment $\bar{\boldsymbol{M}}_{(n)}(\boldsymbol{\xi})$ on the particle in a confined fluid is given by

$$\bar{\boldsymbol{M}}^t_{(n)}(\boldsymbol{\xi}) = \boldsymbol{M}^t_{(n)}(\boldsymbol{\xi}) + [M]^t([I] - [N])^{-1}[N_{(:,n)}], \tag{5.17}$$

where

$$[N_{(:,n)}] = \begin{bmatrix} \boldsymbol{N}_{(0,n)} \\ \boldsymbol{N}_{(1,n)} \\ \vdots \\ \boldsymbol{N}_{(m,n)} \\ \vdots \end{bmatrix}. \tag{5.18}$$

6. Error estimate in truncation

The exact results obtained for velocity field, force and torque in (4.14), (5.9) and (5.13) are expressed in terms of infinite matrices. In practical application, it is not possible to take into account all the entries of these matrices. In fact, in the overwhelming majority of cases, only lower order analytical expressions for Faxén operators and multipoles singularities are available and, moreover, there are no recursive relations able to predict higher-order terms even for the simplest geometries. Furthermore, whenever complex geometries are considered, for which no analytical solutions are available, numerical approaches represent the only feasible alternative in order to evaluate moments and multipoles, and approximations or series truncations become necessary.

Therefore, a central issue in the practical applications of reflection methods is the determination of the order of magnitude of the error committed in the approximations/truncations as function of the geometric dimensionless ratio ℓ_b/ℓ_d. Specifically, consider the error deriving by considering only the first moments and multipoles up to the Kth order in the exact expressions (4.14), (5.9) and (5.13), hence by substituting to $[M]$ its truncated counterpart $[M_{(0:K)}]$ (where, according the notation introduced in (4.3), $[M_{(0:K)}]$ is the vector collecting all the unbounded moments from the zeroth to the Kth order) and similarly for the other infinite matrices, $[N] \rightarrow [N_{(0:K,0:K)}]$, $[G] \rightarrow [G_{(0:K)}]$,

$$\left| \boldsymbol{v}(\boldsymbol{x}) - \boldsymbol{u}(\boldsymbol{x}) - \frac{[M_{(0:K)}]^t([I_{(0:K,0:K)}] - [N_{(0:K,0:K)}])^{-1}[G_{(0:K)}]}{8\pi\mu} \right|. \tag{6.1}$$

To this aim, consider the (4.5) rewritten in the form

$$v_a^{[1]}(\boldsymbol{x}) + v_a^{[2]}(\boldsymbol{x}) = \frac{[M_{(0:K)}]^t[G_{(0:K)}]}{8\pi\mu} + \frac{1}{8\pi\mu} \sum_{m=K+1}^{\infty} \frac{\left(\boldsymbol{M}_{(m)}\right)^t \boldsymbol{G}_{(m)}}{m!}. \tag{6.2}$$

Enforcing the dimensional analysis developed in Appendix A, specifically (A5) and (A7) providing

$$M_{\beta\boldsymbol{\beta}_{K+1}}(\boldsymbol{\xi}) = \mu U_c O\left(\ell_b^{K+2}\right); \quad \nabla_{\boldsymbol{\beta}_{K+1}} G_{a\beta}(\boldsymbol{x}, \boldsymbol{\xi}) = O\left(1/\ell_f^{K+2}\right), \tag{6.3}$$

the leading-order term in the series on the right-hand side of (6.2) is

$$|\boldsymbol{M}^t_{(K+1)}\boldsymbol{G}_{(K+1)}| = \mu U_c O\left(\frac{\ell_b}{\ell_f}\right)^{K+2}, \tag{6.4}$$

with U_c being the characteristic magnitude of the ambient velocity field. Therefore, truncating the series up to the Kth order, the order of magnitude of the remainder follows

$$v_a^{[1]}(\boldsymbol{x}) + v_a^{[2]}(\boldsymbol{x}) = \frac{[M_{(0:K)}]^t[G_{(0:K)}]}{8\pi\mu} + U_c O\left(\frac{\ell_b}{\ell_f}\right)^{K+2}. \tag{6.5}$$

The velocity fields due to the next reflections, hence for $k = 1$, can be written as

$$\begin{aligned} v_a^{[3]}(\boldsymbol{x}) + v_a^{[4]}(\boldsymbol{x}) &= \frac{[M_{(0:K)}]^t[N_{(0:K,0:K)}][G_{(0:K)}]}{8\pi\mu} \\ &\quad + \frac{1}{8\pi\mu}\sum_{m=K+1}^{\infty}\sum_{n=K+1}^{\infty}\frac{\left(\boldsymbol{M}_{(m)}\right)^t\boldsymbol{N}_{(m,n)}\,\boldsymbol{G}_{(n)}}{m!}, \end{aligned} \tag{6.6}$$

where the leading-order term in the series, estimated via (A5), (A7) and (A12), is

$$|\boldsymbol{M}^t_{(K+1)}\boldsymbol{N}_{(K+1,K+1)}\boldsymbol{G}_{(K+1)}| = \mu U_c O\left(\frac{\ell_b}{\ell_f}\frac{\ell_b}{2\ell_d}\right)^{K+2}. \tag{6.7}$$

Since $\ell_b/(2\ell_d) < 1$, the term in (6.7) is always smaller than the term in (6.4), thus

$$|\boldsymbol{M}^t_{(K+1)}\boldsymbol{N}_{(K+1,K+1)}\boldsymbol{G}_{(K+1)}| = \mu U_c O\left(\frac{\ell_b}{\ell_f}\right)^{K+2} \tag{6.8}$$

and (6.6) can be rewritten as

$$v_a^{[3]}(\boldsymbol{x}) + v_a^{[4]}(\boldsymbol{x}) = \frac{[M_{(0:K)}]^t[N_{(0:K,0:K)}][G_{(0:K)}]}{8\pi\mu} + U_c\, O\left(\frac{\ell_b}{\ell_f}\right)^{K+2}. \tag{6.9}$$

Reiterating the same procedure for the higher-order reflected velocity fields, hence for $k > 1$, we obtain

$$v_a^{[2k+1]}(\boldsymbol{x}) + v_a^{[2k+2]}(\boldsymbol{x}) = \frac{[M_{(0:K)}]^t[N_{(0:K,0:K)}]^k[G_{(0:K)}]}{8\pi\mu} + U_c\, O\left(\frac{\ell_b}{\ell_f}\right)^{K+2}, \quad k = 1, 2, \ldots. \tag{6.10}$$

Therefore, the truncation error committed considering only up to Kth-order terms in the infinity matrix expressions entering (4.14) satisfies the scaling relations

$$\boldsymbol{v}(\boldsymbol{x}) - \boldsymbol{u}(\boldsymbol{x}) = \frac{[M_{(0:K)}]^t([I_{(0:K,0:K)}] - [N_{(0:K,0:K)}])^{-1}[G_{(0:K)}]}{8\pi\mu} + U_c O\left(\frac{\ell_b}{\ell_f}\right)^{K+2}. \tag{6.11}$$

A similar analysis can be extended to forces and torques, obtaining

$$\boldsymbol{F} - \boldsymbol{F}^{[\infty]} = -[M_{(0:K)}]^t([I_{(0:K,0:K)}] - [N_{(0:K,0:K)}])^{-1}[N_{(0:K,0)}] + F_c O\left(\frac{\ell_b}{\ell_d}\right)^{K+2} \tag{6.12}$$

and

$$\boldsymbol{T} - \boldsymbol{T}^{[\infty]} = [M_{(0:K)}]^t([I_{(0:K,0:K)}] - [N_{(0:K,0:K)}])^{-1}[L_{(0:K)}] + T_c O\left(\frac{\ell_b}{\ell_d}\right)^{K+2}, \tag{6.13}$$

where $F_c = \mu\ell_b U_c$ and $T_c = \mu\ell_b^2 U_c$.

The scaling analysis of the truncation error addressed previously can be applied to the approximations of the hydromechanical properties addressed in the literature. In the following, we analyse and discuss, from the point of view of the present theory, the classical literature results of hydromechanics of bodies in confined Stokes flow, extending such expressions to more general BCs, geometries and motions of the bodies.

6.1. *The approximation for $K = 0$ and Brenner's formula*

An explicit approximation for the force acting on an arbitrary body translating in a confined fluid has been first derived by Brenner (1964*a*) in terms of the resistance matrix of the body in the unbounded fluid and the regular part of the Green function at the position of the body. Within the present formalism, the Brenner (1964*a*) formula for the force is

$$\boldsymbol{F} = \boldsymbol{F}^{[\infty]} \left(I + \frac{\boldsymbol{W}_{(0)} \boldsymbol{R}}{8\pi\mu} \right)^{-1} + F_c O \left(\frac{\ell_b}{\ell_d} \right)^2, \tag{6.14}$$

where $R_{\beta\gamma} = -8\pi\mu m_{\beta\gamma}$ is the resistance matrix of the body in the unbounded fluid.

For $K = 0$ in (6.11)–(6.13), substituting $\boldsymbol{M}^t_{(0)} = -\boldsymbol{F}^{[\infty]}$, we have the zeroth-order approximation of the velocity field

$$\boldsymbol{v}(\boldsymbol{x}) - \boldsymbol{u}(\boldsymbol{x}) = -\frac{\boldsymbol{F}^{[\infty]}(I - \boldsymbol{N}_{(0,0)})^{-1} \boldsymbol{G}_{(0)}}{8\pi\mu} + U_c O \left(\frac{\ell_b}{\ell_f} \right)^2, \tag{6.15}$$

the force

$$\boldsymbol{F} - \boldsymbol{F}^{[\infty]} = \boldsymbol{F}^{[\infty]}(I - \boldsymbol{N}_{(0,0)})^{-1} \boldsymbol{N}_{(0,0)} + F_c O \left(\frac{\ell_b}{\ell_d} \right)^2 \tag{6.16}$$

and the torque

$$\boldsymbol{T} - \boldsymbol{T}^{[\infty]} = -\boldsymbol{F}^{[\infty]}(I - \boldsymbol{N}_{(0,0)})^{-1} \boldsymbol{L}_{(0)} + T_c O \left(\frac{\ell_b}{\ell_d} \right)^2, \tag{6.17}$$

with I being the 3×3 identity matrix.

By the dimensional analysis developed in Appendix B.1, the velocity field (6.15) becomes

$$\boldsymbol{v}(\boldsymbol{x}) = \boldsymbol{u}(\boldsymbol{x}) - \boldsymbol{F}^{[\infty]} \left(I + \frac{\boldsymbol{W}_{(0)} \boldsymbol{R}}{8\pi\mu} \right)^{-1} \frac{\boldsymbol{G}_{(0)}}{8\pi\mu} + U_c O \left(\frac{\ell_b}{\ell_f} \right)^2, \tag{6.18}$$

the force (6.16) returns, as expected, the Brenner's formula

$$\boldsymbol{F} = \boldsymbol{F}^{[\infty]} \left(I + \frac{\boldsymbol{W}_{(0)} \boldsymbol{R}}{8\pi\mu} \right)^{-1} + F_c O \left(\frac{\ell_b}{\ell_d} \right)^2 \tag{6.19}$$

and the torque (6.17) is

$$\boldsymbol{T} = \boldsymbol{T}^{[\infty]} - \boldsymbol{F}^{[\infty]} \left(I + \frac{\boldsymbol{W}_{(0)} \boldsymbol{R}}{8\pi\mu} \right)^{-1} \frac{\boldsymbol{W}_{(0)} \boldsymbol{C}}{8\pi\mu} + T_c O \left(\frac{\ell_b}{\ell_d} \right)^2, \tag{6.20}$$

where $C_{\beta\gamma} = 8\pi\mu\varepsilon_{\beta\delta\delta_1} m_{\gamma\delta\delta_1}(\boldsymbol{\xi}, \boldsymbol{\xi})$ is the coupling matrix between forces and rotations of the body in the unbounded fluid (Happel & Brenner 1983; Procopio & Giona 2024).

Equations (6.18), (6.19) and (6.20), requiring solely the Green function of the confinement and the grand-resistance matrix of the body, provide the first-order terms associated with any flow past a body immersed in a confined fluid. In the case the body translates with velocity $\boldsymbol{U}$ in a quiescent fluid, we can consider the disturbance flow associated with an ambient flow past the still body $\boldsymbol{u}(\boldsymbol{x}) = -\boldsymbol{U}$. Therefore, from (6.18) and considering $\boldsymbol{F}^{[\infty]} = -\boldsymbol{U}\boldsymbol{R}$, the velocity field around the translating body is

$$\boldsymbol{w}(\boldsymbol{x}) = \boldsymbol{U}\boldsymbol{R}\left(\boldsymbol{I} + \frac{\boldsymbol{W}_{(0)}\boldsymbol{R}}{8\pi\mu}\right)^{-1}\frac{\boldsymbol{G}_{(0)}}{8\pi\mu} + U_c O\left(\frac{\ell_b}{\ell_f}\right)^2. \tag{6.21}$$

By (6.19), the force is

$$\boldsymbol{F} = -\boldsymbol{U}\boldsymbol{R}\left(\boldsymbol{I} + \frac{\boldsymbol{W}_{(0)}\boldsymbol{R}}{8\pi\mu}\right)^{-1} + F_c O\left(\frac{\ell_b}{\ell_d}\right)^2, \tag{6.22}$$

whereas, by considering that $\boldsymbol{T}^{[\infty]} = -\boldsymbol{U}\boldsymbol{C}$, from (6.20) the torque is

$$\boldsymbol{T} = -\boldsymbol{U}\left(\boldsymbol{C} - \boldsymbol{R}\left(\boldsymbol{I} + \frac{\boldsymbol{W}_{(0)}\boldsymbol{R}}{8\pi\mu}\right)^{-1}\frac{\boldsymbol{W}_{(0)}\boldsymbol{C}}{8\pi\mu}\right) + T_c O\left(\frac{\ell_b}{\ell_d}\right)^2. \tag{6.23}$$

If the particle rotates (without translating) with angular velocity $\boldsymbol{\omega}$, the force on the particle in the unbounded fluid is given by $\boldsymbol{F}^{[\infty]} = -\boldsymbol{\omega}\boldsymbol{C}^t$ (Happel & Brenner 1983) and, therefore, following the same procedure as previously, the velocity field is

$$\boldsymbol{w}(\boldsymbol{x}) = \boldsymbol{\omega}\boldsymbol{C}^t\left(\boldsymbol{I} + \frac{\boldsymbol{W}_{(0)}\boldsymbol{R}}{8\pi\mu}\right)^{-1}\frac{\boldsymbol{G}_{(0)}}{8\pi\mu} + U_c O\left(\frac{\ell_b}{\ell_f}\right)^2, \tag{6.24}$$

the force on the body takes the expression

$$\boldsymbol{F} = -\boldsymbol{\omega}\,\boldsymbol{C}^t\left(\boldsymbol{I} + \frac{\boldsymbol{W}_{(0)}\boldsymbol{R}}{8\pi\mu}\right)^{-1} + F_c O\left(\frac{\ell_b}{\ell_d}\right)^2 \tag{6.25}$$

and the torque, considering $\boldsymbol{T}^{[\infty]} = -\boldsymbol{\omega}\boldsymbol{\Omega}$, can be written as

$$\boldsymbol{T} = -\boldsymbol{\omega}\left[\boldsymbol{\Omega} - \boldsymbol{C}^t\left(\boldsymbol{I} + \frac{\boldsymbol{W}_{(0)}\boldsymbol{R}}{8\pi\mu}\right)^{-1}\frac{\boldsymbol{W}_{(0)}\boldsymbol{C}}{8\pi\mu}\right] + T_c O\left(\frac{\ell_b}{\ell_d}\right)^2, \tag{6.26}$$

where $\boldsymbol{\Omega}$, having entries $\Omega_{\alpha\beta} = -8\pi\mu\varepsilon_{\alpha\gamma\gamma_1}\varepsilon_{\beta\delta\delta_1}m_{\gamma\gamma_1\delta\delta_1}(\boldsymbol{\xi},\boldsymbol{\xi})$, is the angular resistance matrix.

6.2. *Extended Swan and Brady's approximation for rigid motion*

In obtaining the approximate expressions (6.19) and (6.20), valid to the order (ℓ_b/ℓ_d), we have neglected the higher-order terms in the zeroth-order Faxén operator for the force and in the first-order Faxén operator for the torque (see the derivation in Appendix B.1). Supposing that these Faxén operators are exactly known, it is possible to obtain more accurate expressions for the force and the torque on a rigid moving body. This has been found by Swan & Brady (2007, 2010) in the case of confined spherical bodies with no-slip BCs. Specifically, expressing their result in the mobility representation, Swan and Brady provided the velocity $\boldsymbol{U}$ and angular velocity $\boldsymbol{\omega}$ of a sphere under the action of a force $\boldsymbol{F}$ and a torque $\boldsymbol{T}$

$$\boldsymbol{U} = -\boldsymbol{F}\boldsymbol{R}^{-1}(\boldsymbol{I} - \boldsymbol{R}^{-1}\boldsymbol{\Phi}) + \boldsymbol{T}\boldsymbol{\Omega}^{-1}\boldsymbol{\Psi}^{t}\boldsymbol{R}^{-1} \tag{6.27}$$

and

$$\boldsymbol{\omega} = \boldsymbol{F}\boldsymbol{R}^{-1}\boldsymbol{\Psi}\boldsymbol{\Omega}^{-1} - \boldsymbol{T}\boldsymbol{\Omega}^{-1}(\boldsymbol{I} - \boldsymbol{\Omega}^{-1}\boldsymbol{\Theta}), \tag{6.28}$$

where

$$\Phi_{\alpha\beta} = -8\pi\mu\mathcal{F}_{\gamma\beta}\mathcal{F}_{\gamma'\alpha}W_{\gamma\gamma'}(\boldsymbol{\xi},\boldsymbol{\xi}')\big|_{\boldsymbol{\xi}'=\boldsymbol{\xi}}, \tag{6.29}$$

$$\Psi_{\alpha\beta} = 8\pi\mu\mathcal{T}_{\gamma\beta}\mathcal{F}_{\gamma'\alpha}W_{\gamma\gamma'}(\boldsymbol{\xi},\boldsymbol{\xi}')\big|_{\boldsymbol{\xi}'=\boldsymbol{\xi}} \tag{6.30}$$

and

$$\Theta_{\beta\alpha} = -8\pi\,\mu\mathcal{T}_{\gamma\beta}\mathcal{T}_{\alpha'\delta}W_{\gamma\alpha'}(\boldsymbol{\xi},\boldsymbol{\xi}')\big|_{\boldsymbol{\xi}'=\boldsymbol{\xi}}, \tag{6.31}$$

with the Faxén operators being those of a sphere with no-slip BCs.

By using the theory developed previously, it is possible to extend the Swan and Brady expressions to bodies with generic shape and generic reciprocal BCs. Furthermore, it is possible to evaluate the error committed by adopting the Swan and Brady approach to estimate the hydrodynamic interaction. In Appendix B.2, we obtain that the force and torque acting on a body rigid moving with velocity $\boldsymbol{U}$ and angular velocity $\boldsymbol{\omega}$ can be expressed as

$$\boldsymbol{F} = -\boldsymbol{U}\left(\boldsymbol{R} + \left(\boldsymbol{I} - \boldsymbol{\Phi}\,\boldsymbol{R}^{-1}\right)^{-1}\boldsymbol{\Phi}\right) - \boldsymbol{\omega}\left(\boldsymbol{C}^{t} + \boldsymbol{\Psi}^{t}\left(\boldsymbol{I} - \boldsymbol{\Phi}\boldsymbol{R}^{-1}\right)^{-1}\right) + O\left(\frac{\ell_b}{\ell_d}\right)^3 \tag{6.32}$$

and

$$\boldsymbol{T} = -\boldsymbol{U}\left(\boldsymbol{C} + \left(\boldsymbol{I} - \boldsymbol{\Phi}\boldsymbol{R}^{-1}\right)^{-1}\boldsymbol{\Psi}\right) - \boldsymbol{\omega}\left(\boldsymbol{\Omega} + \boldsymbol{\Theta} + \boldsymbol{\Psi}^{t}\boldsymbol{R}^{-1}\left(1 - \boldsymbol{\Phi}\boldsymbol{R}^{-1}\right)^{-1}\boldsymbol{\Psi}\right) + O\left(\frac{\ell_b}{\ell_d}\right)^3, \tag{6.33}$$

where the Faxén operators entering $\boldsymbol{\Phi}$, $\boldsymbol{\Psi}$, $\boldsymbol{\Theta}$, defined in (6.29)–(6.31), are those of a body with generic shape and reciprocal BCs.

In the case of a spherical body, for which $\boldsymbol{C} = \boldsymbol{0}$, (6.32) and (6.33) become

$$\boldsymbol{F} = -\boldsymbol{U}\left(\boldsymbol{R} + \left(\boldsymbol{I} - \boldsymbol{\Phi}\,\boldsymbol{R}^{-1}\right)^{-1}\boldsymbol{\Phi}\right) - \boldsymbol{\omega}\boldsymbol{\Psi}^{t}\left(\boldsymbol{I} - \boldsymbol{\Phi}\boldsymbol{R}^{-1}\right)^{-1} + O\left(\frac{\ell_b}{\ell_d}\right)^4 \tag{6.34}$$

and

$$\boldsymbol{T} = -\boldsymbol{U}\left(\boldsymbol{I} - \boldsymbol{\Phi}\boldsymbol{R}^{-1}\right)^{-1}\boldsymbol{\Psi} - \boldsymbol{\omega}\left(\boldsymbol{\Omega} + \boldsymbol{\Theta} + \boldsymbol{\Psi}^{t}\boldsymbol{R}^{-1}\left(1 - \boldsymbol{\Phi}\boldsymbol{R}^{-1}\right)^{-1}\boldsymbol{\Psi}\right) + O\left(\frac{\ell_b}{\ell_d}\right)^5. \tag{6.35}$$

From these equations it is possible to obtain the Swan and Brady 'mobility' representation (6.27) and (6.28) by inverting the block grand-resistance matrix (Bhatia 1997) and considering that, for a spherical particle, $\boldsymbol{\Phi} = O(\ell_b/\ell_d)$, $\boldsymbol{\Psi} = O(\ell_b/\ell_d)^2$ and $\boldsymbol{\Theta} = O(\ell_b/\ell_d)^3$. As shown in Brenner (1964*b*), there exists a vast class of bodies for which, choosing the centre of hydrodynamic reaction as centre of rotation, the coupling between translation and rotation vanishes, then $\boldsymbol{C} = \boldsymbol{0}$. Providing that the geometrical moments entering the Faxén operators are evaluated with respect to the centre of hydrodynamic

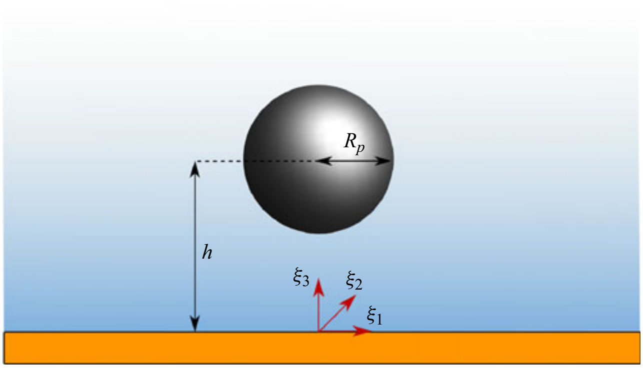

Figure 3. Schematic representation of a sphere near a plane wall.

rotation, for all these bodies it is possible to employ (6.34) and (6.35) obtaining, hence, an improved error in the truncation.

Equations (6.32)–(6.33) and (6.34)–(6.35) are fundamental scaling relations permitting to obtain good approximations for the resistance on bodies (especially if possess special symmetries) in confined systems by the knowledge of solely the zeroth- and first-order (for torque) Faxén operators. However, although such corrections improve the approximations in evaluating force and torques on body in confined fluids, the scaling analysis indicates that the approximate relation (6.34) (and, hence, the Swan and Brady expressions) cannot provide correctly the term $O(\ell_b/\ell_d)^4$ for the force. In the Faxén's expressions for a sphere translating near a plane wall and for a sphere translating between two parallel plane walls (see Happel & Brenner 1983, p. 327), a non-vanishing term $O(\ell_b/\ell_d)^4$ has been found, whereas in Swan & Brady (2007, 2010) the term $O(\ell_b/\ell_d)^4$ is considered vanishing, but the terms $O(\ell_b/\ell_d)^5$ (which fortuitously agrees with that obtained by Faxén performing high-order reflections) has been obtained. In the next section, we apply the exact expression (6.12) for the force on a sphere translating near a plane wall truncated to the order $O(\ell_b/\ell_d)^5$ and we find that, in accordance with the Faxén result, the term $O(\ell_b/\ell_d)^4$ is not vanishing.

7. A sphere near a plane wall

Next, consider the archetypical hydrodynamic problem of a sphere with radius R_p and centre at distance h from a plane, as depicted in figure 3. Furthermore, consider Navier-slip BCs (2.5) at the surface of the sphere and no-slip BC at the surface of the plane wall.

For this hydrodynamic system, both the Faxén operator of the body and the Green function of the confinement, required to construct analytically the $[N]$-matrix in (4.6), are available in the literature up to the second order. Specifically, the zeroth-, first- and second-order Faxén operators with pole at the centre of the sphere can be found in Procopio & Giona (2024), whereas the Green function and its derivatives in the semi-space have been derived by Blake (1971); Blake & Chwang (1974); Procopio & Giona (2023). Both the Faxén operators and the multipoles evaluated at the position of the sphere, useful for the computation of the $[N]$-matrix, are reported in the supplementary material available at https://doi.org/10.1017/jfm.2024.651 expressed in the Cartesian coordinate system (ξ_1, ξ_2, ξ_3) represented in figure 3.

According to the definition (3.17), the entries of the $[N]$-matrix, representing the hydrodynamic interaction between the sphere and the plane, are obtained by applying the

Faxén operators to the regular part of the multipoles. Therefore, by the knowledge of the Faxén operators up to the second order, it is possible to construct the matrix

$$[N_{(0:2,0:2)}] = \begin{bmatrix} \boldsymbol{N}_{(0,0)} & \boldsymbol{N}_{(0,1)} & \dfrac{\boldsymbol{N}_{(0,2)}}{2!} \\ \boldsymbol{N}_{(1,0)} & \boldsymbol{N}_{(1,1)} & \dfrac{\boldsymbol{N}_{(1,2)}}{2!} \\ \boldsymbol{N}_{(2,0)} & \boldsymbol{N}_{(2,1)} & \dfrac{\boldsymbol{N}_{(2,2)}}{2!} \end{bmatrix}. \tag{7.1}$$

The entries of the submatrix

$$\boldsymbol{N}_{(0,0)} = \begin{bmatrix} N_{1\,1} & N_{1\,2} & N_{1\,3} \\ N_{2\,1} & N_{2\,2} & N_{2\,3} \\ N_{3\,1} & N_{3\,2} & N_{3\,3} \end{bmatrix} \tag{7.2}$$

expressed in the Cartesian coordinate system (ξ_1, ξ_2, ξ_3), are

$$\left.\begin{aligned} N_{1\,1} &= \mathcal{F}_{\gamma'1} W_{\gamma'1}(\boldsymbol{\xi}', \boldsymbol{\xi})\big|_{\boldsymbol{\xi}'=\boldsymbol{\xi}=(0,0,h)} = \frac{9R_p(1+2\hat{\lambda})}{16h(1+3\hat{\lambda})} - \frac{R_p^3}{16h^3(1+3\hat{\lambda})}, \\ N_{2\,2} &= \mathcal{F}_{\gamma'2} W_{\gamma'2}(\boldsymbol{\xi}', \boldsymbol{\xi})\big|_{\boldsymbol{\xi}'=\boldsymbol{\xi}=(0,0,h)} = \frac{9R_p(1+2\hat{\lambda})}{16h(1+3\hat{\lambda})} - \frac{R_p^3}{16h^3(1+3\hat{\lambda})}, \\ N_{3\,3} &= \mathcal{F}_{\gamma'3} W_{\gamma'3}(\boldsymbol{\xi}', \boldsymbol{\xi})\big|_{\boldsymbol{\xi}'=\boldsymbol{\xi}=(0,0,h)} = \frac{9R_p(1+2\hat{\lambda})}{8h(1+3\hat{\lambda})} - \frac{R_p^3}{4h^3(1+3\hat{\lambda})}, \\ N_{1\,2} &= N_{1\,3} = N_{2\,1} = N_{3\,1} = N_{3\,2} = N_{2\,3} = 0, \end{aligned}\right\} \tag{7.3}$$

with $\hat{\lambda} = \lambda/R_p$ being the dimensionless slip length of the fluid–sphere interface. The entries of the other submatrices entering (7.1) can be obtained by the Faxén operators and multipoles reported in the supplementary material.

7.1. *Force and torque on a translating sphere near a plane wall*

Consider a spherical body translating with velocity $\boldsymbol{U}$, hence an ambient flow $\boldsymbol{u}(\boldsymbol{x}) = -\boldsymbol{U}$. The force acting onto the sphere is given by (6.12). Assuming $K = 3$, we have

$$\boldsymbol{F} = \boldsymbol{F}^{[\infty]} - [M_{(0:3)}]^t([I_{(0:3,0:3)}] - [N_{(0:3,0:3)}])^{-1}[N_{(0:3,0)}] + F_c O\left(\frac{\ell_b}{\ell_d}\right)^5, \tag{7.4}$$

where

$$\boldsymbol{F}^{[\infty]} = -\boldsymbol{M}^t_{(0)} = -6\pi\mu R_p \left(\frac{1+2\hat{\lambda}}{1+3\hat{\lambda}}\right)\boldsymbol{U} \tag{7.5}$$

is the well-known Hadamard–Rybczynski force, $\boldsymbol{M}_1 = \boldsymbol{M}_{(3)} = 0$ and, as shown in Appendix C.1,

$$\boldsymbol{M}^t_{(2)} = -\frac{R_p^2}{3(1+2\hat{\lambda})}\boldsymbol{F}^{[\infty]}\boldsymbol{I}_{(0,2)}, \tag{7.6}$$

where $\boldsymbol{I}_{(0,2)}$ is a matrix obtained by the vectorisation of the multi-index $(\beta\beta_1\beta_2)$ of the tensor $\delta_{\gamma\beta}\delta_{\beta_1\beta_2}$. As shown in Appendix C.1, since $\boldsymbol{M}_{(3)} = 0$, the submatrices $\boldsymbol{N}_{(3,q)}$

and $\boldsymbol{N}_{(q,3)}$ (with $q = 0, 1, 2, 3$) entering $[N_{(0:3,0:3)}]$ and $[N_{(0:3,0)}]$ in (7.4) are immaterial and can be assumed vanishing (in point of fact, we show in Appendix C.1, that only the submatrix $\boldsymbol{N}_{(0,p)}$, with $p = 0, 1, 2$, contribute to the force obtained by (7.4)). After substituting the entries of the N-matrix in (7.4) and after some algebra we obtain

$$\boldsymbol{F} = \boldsymbol{F}^{[\infty]} \begin{pmatrix} \dfrac{1}{1-\beta_{\|}} & 0 & 0 \\ 0 & \dfrac{1}{1-\beta_{\|}} & 0 \\ 0 & 0 & \dfrac{1}{1-\beta_{\perp}} \end{pmatrix} + O\left(\frac{R_p}{h}\right)^5, \tag{7.7}$$

where

$$\beta_{\|} = \frac{9R_p}{16h}\left(\frac{1+2\hat{\lambda}}{1+3\hat{\lambda}}\right) - \frac{R_p^3}{8h^3(1+3\hat{\lambda})} + \frac{45R_p^4}{256h^4}\left(\frac{(1+2\hat{\lambda})^2}{(1+3\hat{\lambda})(1+5\hat{\lambda})}\right) \tag{7.8}$$

and

$$\beta_{\perp} = \frac{9R_p}{8h}\left(\frac{1+2\hat{\lambda}}{1+3\hat{\lambda}}\right) - \frac{R_p^3}{2h^3(1+3\hat{\lambda})} + \frac{135R_p^4}{256h^4}\left(\frac{(1+2\hat{\lambda})^2}{(1+3\hat{\lambda})(1+5\hat{\lambda})}\right). \tag{7.9}$$

For $\hat{\lambda} = 0$ (i.e. in the no-slip case), existing literature results can be recovered. In fact, the force $F_{\perp}$ on a sphere translating perpendicularly to the plane wall with velocity $U_{\perp}$ is in perfect agreement with the Taylor series expansion of the exact solution obtained by Brenner (1961), which reads

$$\frac{F_{\perp}}{6\pi\mu R_p U_{\perp}} = 1 + \frac{9R_p}{8h} + \frac{81{R_p}^2}{64h^2} + \frac{473{R_p}^3}{512h^3} + \frac{4113{R_p}^4}{4096h^4} + O\left(\frac{R_p}{h}\right)^5 \tag{7.10}$$

and $\beta_{\|}$ reduces to the same expression obtained by Faxén (see Happel & Brenner 1983, p. 327).

As expected by the dimensional analysis performed in § 6, by using the approximate Brenner's relation (6.22), only the first terms $O(R_p/h)$ on the right-hand side of (7.8) and (7.9) are correctly obtained, whereas by using the Swan and Brady approximations (6.34) also the second terms $O(R_p/h)^3$ are correctly evaluated, but the third $O(R_p/h)^4$ term is erroneously vanishing. Figures 4 and 5 depict the results obtained in (7.7)–(7.9) and by the approximated relations developed in §§ 6.1 and 6.2 compared with the exact results (such as those deriving by solving the Goren (1979) equations) and to FEM simulations (in the cases the exact results are not available in the literature). From the visual inspection of figures 4 and 5, it readily follows that (7.7) provides an accurate representation of the force on a spherical body valid for gaps $\delta = (h - R_p) \gtrsim R_p$ or even smaller, if one considers all the terms for $\beta_{\|}$ and $\beta_{\perp}$ entering (7.8) and (7.9). Further improvements of the expansion, taking into account higher-order Faxén operators, could increase the range of validity of the theoretical expressions to smaller gap values.

It can be observed that there is a larger error in the solution obtained by the Swan and Brady approximation (6.34) to the order $O(R_p/h)^3$ compared with the solution obtained by the Brenner approximation (6.22) to the order $O(R_p/h)$, despite the higher-order reflection considered. This additional error arises from the negative terms in the denominator of the expressions (7.8) and (7.9), associated with the dipole potential of the Stokes solution for the sphere translating in the unbounded fluid, which induce a slight 'boost' upon reflection by the plane.

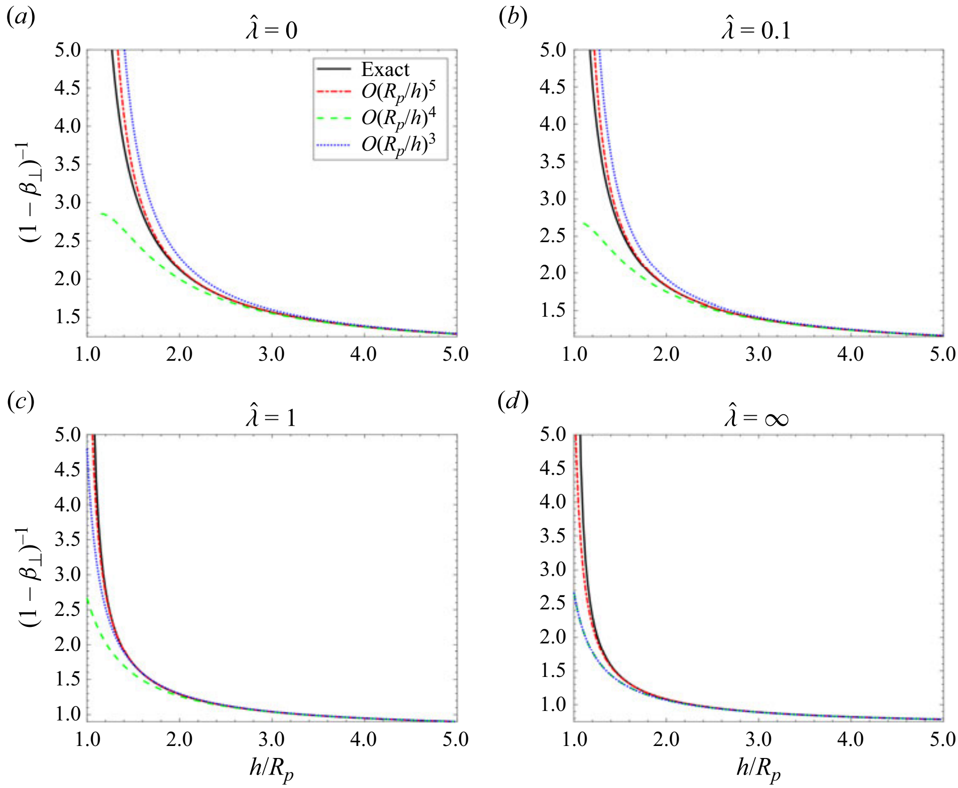

Figure 4. Dimensionless force on a spherical body translating perpendicularly to a planar wall for different slip lengths on the surface of the sphere. Solid black lines represent exact results obtained by solving the equations provided by Goren (1979), red dashed-dotted lines depict (7.7) taking into account all the terms, green dashed lines represent (7.7) where the terms $O(R_p/h)^4$ are neglected (corresponding to the approximated relation (6.34)) and blue dotted lines represent (7.7) where the terms $O(R_p/h)^3$ are neglected (corresponding to the approximated relation (6.22)). For complete slip ($\hat{\lambda} = \infty$), blue dotted and green dashed lines are practically coincident.

According (6.13), the torque on the translating sphere with velocity $\boldsymbol{U}$ truncated to $K = 3$ reads

$$\boldsymbol{T} = \boldsymbol{T}^{[\infty]} + [M_{(0:3)}]^t([I_{(0:3,0:3)}] - [N_{(0:3,0:3)}])^{-1}[L_{(0:3)}] + T_c O\left(\frac{\ell_b}{\ell_d}\right)^5. \tag{7.11}$$

Substituting the expressions for the entries of the N-matrix and considering the error estimated in Appendix C.2 (or, equivalently, considering the (7.20) and the symmetry of the grand-resistance matrix), after some algebra one obtains

$$\boldsymbol{T} = R_p \boldsymbol{F}^{[\infty]} \begin{pmatrix} 0 & -\gamma & 0 \\ \gamma & 0 & 0 \\ 0 & 0 & 0 \end{pmatrix} + O\left(\frac{R_p}{h}\right)^6 \tag{7.12}$$

or, by (7.5),

$$\boldsymbol{T} = -6\pi\mu R_p^2 \left(\frac{1+2\hat{\lambda}}{1+3\hat{\lambda}}\right) \boldsymbol{U} \begin{pmatrix} 0 & -\gamma & 0 \\ \gamma & 0 & 0 \\ 0 & 0 & 0 \end{pmatrix} + O\left(\frac{R_p}{h}\right)^6, \tag{7.13}$$

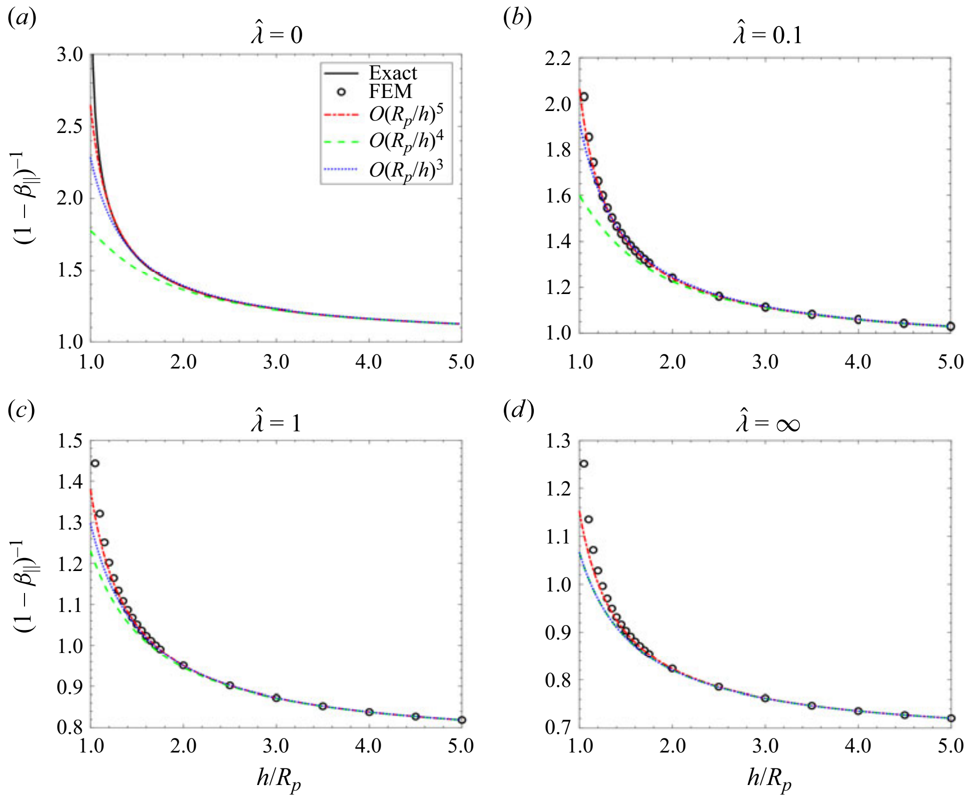

Figure 5. Dimensionless force on a spherical body translating parallel to a plane wall for different slip lengths on the surface of the sphere. The solid black line represents the exact no-slip result obtained by solving the equations provided by O'Neill (1964), black circles are the results of FEM simulations, red dashed-dotted lines depict (7.7) taking into account all the terms, green dashed lines represent (7.7) where the terms $O(R_p//h)^4$ are neglected (corresponding to the approximated relation (6.34)) and blue dotted lines represent (7.7) where the terms $O(R_p/h)^3$ are neglected (corresponding to the approximated relation (6.22)). For complete slip ($\hat{\lambda} = \infty$), blue and green dashed lines are practically coincident.

where

$$\gamma = \frac{1}{8}\left(\frac{R_p}{h}\right)^4 \left(\frac{1}{(1+2\hat{\lambda})(1+3\hat{\lambda})} - \frac{3}{8}\left(\frac{R_p}{h}\right)\frac{(1+5\hat{\lambda}+15\hat{\lambda}^2)}{(1+3\hat{\lambda})^2(1+5\hat{\lambda})}\right). \tag{7.14}$$

As expected from the dimensional analysis performed in § 6.1 (6.23), the $K = 0$-order approximation cannot predict the leading-order term $O(R_p/h)^4$ as in (7.13)–(7.14). In fact, since the coupling matrix $\boldsymbol{C}$ of a sphere in the unbounded fluid is vanishing, the torque on a translating sphere near a plane would vanishing according to this approximation. Using the approximation (6.35) it is possible to obtain correctly the leading-order term $O(R_p/h)^4$ in (7.14), but not the term $O(R_p/h)^5$.

The results obtained by (7.14) truncated to the orders $O(R_p/h)^4$ and $O(R_p/h)^5$ are compared in figure 6 with the exact solutions provided by O'Neill (1964) for no-slip BCs assumed on the surface of the sphere and with FEM simulations performed for $\hat{\lambda} = 0.1, 0.5, 1$.

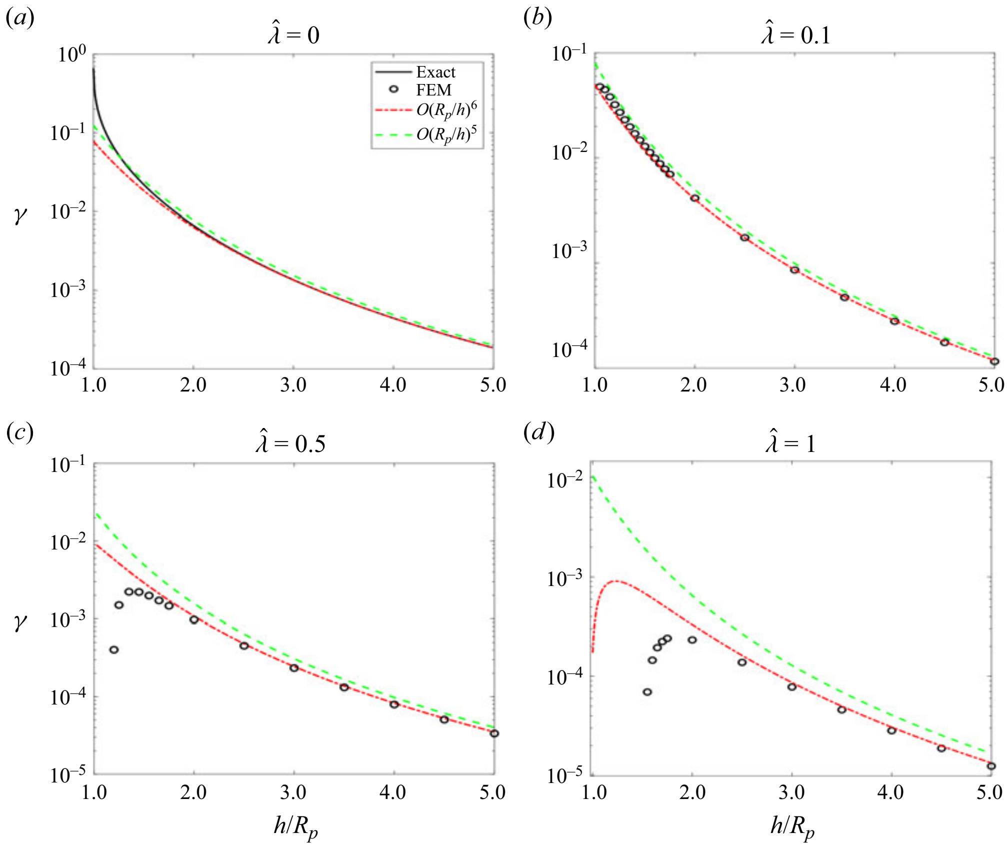

Figure 6. Dimensionless torque on a spherical body translating parallel to a plane wall for different slip lengths on the surface of the sphere. The solid black line represents the exact no-slip result obtained by solving the equations by O'Neill (1964), black circles are the results of FEM simulations, red dashed-dotted lines correspond to (7.14) taking into account all the terms and green dashed lines correspond to (7.14) neglecting the term $O(R_p/h)^5$, corresponding to the approximated relation (6.35).

7.2. *Torque and force on a rotating sphere near a plane wall*

The torque truncated to $K = 4$ on a sphere rotating near a plane wall is obtained by considering

$$\boldsymbol{T} = \boldsymbol{T}^{[\infty]} + [M_{(0:4)}]^t([I_{(0:4,0:4)}] - [N_{(0:4,0:4)}])^{-1}[L_{(0:4)}] + T_c O\left(\frac{\ell_b}{\ell_d}\right)^6, \tag{7.15}$$

where $\boldsymbol{M}_{(0)} = \boldsymbol{M}_{(2)} = \boldsymbol{M}_{(4)} = 0$ and, as shown in Appendix C.3,

$$\boldsymbol{M}_{(1)} = \frac{\boldsymbol{T}^{[\infty]}\boldsymbol{\varepsilon}}{2}. \tag{7.16}$$

In Appendix C.3, we show that $\boldsymbol{M}_{(3)}$, $\boldsymbol{L}_{(3)}$, $\boldsymbol{N}_{(q,3)}$ and $\boldsymbol{N}_{(3,q)}$ (with $q = 0, 1, 2, 3$) are immaterial for this approximation order and, hence, they can be assumed to be zero in (7.15). By substituting the other entries of the N-matrix, we obtain

$$\boldsymbol{T} = \boldsymbol{T}^{[\infty]}\begin{pmatrix} 1+\nu_\parallel & 0 & 0 \\ 0 & 1+\nu_\parallel & 0 \\ 0 & 0 & 1+\nu_\perp \end{pmatrix} + O\left(\frac{R_p}{h}\right)^6, \tag{7.17}$$

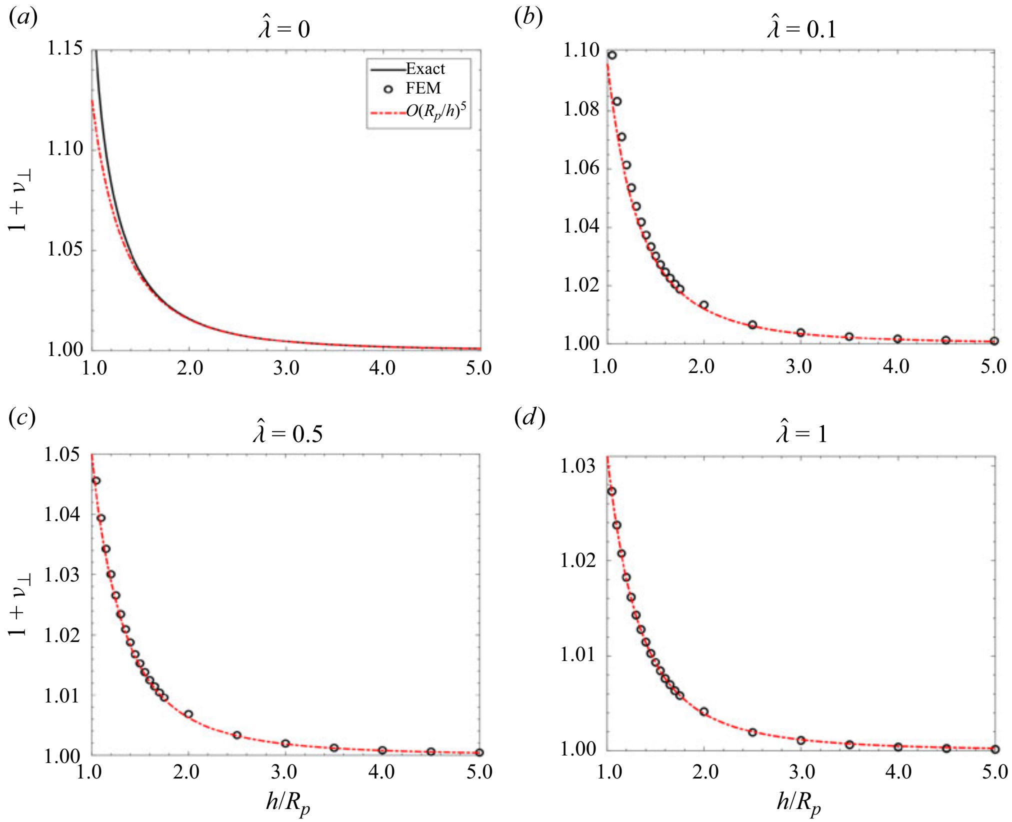

Figure 7. Dimensionless torque on a spherical body rotating with angular velocity perpendicular to a plane wall for different slip lengths on the surface of the sphere. The solid black line represents the exact no-slip result obtained by solving the equations provided by Dean & O'Neill (1963), black circles are the results of FEM simulations and red dashed-dotted lines represent (7.17) which, in the present case, is equivalent to (6.35).

where

$$\nu_\parallel = \frac{15R_p^3}{16h^3}\left(\frac{1}{1+3\hat{\lambda}}\right) \tag{7.18}$$

and

$$\nu_\perp = \frac{R_p^3}{8h^3}\left(\frac{1}{1+3\hat{\lambda}}\right). \tag{7.19}$$

The result expressed by (7.17) can be obtained by applying the extended Swan and Brady approximation (6.35). The graph of (7.17) is depicted in figures 7 and 8, compared with the exact expressions for a sphere with no-slip BCs provided by Jeffery (1915) and Dean & O'Neill (1963) and with FEM simulations for $\hat{\lambda} = 0.1, 0.5, 1$.

The force acting on a rotating sphere near a plane wall can be deduced from

$$\boldsymbol{F} = [M_{(0:4)}]^t([I_{(0:4,0:4)}] - [N_{(0:4,0:4)}])^{-1}[N_{(0:4,0)}] + F_c O\left(\frac{\ell_b}{\ell_d}\right)^6. \tag{7.20}$$

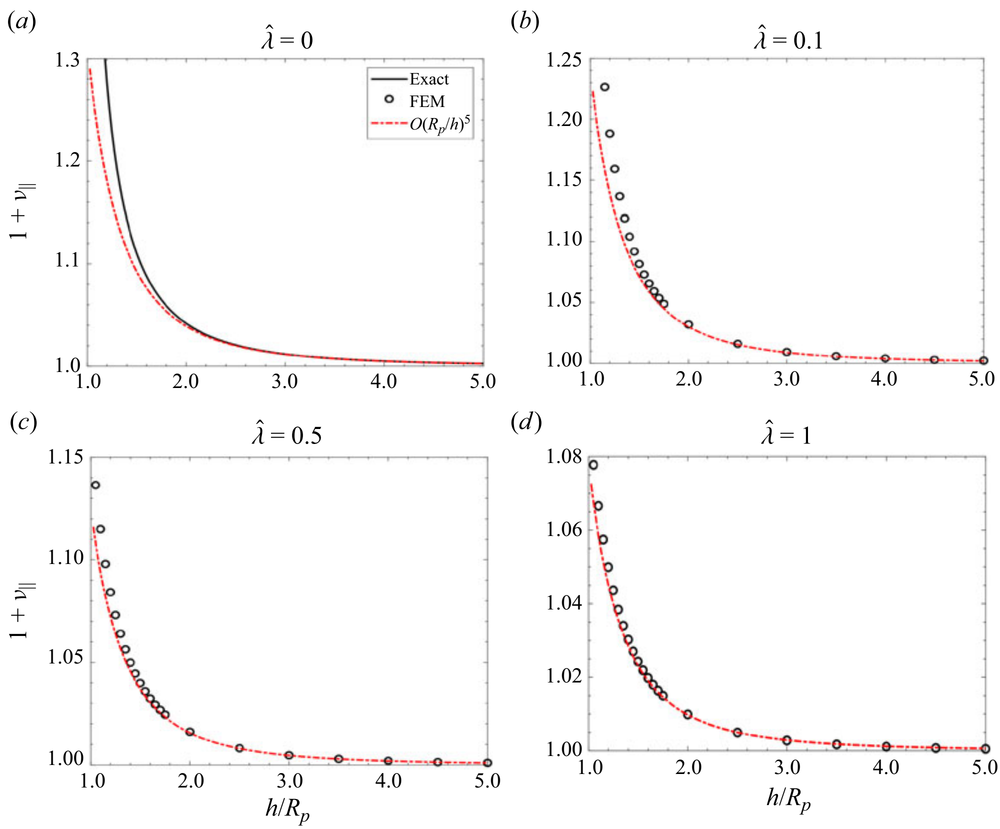

Figure 8. Dimensionless torque on a spherical body rotating with angular velocity parallel to a plane wall for different slip lengths on the sphere. The solid black line represents the exact no-slip result obtained by solving the equations provided by Dean & O'Neill (1963), black circles are the results of FEM simulations and red dashed-dotted lines represent (7.17) which, in the present case, is equivalent to (6.35).

The same result admits a more straightforward derivation by considering the linearity between $\boldsymbol{F}$ and $\boldsymbol{\omega}$ expressed by the coupling matrix $\bar{\boldsymbol{C}}$

$$\boldsymbol{F} = -\boldsymbol{\omega}\bar{\boldsymbol{C}} + O\left(\frac{R_p}{h}\right)^6. \tag{7.21}$$

Enforcing the symmetry of the grand-resistance matrix (see Appendix A in Procopio & Giona (2022) or for the case of a body in a confined fluid considering Navier-slip BCs), we have

$$\bar{\boldsymbol{C}} = \bar{\boldsymbol{D}}^t, \tag{7.22}$$

where $\bar{\boldsymbol{D}}$ is the coupling matrix entering the expression $\boldsymbol{T} = -\boldsymbol{U}\bar{\boldsymbol{D}}$ in (7.13). Therefore,

$$\boldsymbol{F} = -6\pi\mu R_p^2 \left(\frac{1+2\hat{\lambda}}{1+3\hat{\lambda}}\right) \boldsymbol{\omega} \begin{pmatrix} 0 & \gamma & 0 \\ -\gamma & 0 & 0 \\ 0 & 0 & 0 \end{pmatrix} + O\left(\frac{R_p}{h}\right)^6, \tag{7.23}$$

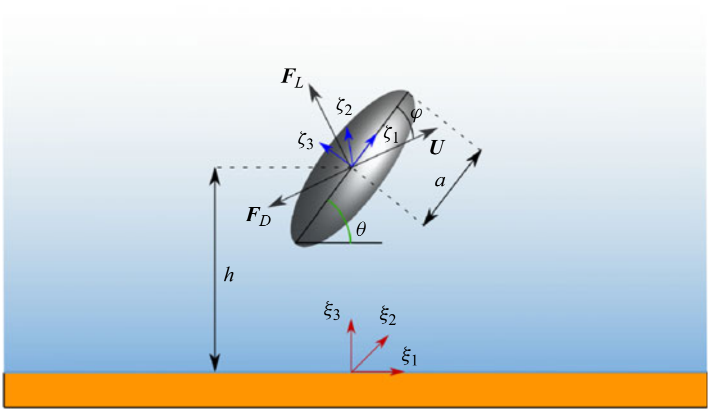

Figure 9. Schematic representation of a prolate spheroid near a plane wall. The prolate spheroid translates with velocity $\boldsymbol{U}$, forming an angle ϕ with the major axis of the spheroid. Here $\boldsymbol{F}_d$ is the hydrodynamic drag force experienced by the body aligned with $\boldsymbol{U}$ and $\boldsymbol{F}_L$ the hydrodynamic lift force orthogonal to $\boldsymbol{U}$.

where γ is given in (7.14). Analogously to (7.12)

$$\boldsymbol{F} = \frac{\boldsymbol{T}^{[\infty]}}{R_p} \begin{pmatrix} 0 & \delta & 0 \\ -\delta & 0 & 0 \\ 0 & 0 & 0 \end{pmatrix} + O\left(\frac{R_p}{h}\right)^6, \tag{7.24}$$

where

$$\delta = \left(1 + 2\hat{\lambda}\right) \frac{3\gamma}{4}. \tag{7.25}$$

8. Force on a translating prolate spheroid near a plane wall

In this section, we investigate the effect of the shape and of the orientation of a body in a confined fluid on the hydrodynamic interactions between the body and the confinement in light of the theory developed here. To this aim, we consider a prolate spheroid translating in the Stokes fluid with velocity $\boldsymbol{U}$ near a plane wall, at distance h between its centroid and the plane. Unlike the spherical case addressed in the previous section, two additional geometrical parameters should be introduced: the eccentricity e of the spheroid, accounting for the effects of the shape of the body on its hydromechanics, and the angle θ between the symmetry axis of the prolate spheroid and the plane (see figure 9), accounting for the effects of the orientation of the body. In order to highlight these effects, the translational motion of the spheroid without rotation is considered, although a full hydromechanic analysis of this system can be developed within the present approach. To obtain the hydrodynamic force acting on the spheroid, we employ the approximate expressions obtained in §§ 6.1 and 6.2, and we show that, owing to these approximations, accurate expressions for the hydromechanics of particles in confined fluid can be derived solely from the knowledge of the unbounded resistance matrix or the lower-order Faxén operators.

We consider a prolate spheroid defined by the surface equation

$$\frac{\zeta_1^2}{a^2} + \frac{\zeta_2^2 + \zeta_3^2}{b^2} = 1, \tag{8.1}$$

where $(\zeta_1, \zeta_2, \zeta_3)$ is a Cartesian coordinate system with origin at the centroid, a the semi-length of the major axis and b the semi-length of the minor axis (see figure 9).

The resistance matrix of a prolate spheroid with no-slip BCs in the unbounded fluid, expressed in the coordinate system $(\zeta_1, \zeta_2, \zeta_3)$, is $\boldsymbol{R} = 16\pi\mu c \boldsymbol{A}(e)$ (Kim & Karrila 2005) where e is the eccentricity of the spheroid, $c = ae$ the focal length and

$$\boldsymbol{A}(e) = \begin{pmatrix} \dfrac{e^2}{(1+e^2)\log\left(\dfrac{1+e}{1-e}\right) - 2e} & 0 & 0 \\ 0 & \dfrac{2e^2}{(1-3e^2)\log\left(\dfrac{1+e}{1-e}\right) - 2e} & 0 \\ 0 & 0 & \dfrac{2e^2}{(1-3e^2)\log\left(\dfrac{1+e}{1-e}\right) - 2e} \end{pmatrix}. \tag{8.2}$$

Substituting the resistance matrix into (6.14), the first-order approximation is straightforward

$$\boldsymbol{F} = \boldsymbol{F}^{[\infty]}\left(\boldsymbol{I} + 2\frac{c}{h}\boldsymbol{w}(\theta)\boldsymbol{A}(e)\right)^{-1} + O\left(\frac{a}{h}\right)^2, \tag{8.3}$$

where $\boldsymbol{F}^{[\infty]} = -16\pi\mu c\boldsymbol{U}\boldsymbol{\cdot}\boldsymbol{A}(e)$ and $\boldsymbol{w}(\theta)$, having as its entries the regular part of the Green function $-W_{\alpha\beta}(\boldsymbol{\zeta}/h, \boldsymbol{\zeta}/h)$ at the position of the centroid $\boldsymbol{\zeta} = (0, 0, 0)$, reads

$$w_{\alpha\beta}(\theta) = -\begin{pmatrix} \frac{3}{8}(3-\cos(2\theta)) & 0 & \frac{3}{8}\sin(2\theta) \\ 0 & \frac{3}{4} & 0 \\ \frac{3}{8}\sin(2\theta) & 0 & \frac{3}{8}(3+\cos(2\theta)) \end{pmatrix}. \tag{8.4}$$

To obtain the higher-order terms providing the hydrodynamic force, we can employ the zeroth-order Faxén operator for the prolate spheroid available in the literature (Hasimoto 1983; Kim 1985; Kim & Karrila 2005) by using the extended Swan and Brady relations obtained in § 6.2. Specifically, the zeroth-order Faxén operator can be expressed as

$$\mathcal{F}_{\beta\gamma} = \frac{R_{\beta\gamma}}{16\pi\mu c}\int_{\boldsymbol{\Gamma}} d\boldsymbol{\Gamma}\left(1 + \frac{(1-e^2)(c^2-\zeta_1^2)\Delta_\zeta}{4e^2}\right), \tag{8.5}$$

where Δ_ζ is the Laplacian acting on the coordinates $(\zeta_1, \zeta_2, \zeta_3)$, the curve $\boldsymbol{\Gamma}$ is the line segment between the two foci at $\zeta_1 = \pm c$ of the spheroid with parametrisation

$$\boldsymbol{\Gamma}(s) = \begin{cases} \zeta_1(s) = s, \\ \zeta_2(s) = 0, \\ \zeta_3(s) = 0, \end{cases} \quad s \in [-c, c] \tag{8.6}$$

and $\mathrm{d}\boldsymbol{\Gamma} \equiv \mathrm{d}s$ is its measure element.

The geometrical moments entering the Faxén operator (8.5) are expressed with respect to the centroid (being the centre of hydrodynamic reaction) as pole. For the symmetry of the spheroid, a rotation around this point is uncoupled to the translations, thus providing

$\boldsymbol{C} = \boldsymbol{0}$. Therefore, we can use (6.34) assuming $\boldsymbol{\omega} = \boldsymbol{0}$, which, after some algebra, attains the more compact form

$$\boldsymbol{F} = -U\boldsymbol{R}(\boldsymbol{I} - \boldsymbol{R}^{-1}\boldsymbol{\Phi})^{-1} + O\left(\frac{a}{h}\right)^4. \tag{8.7}$$

From (8.7), in order to obtain the hydrodynamic force acting on the spheroid by (8.7), it is necessary to evaluate the matrix $\boldsymbol{\Phi}$ defined by (6.29), which, considering the Faxén operator (8.5), reads

$$\begin{aligned}\Phi_{\beta\gamma} = -\frac{R_{\delta'\beta}R_{\delta\gamma}}{32\pi\mu c^2}\Bigg[&\int_{-c}^{c}\mathrm{d}s'\int_{-c}^{c}\mathrm{d}s\, W_{\delta'\delta}\left(\boldsymbol{\zeta}'(s'), \boldsymbol{\zeta}(s)\right)\\ &+\frac{1-e^2}{4e^2}\int_{-c}^{c}\mathrm{d}s'\int_{-c}^{c}\mathrm{d}s\,(c^2-s^2)\Delta_\zeta W_{\delta'\delta}\left(\boldsymbol{\zeta}'(s'), \boldsymbol{\zeta}(s)\right)\\ &+\frac{1-e^2}{4e^2}\int_{-c}^{c}\mathrm{d}s'\int_{-c}^{c}\mathrm{d}s\,(c^2-s'^2)\Delta_{\zeta'} W_{\delta'\delta}\left(\boldsymbol{\zeta}'(s'), \boldsymbol{\zeta}(s)\right)\Bigg] + O(a/h)^4,\end{aligned} \tag{8.8}$$

where the primed subscripts $\delta' = 1, 2, 3$ refer to the coordinate system at the point $\boldsymbol{\zeta}'$.

Substituting (8.8) into (8.7), we finally obtain

$$\boldsymbol{F} = \boldsymbol{F}^{[\infty]}\left(\boldsymbol{I} + \frac{c}{2h}\boldsymbol{P}\left(\frac{c}{h},\theta\right)\boldsymbol{A}(e) + \left(\frac{c}{h}\right)^3\left(\frac{1-e^2}{8e^2}\right)\boldsymbol{Q}\left(\frac{c}{h},\theta\right)\boldsymbol{A}(e)\right)^{-1} + O\left(\frac{a}{h}\right)^4, \tag{8.9}$$

where the entries of $\boldsymbol{P}(c/h,\theta)$ and $\boldsymbol{Q}(c/h,\theta)$ are, respectively,

$$P_{\delta'\delta}\left(\frac{c}{h},\theta\right) = \int_{-1}^{1}\mathrm{d}s'\int_{-1}^{1}\mathrm{d}s\, W_{\delta'\delta}\left(\boldsymbol{\zeta}'(s')\frac{c}{h}, \boldsymbol{\zeta}(s)\frac{c}{h}\right) \tag{8.10}$$

$$\begin{aligned}Q_{\delta'\delta}\left(\frac{c}{h},\theta\right) = \Bigg[&\int_{-1}^{1}\mathrm{d}s'\int_{-1}^{1}\mathrm{d}s(1-s^2)\Delta_\zeta W_{\delta'\delta}\left(\boldsymbol{\zeta}'(s')\frac{c}{h}, \boldsymbol{\zeta}(s)\frac{c}{h}\right)\\ &+\int_{-1}^{1}\mathrm{d}s'\int_{-1}^{1}\mathrm{d}s(1-s'^2)\Delta_{\zeta'} W_{\delta'\delta}\left(\boldsymbol{\zeta}'(s')\frac{c}{h}, \boldsymbol{\zeta}(s)\frac{c}{h}\right)\Bigg].\end{aligned} \tag{8.11}$$

To perform the derivatives and integrals along the segment between the foci of the spheroid entering (8.8) (or the normalised integrals entering (8.10) and (8.11)) independently of the orientation of the prolate spheroid, it is fundamental to employ the representation of the Green function invariant both at the field and the pole points, corresponding to the ‘bi-invariant’ form of the regular part of the Green function in the semi-space obtained in Procopio & Giona (2023)

$$\begin{aligned}W_{b\beta}(\boldsymbol{x},\boldsymbol{\zeta}) = S_{b\beta}(\boldsymbol{x}-\boldsymbol{\zeta}^*) - (\boldsymbol{\zeta}^*-\boldsymbol{\zeta})\boldsymbol{\cdot}\boldsymbol{n}\, J_{\beta\gamma*}\\ \times\left[n_{\delta*}\nabla_{\gamma*}S_{b\delta*}(\boldsymbol{x}-\boldsymbol{\zeta}^*) - \frac{(\boldsymbol{\zeta}^*-\boldsymbol{\zeta})\boldsymbol{\cdot}\boldsymbol{n}}{2}\Delta_{\zeta^*}S_{a\gamma^*}(\boldsymbol{x}-\boldsymbol{\zeta}^*)\right],\end{aligned} \tag{8.12}$$

with $\boldsymbol{x} \equiv \boldsymbol{\zeta}'$ and where $\boldsymbol{n} = (\sin\theta, 0, \cos\theta)$ is the normal to the plane wall inward to the fluid, $\boldsymbol{J} = \boldsymbol{I} - 2\boldsymbol{n}\otimes\boldsymbol{n}$ the mirror operator (that in Procopio & Giona (2023) has been shown to coincide with the parallel propagator between the fluid space and the reflected space), $\boldsymbol{\zeta}^* = \boldsymbol{J}\boldsymbol{\cdot}\boldsymbol{\zeta} - 2h\,\boldsymbol{n}$ is the reflected point by the plane and the starred subscripts, such as β^*, refers to the coordinate system at the mirror point $(\zeta_1^*, \zeta_3^*, \zeta_3^*)$.

Solving the integrals (8.10) and (8.11) with the regular part of the Green function (8.11) (normalised accordingly) and expanding the results in Taylor series of (c/h), we obtain

$$F = 16\pi\mu c U A(e)\left(I + \frac{c}{2h} p_0(\theta) A(e) + \left(\frac{c}{2h}\right)^3 \left(p_2(\theta) + \frac{1-e^2}{4e^2} q_0(\theta)\right) A(e)\right)^{-1} + O\left(\frac{a}{h}\right)^4, \tag{8.13}$$

where $p_0(\theta) = 4\, w(\theta)$,

$$p_2 = \begin{pmatrix} \dfrac{60\cos(2\theta) - 9\cos(4\theta) + 5}{96} & 0 & \dfrac{3}{4}\sin\theta\cos^3\theta \\ 0 & \dfrac{9\cos(2\theta)+1}{24} & 0 \\ \dfrac{3}{4}\sin\theta\cos^3\theta & 0 & \cos(2\theta) + \dfrac{9\cos(4\theta)+55}{96} \end{pmatrix} \tag{8.14}$$

and

$$q_0 = \begin{pmatrix} \dfrac{20}{3} - 4\cos(2\theta) & 0 & 8\sin(\theta)\cos(\theta) \\ 0 & \dfrac{8}{3} & 0 \\ 8\sin(\theta)\cos(\theta) & 0 & 4\cos(2\theta) + \dfrac{20}{3} \end{pmatrix}. \tag{8.15}$$

From (8.13), we can evince that the second-order term $O(a/h)^2$ in the inverse matrix entering the expression of the force is vanishing for any orientation θ of the prolate spheroid. Therefore, comparing this result with (8.3), we can conclude that the error committed by using the $K = 0$ approximation is $O(a/h)^3$, hence smaller than $O(a/h)^2$ expected from general considerations.

When particle dynamics is considered, it might be useful to express the force in the fixed reference frame of the plane. Specifically, considering the coordinate system with origin on the plane (see figure 9)

$$\begin{cases} \xi_1 = \zeta_1 \cos\theta - \zeta_3 \sin\theta, \\ \xi_2 = \zeta_2, \\ \xi_3 = \zeta_1 \sin\theta + \zeta_3 \cos\theta - h, \end{cases} \tag{8.16}$$

the entries of the matrices $p_0(\theta)$, $p_2(\theta)$, $q_0(\theta)$, expressed in this system, read

$$p_0(\theta) = \begin{pmatrix} -3 & 0 & 0 \\ 0 & -3 & 0 \\ 0 & 0 & -6 \end{pmatrix}, \tag{8.17}$$

$$
\boldsymbol{p}_2(\theta) = \begin{pmatrix} \dfrac{11\cos(2\theta)+3}{24} & 0 & -\dfrac{\sin(2\theta)}{6} \\ 0 & \dfrac{9\cos(2\theta)+1}{24} & 0 \\ -\dfrac{\sin(2\theta)}{6} & 0 & \dfrac{7\cos(2\theta)+3}{6} \end{pmatrix}, \tag{8.18}
$$

$$
\boldsymbol{q}_0(\theta) = \begin{pmatrix} \dfrac{8}{3} & 0 & 0 \\ 0 & \dfrac{8}{3} & 0 \\ 0 & 0 & \dfrac{32}{3} \end{pmatrix}. \tag{8.19}
$$

An expression for the mobility, conceptually analogous to (8.13), has been proposed by Mitchell & Spagnolie (2015) using a Swan and Brady approach, directly extended to the ellipsoids. However, it can be observed that the entries of the mobility matrix reported in Mitchell & Spagnolie (2015) do not match the entries of the mobility of the sphere obtained by Swan & Brady (2007) (or obtainable by inverting the resistance matrix provided in § 7.1) in the limit of vanishing eccentricity $e \to 0$. On the other hand, by inverting the resistance matrix entering (8.13), the limit of spherical bodies is correctly matched. For instance, the velocity of the spheroid U along the plane under the effect of an external force F^{ext} parallel to the plane reads

$$
\frac{6\pi\mu a U}{F^{ext}} = \frac{3}{8}\left(\frac{\cos^2(\theta)}{eA_{11}(e)} + \frac{\sin^2(\theta)}{eA_{33}(e)}\right) - \left(\frac{a}{h}\right)\frac{9}{16} + \left(\frac{a}{h}\right)^3 \frac{\left(11e^2\cos(2\theta) - 13e^2 + 16\right)}{128}, \tag{8.20}
$$

where $A_{11}(e)$ and $A_{33}(e)$ are the entries of the matrix $\boldsymbol{A}(e)$ in (8.2) in the coordinate system $(\zeta_1, \zeta_2, \zeta_3)$. Since $eA_{11}(e) \to 3/8$ and $eA_{33}(e) \to 3/8$ in the limit $e \to 0$, (8.20) yields the mobility

$$
\frac{6\pi\mu a U}{F^{ext}} = 1 - \left(\frac{a}{h}\right)\frac{9}{16} + \left(\frac{a}{h}\right)^3 \frac{1}{8} \tag{8.21}
$$

of a sphere in this limit. Equation (8.20) differs from that provided by Mitchell & Spagnolie (2015) for terms $O(a/h)^0$ and $O(a/h)^3$. The discrepancy is likely due to the fact that the relations derived by Mitchell & Spagnolie (2015) were obtained by differentiating only at the field point of the Green function to obtain higher-order terms, also in those cases the derivative at the pole point was necessary (for example to obtain terms $\nabla_\beta \nabla_{\beta'} W(\boldsymbol{\xi}, \boldsymbol{\xi}')$), since the pole point cannot be differentiated in the Blake's formulation (Blake 1971) of the Green function bounded by a no-slip plane (see Liron & Mochon (1976) or Spagnolie & Lauga (2012) for a discussion on this point). As regards this technical but important issue, bitensorial calculus represents the proper geometrical setting for addressing the differentiation problems, owing to its bi-invariance both with respect to field and pole point coordinates.

The comparison of the theoretical relations (8.3) and (8.13) and the numerical FEM simulations depicted in figures 10 and 11, shows that the theoretical approximated relations provide accurate results up to $h \approx 2a$, independently of the orientation of the spheroid. More specifically, figure 10 depicts the drag force F_d (hence, the force aligned with the translatory direction, see figure 9) experienced by the spheroid translating with velocity parallel to the plane along the axis ξ_1 and intensity U. It can be observed that, for small values of the eccentricity e, the approximation (8.13), truncated to the order $O(a/h)^4$, provides a worse approximation with respect to (8.3) truncated to a lower order. This phenomenon could indeed be expected by considering the case of a spherical body addressed in § 7.1, where it is shown that the approximation for the drag force is improved once the next correction term $O(R_p/h)^4$ is accounted for. However, it is possible to observe in figure 10 that, for higher values of the eccentricity e, the error decreases with the inclusion of the next correction term $O(a/h)^3$. As shown in figure 11 for the lift force (i.e. the force orthogonal to the translation of the body, see figure 9) experienced by prolate spheroid moving parallel to the plane along the axis ξ_1, (8.13) provides a better approximation with respect to the lower-order truncation (8.3) for any value of eccentricity e.

In contrast to the case of a spheroid in a unbounded flow, the plane wall generates a lift force $\boldsymbol{F}_L$ even when the translation occurs along the principal axes of the spheroid, as shown in figure 12(*a*). This implies that, if we want to move the spheroid along its principal axes, the external force applied to it cannot be aligned with the axes itself. Specifically, the lift force always opposes the approach of the body to the plane, pointing towards the plane when the direction of motion points out of the plane and vice versa. In figure 12(*b–d*), it is possible to observe that the hydrodynamic effects of the plane wall on the resistance of the spheroid determine a lift force that may have an opposite sign with respect to the case of the unbounded flow. This occurs when the orientation of the spheroid is $\theta = \pi/2$ or $\theta = \pi/4$, whereas for $\theta = 0$ the spheroid experiences a lift force in the same direction of the unbounded case. This implies that if the spheroid is perpendicular to the plane and we want to move it in a direction forming an angle $\phi = \pi/4$ with its axis of symmetry, an external force in a direction forming a smaller angle with the axis should be applied. This is opposite to the unbounded case, where the force direction must have a greater angle.

9. Conclusions

The aim of this article was to provide useful mathematical–physical tools for studying the hydromechanics of bodies in confined fluids in its general setting.

By decomposing the hydrodynamics of a body in a confined Stokes fluid into two simpler problems, separately related to the body in the unbounded fluid, and to the confinement in the absence of the body, the method developed in this article allows us to overcome the typical difficulties arising from the intrinsic complexity of the geometries of such systems.

Two main significant advantages emerge straightforwardly from this decomposition, mainly represented by the mathematical factorisations in (4.14) and (5.17). (i) The decomposition provides a simpler and more systematic analysis of the problems concerning the hydrodynamics of bodies in confined fluids, without requiring special symmetries, as shown in the archetypal examples of a sphere near a plane wall reported in § 7 or of a spheroid near a plane wall in § 8, where the hydrodynamic resistance matrices are derived by simply applying the general equations, without enforcing any special symmetry of the systems. (ii) The decomposition may represent the theoretical starting point in the development of new numerical methods. Specifically, it is possible to collect a widely enough system of Faxén operators for bodies (estimating the geometrical moments using classical numerical methods) and of multipole fields for the confinements (solely the value of the regular part at the pole is necessary) to obtain, by combining them, a large number of solutions of hydromechanics problems related to bodies suspended in confined fluids. In this way, it is possible to reduce significantly either the computational cost or the amount of collected data necessary for the numerical solution of the hydromechanic problem. In addition, in the cases when the geometrical moments or

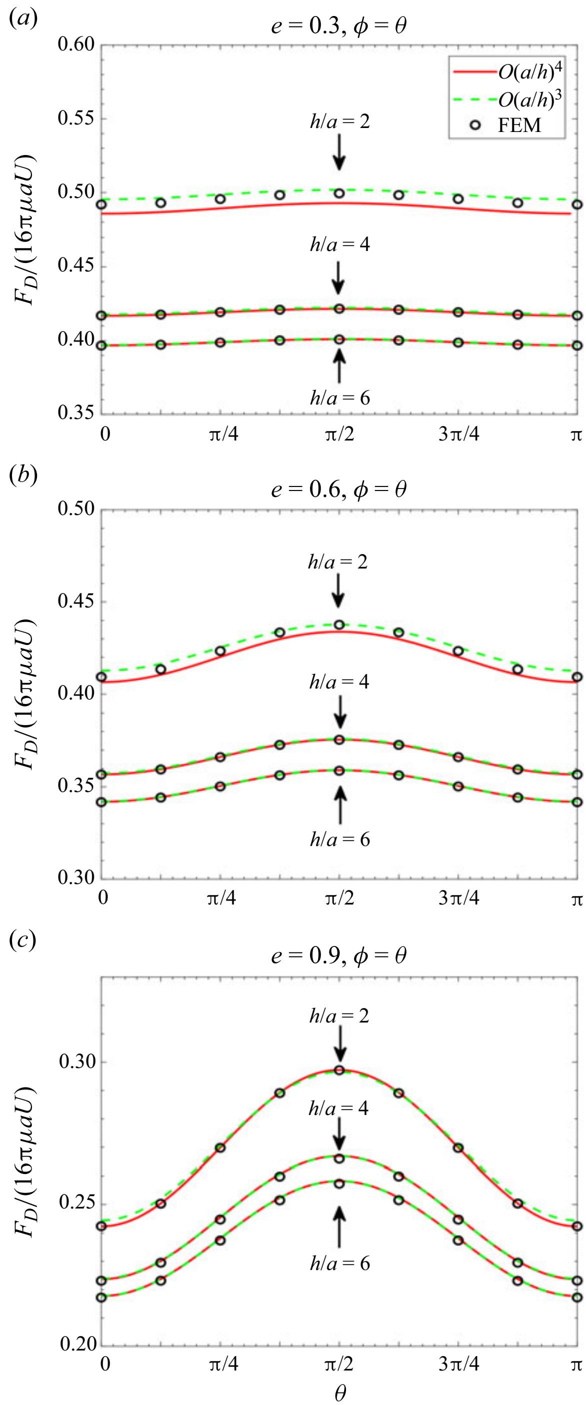

Figure 10. Dimensionless drag force acting on prolate spheroids with eccentricity $e = 0.3, 0.6, 0.9$ translating parallel to the plane wall along the axis ξ_1 with intensity U as a function of the orientation angle θ (see figure 9) for different distances h between the centroid and the plane wall. Symbols represent FEM simulations, green dashed lines the $O(a/h)^3$ approximation (8.3) and red lines the $O(a/h)^4$ approximation (8.12).

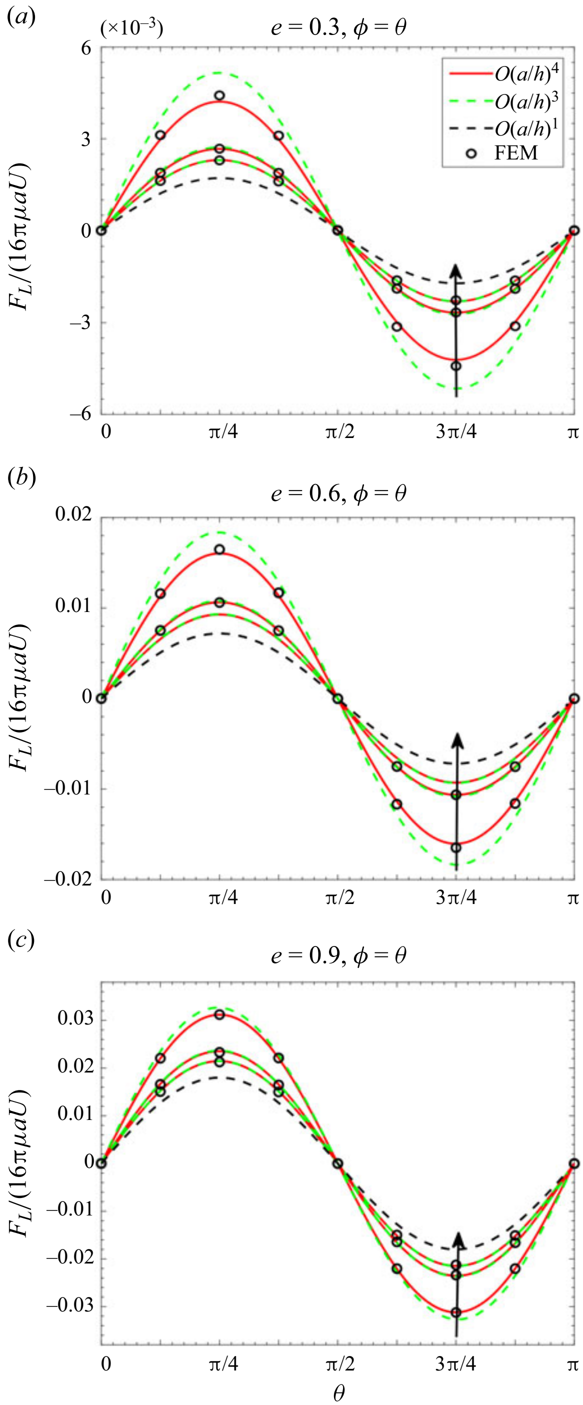

Figure 11. Dimensionless lift force acting on prolate spheroids with eccentricity $e = 0.3, 0.6, 0.9$ translating parallel to the plane wall along the axis ξ_1 with intensity U as a function of the orientation angle θ (see figure 9) for different distances h between the centroid and the plane wall. The arrows indicate increasing distances $h/a = 2, 4, 6, \infty$. Symbols represents FEM simulations, black dashed lines the unbounded case, green dashed lines the $O(a/h)^3$ approximation (8.3) and red lines the $O(a/h)^4$ approximation (8.12).

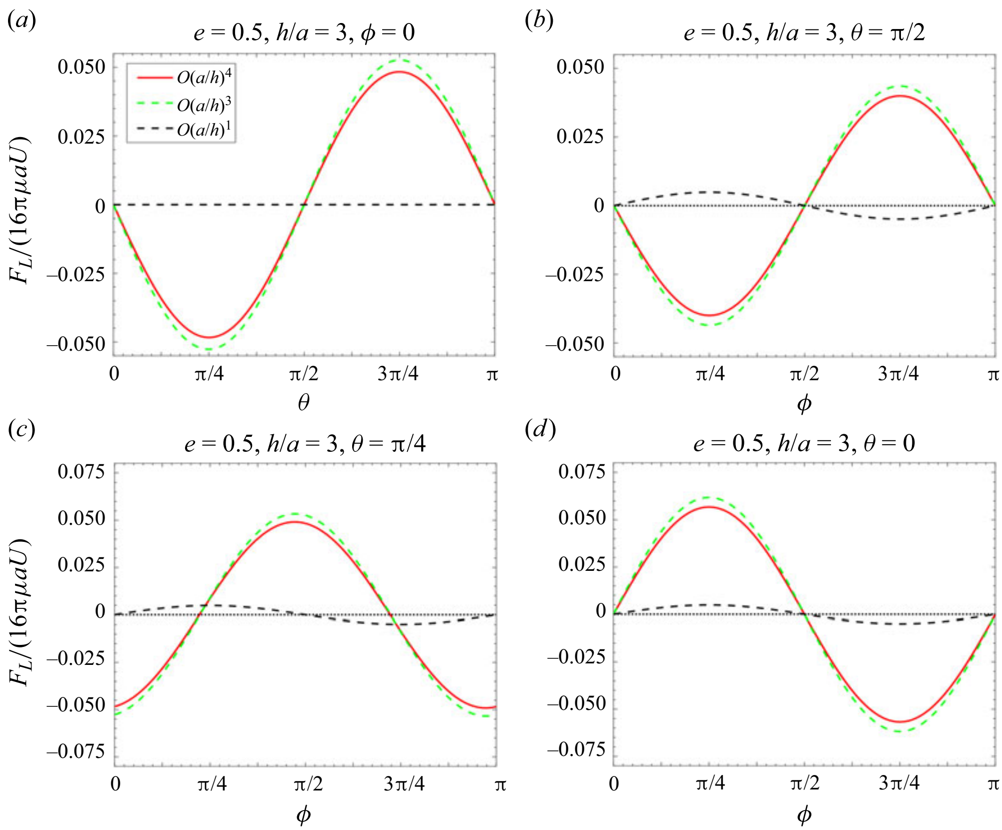

Figure 12. Dimensionless lift force acting on a prolate spheroid with eccentricity $e = 0.5$ at distance $h = 3a$. Panel (a) depicts the lift force acting on a spheroid translating along its principal axis as a function of the orientation angle θ. Panels (b–d) depict the lift force as a function of the angle ϕ between the velocity of the body and its symmetry axis (see figure 9) for different orientations of the spheroid. Specifically, in panel (b) the spheroid is normal to the plane, in panel (c) forms an angle $\theta = \pi/4$ with the plane and in panel (d) is parallel to the plane. The black dashed lines represent the force on prolate spheroids in the unbounded flow, the green dashed lines the $O(a/h)^3$ approximation (8.3) and the red lines the $O(a/h)^4$ approximation (8.12).

the Green function are not available, the present approach leads to efficient numerical strategies. For instance, consider the case of a spheroid near a plane wall as addressed in § 8, and suppose to estimate the 6×6 resistance matrix for the force and the torque by FEM simulations (or, equivalently, by other numerical methods such as BEM). With the eccentricity of the spheroid fixed, assume we are interested in the entries of the resistance matrix for all the positions from ranging $h = a$ to $h = 100a$ and for all the orientations from $\theta = 0$ to $\theta = \pi/2$ with a resolution $\delta h = \delta\theta = 10^{-2}$. To this end, 6 FEM simulations for each configuration are needed, providing a total number of 9 386 148 FEM simulations. On the other hand, assuming that no geometric moments are known for the spheroid (without considering the symmetries of the body), we need less then 1092 FEM simulations of the unbounded (one for each ambient flow) in order to obtain the geometrical moments $m_{\alpha\boldsymbol{\alpha}_m\beta\boldsymbol{\beta}_n}(\boldsymbol{\xi}, \boldsymbol{\xi})$ up to the order $m = n = 5$ (for any order n of the geometrical moments, we need, in principle, 3^{n+1} different ambient flows) providing the entries of the resistance matrix truncated to an order $O(a/h)^{10}$ according to (B5). This number reduces to 126 if the symmetry of the spheroids is enforced (for any order n of the geometrical moments, we need, in principle, 2^{n+1} different ambient flows).

Another non-secondary advantage provided by the explicit expressions obtained in this article is that the result found do not depend on the specific BCs chosen, provided they are linear and satisfy BC reciprocity. This can be helpful in dealing with complex combinations of BCs, such as in systems involving Janus particles or stick–slip surfaces. Furthermore, by this approach, it is possible, as addressed in §§ 6.1 and 6.2, to extend and generalise the classical approximated expressions for the grand-resistance matrix of bodies with no-slip BCs in confined fluids to the more general case of arbitrary linear reciprocal BCs.

Obviously, the infinite matrices entering the exact solution (4.14) and (5.17), should be necessarily truncated/approximated in all the practical calculations, leading to unavoidable truncation errors that have been thoroughly analysed and estimated in § 6. However, as addressed in § 7 for the case of a sphere translating and rotating near a plane wall, accurate results can be achieved, even for gaps smaller than the characteristic length of the body, by considering Faxén operators up to the second order.

Unfortunately, as shown in Appendix A, although the convergence of the reflection method is ensured for gaps $\delta \gtrsim 1.65\, \ell_b$, the reflection method could fail in describing hydrodynamic problems in the lubrication limit for vanishing gaps $\delta \rightarrow 0$. It would be interesting, to test further the range of validity of the reflection method by identifying the exact critical gap starting from which the reflection method diverge in prototype system (such as a sphere near a plane). Explicit expressions provided in this work are an invaluable tool to achieve this aim, since they allow to compute even higher-order terms entering the characteristic expressions of the reflection method. A possible approach to overcome the reflection method limit, related to the convergence in the small gap limit, is to construct the total solutions by matching the reflection solution with the lubrication solution, applying matching methods (see, for example, Jeffrey & Onishi 1984; Swan & Brady 2010). This method is widely employed in Stokesian dynamics (Guazzelli & Morris 2012), wherein the interaction between multiple particles is constructed based on the hydrodynamic solution in the far field between two isolated particles and, next, matched with lubrication solutions. Making use of (4.15), (5.9), (5.13) and (5.17), the interactions between two particles in the far field can be derived even in the confined case (i.e. considering two particles in a confined flow). This potentially paves the way for extending Stokesian dynamics methods to confined cases as well.

In any case, the detailed description of the hydrodynamics of two surfaces getting in touch, for which many questions are still open (Procopio & Giona 2022), is very complex and would require the hydrodynamic description to be complemented with other microscopic factors (such as the accurate estimate of the slip length or the inclusion of Casimir (Klimchitskaya, Mohideen & Mostepanenko 2009) and electrostatic effects), and this goes beyond the mere lubrication analysis.

Supplementary material. Supplementary material is available at https://doi.org/10.1017/jfm.2024.651.

Declaration of interests. The authors report no conflict of interest.

Author ORCIDs.
Giuseppe Procopio https://orcid.org/0000-0001-6313-790X;
Massimiliano Giona https://orcid.org/0000-0001-5875-0160.

Appendix A. Analysis of series convergence

In this Appendix the convergence of the series introduced in §§ 3 and 4 is investigated.

To begin with, let us consider the convergence of the series (3.12) yielding the first two terms $\boldsymbol{v}^{[1]}(\boldsymbol{x}) + \boldsymbol{v}^{[2]}(\boldsymbol{x})$ in the reflection formula (3.1). Equation (3.12) can be compactly expressed in matrix form as

$$\boldsymbol{v}^{[1]}(\boldsymbol{x}) + \boldsymbol{v}^{[2]}(\boldsymbol{x}) = \frac{[M]^t[G]}{8\pi\mu}. \tag{A1}$$

It is easy to verify that the row by column multiplication $[M]^t[G]$ corresponds to the sum of products between the elements $\boldsymbol{M}_{(m)}$ and $\boldsymbol{G}_{(m)}$, i.e.

$$[M]^t[G] = \sum_m^\infty \frac{\left(\boldsymbol{M}_{(m)}\right)^t \boldsymbol{G}_{(m)}}{m!} \tag{A2}$$

and using the Cauchy–Schwarz inequality we have

$$\left|[M]^t[G]\right| = \left|\sum_m^\infty \frac{\left(\boldsymbol{M}_{(m)}\right)^t \boldsymbol{G}_{(m)}}{m!}\right| \le \sum_m^\infty \frac{\left|\left(\boldsymbol{M}_{(m)}\right)^t \boldsymbol{G}_{(m)}\right|}{m!} \le \sum_m^\infty \frac{\left\|\boldsymbol{M}_{(m)}\right\| \left\|\boldsymbol{G}_{(m)}\right\|}{m!}, \tag{A3}$$

where $\|\cdot\|$ represents the norm of a matrix.

In order to obtain an upper bound for the rightmost term in (A3), an estimate for the norms $\|\boldsymbol{M}_{(m)}\|$ and $\|\boldsymbol{G}_{(m)}\|$ is required. According to the reflection procedure followed in § 3, the moments $M_{\alpha\boldsymbol{\alpha}_m}(\boldsymbol{\xi})$ refer to a body with characteristic length ℓ_b, immersed in a unbounded ambient flow $\boldsymbol{u}(\boldsymbol{x})$, with characteristic velocity U_c. Therefore, by dimensional analysis, the force field distribution $\boldsymbol{\psi}(\boldsymbol{x})$, matching the BCs according to (2.12), and the position vector $(\boldsymbol{x} - \boldsymbol{\xi})$ can be normalised as follows:

$$(\hat{\boldsymbol{x}} - \hat{\boldsymbol{\xi}}) = \frac{(\boldsymbol{x} - \boldsymbol{\xi})}{\ell_b}, \quad \hat{\boldsymbol{\psi}}(\boldsymbol{x}) = \frac{\boldsymbol{\psi}(\boldsymbol{x})}{\dfrac{\mu U_c}{\ell_b^2}}. \tag{A4}$$

By definition of the moments (2.13), the entries of the moments can be normalised by

$$\hat{M}_{\alpha\boldsymbol{\alpha}_m}(\boldsymbol{\xi}) = \frac{M_{\alpha\boldsymbol{\alpha}_m}(\boldsymbol{\xi})}{\mu U_c \ell_b^{m+1}} \tag{A5}$$

so that $\hat{M}_{\alpha\boldsymbol{\alpha}_m}(\boldsymbol{\xi}) \sim O(1)$, and we can define the characteristic velocity U_c such that $|\hat{M}_{\alpha\boldsymbol{\alpha}_m}(\boldsymbol{\xi})| \le 1$, strictly. Therefore, if $\hat{\boldsymbol{M}}_{(m)}$ is the $(m+1)$-dimensional vector with $\hat{M}_{\alpha\boldsymbol{\alpha}_m}(\boldsymbol{\xi})$ as its entries, we have

$$\left\|\boldsymbol{M}_{(m)}\right\| = \left\|\hat{\boldsymbol{M}}_{(m)}\right\| \mu U_c \ell_b^{m+1} \le 3^{(m+1)/2} \mu U_c \ell_b^{m+1}. \tag{A6}$$

On the other hand, since the leading term in the Green function derivatives (2.10), is the derivative of the Stokeslet, we can normalise the entries of the mth-order derivative of the Green function evaluated at the field point by a characteristic distance ℓ_f between the body and the field point as

$$\hat{\nabla}_{\boldsymbol{\alpha}_m}\hat{G}_{a\alpha}(\boldsymbol{x},\boldsymbol{\xi}) = \ell_f^{m+1}\nabla_{\boldsymbol{\alpha}_m}G_{a\alpha}(\boldsymbol{x},\boldsymbol{\xi}) \tag{A7}$$

with $\ell_f > \ell_b$ defined so that

$$\left\|\boldsymbol{G}_{(m)}\right\| = \frac{\left\|\hat{\boldsymbol{G}}_{(m)}\right\|}{\ell_f^{m+1}} \leq \frac{3^{(m+1)/2}}{\ell_f^{m+1}}, \tag{A8}$$

with $\hat{\boldsymbol{G}}_{(m)}$ being the vector admitting $\hat{\nabla}_{\boldsymbol{\alpha}_m}\hat{G}_{a\alpha}(\boldsymbol{x},\boldsymbol{\xi})$ as its entries.

Therefore, since $\ell_f > \ell_b$, the velocity field $\boldsymbol{v}^{[1]}(\boldsymbol{x}) + \boldsymbol{v}^{[2]}(\boldsymbol{x})$ is bounded by

$$\left|\boldsymbol{v}^{[1]}(\boldsymbol{x}) + \boldsymbol{v}^{[2]}(\boldsymbol{x})\right| = \frac{\left|[M]^t[G]\right|}{8\pi\mu} \leq \frac{U_c}{8\pi}\sum_m^\infty \frac{3^{m+1}}{m!}\left(\frac{\ell_b^{m+1}}{\ell_f^{m+1}}\right) = \frac{U_c}{8\pi}\left(3\frac{\ell_b}{\ell_f}\right)\mathrm{e}^{(3\ell_b/\ell_f)}. \tag{A9}$$

Next, consider the velocity field $\boldsymbol{v}^{[3]}(\boldsymbol{x}) + \boldsymbol{v}^{[4]}(\boldsymbol{x})$, given in matrix form by (4.8)

$$\boldsymbol{v}^{[3]}(\boldsymbol{x}) + \boldsymbol{v}^{[4]}(\boldsymbol{x}) = \frac{[M]^t[N][G]}{8\pi\mu}, \tag{A10}$$

for which, analogously to the inequalities (A3), we have

$$\begin{aligned}\left|[M']^t[N][G]\right| &= \left|\sum_m^\infty\sum_n^\infty \frac{\left(\boldsymbol{M}_{(m)}\right)^t\boldsymbol{N}_{(m,n)}\boldsymbol{G}_{(n)}}{m!n!}\right| \leq \sum_m^\infty\sum_n^\infty \frac{\left|\left(\boldsymbol{M}_{(m)}\right)^t\boldsymbol{N}_{(m,n)}\boldsymbol{G}_{(n)}\right|}{m!n!} \\ &\leq \sum_m^\infty\sum_n^\infty \frac{\left\|\boldsymbol{M}_{(m)}\right\|\left\|\boldsymbol{N}_{(m,n)}\right\|\left\|\boldsymbol{G}_{(n)}\right\|}{m!n!}.\end{aligned} \tag{A11}$$

By definition (3.17), the entries of the matrices $\boldsymbol{N}_{(m,n)}$ are nth-order moments evaluated for a body immersed in an ambient flow corresponding to the regular part of the mth derivative of the Green function. Since the regular part of the Green function is a disturbance field for the Stokeslet with pole in the body generated by the walls of the confinement, its characteristic magnitude can be considered as that of a Stokeslet with pole at distance $2\ell_d$, ℓ_d being the characteristic distance between the body and the nearest walls from the body. Thus, the characteristic magnitude of its mth-order derivatives can be estimated as $\boldsymbol{W}_{(m)} = O(1/(2\ell_d)^{m+1})$, hence, by the same arguments used for $M_{\alpha\boldsymbol{\alpha}_m}$, we have

$$\hat{N}_{\alpha\boldsymbol{\alpha}_m\beta\boldsymbol{\beta}_n}(\boldsymbol{\xi}) = \frac{N_{\alpha\boldsymbol{\alpha}_m\beta\boldsymbol{\beta}_n}(\boldsymbol{\xi})}{\mu W_c^{(m)}\ell_b^{n+1}} = \frac{N_{\alpha\boldsymbol{\alpha}_m\beta\boldsymbol{\beta}_n}(\boldsymbol{\xi})}{\dfrac{\mu\ell_b^{n+1}}{(2\ell_d)^{m+1}}}. \tag{A12}$$

Therefore, given that $\|\hat{\boldsymbol{N}}_{(m,n)}\| \sim O(1)$ is the norm of the matrix with normalised entries $\hat{N}_{\alpha\boldsymbol{\alpha}_m\beta\boldsymbol{\beta}_n}(\boldsymbol{\xi})$, there exists a constant $C^{(1)}_{m,n}$, such that $|\|\hat{\boldsymbol{N}}_{(m,n)}\|| \leq C^{(1)}_{m,n}$, and

$$\left\|\boldsymbol{N}_{(m,n)}\right\| = \left\|\hat{\boldsymbol{N}}_{(m,n)}\right\|\frac{(\ell_b)^{n+1}}{(2\ell_d)^{m+1}} \leq C^{(1)}_{m,n}3^{(m+n+2)/2}\frac{(\ell_b)^{n+1}}{(2\ell_d)^{m+1}}. \tag{A13}$$

By considering the inequalities (A6), (A8) and (A13), the velocity field $\boldsymbol{v}^{[3]}(\boldsymbol{x}) + \boldsymbol{v}^{[4]}(\boldsymbol{x})$ is bounded by

$$\begin{aligned}\left|\boldsymbol{v}^{[3]}(\boldsymbol{x}) + \boldsymbol{v}^{[4]}(\boldsymbol{x})\right| &= \frac{\left|[M]^t[N][G]\right|}{8\pi\mu} \\ &\leq C^{(1)}_{m,n}\frac{U_c}{8\pi}\left(\frac{3\ell_b}{\ell_f}\right)\left(\frac{3\ell_b}{2\ell_d}\right)\sum_m^\infty\sum_n^\infty\frac{1}{m!n!}\left(\frac{3\ell_b}{\ell_f}\right)^m\left(\frac{3\ell_b}{2\ell_d}\right)^n \\ &= C^{(1)}\frac{U_c}{8\pi}\left(\frac{3\ell_b}{\ell_f}\right)\mathrm{e}^{3\ell_b/\ell_f}\left(\frac{3\ell_b}{2\ell_d}\right)\mathrm{e}^{3\ell_b/2\ell_d},\end{aligned} \tag{A14}$$

where $C^{(1)} = \sup_{m,n} C^{(1)}_{m,n} \sim O(1)$. Iterating the same procedure for all $k = 0, 1, 2, 3, \ldots$, we have

$$\begin{aligned}\left|\boldsymbol{v}^{[2k+1]}(\boldsymbol{x}) + \boldsymbol{v}^{[2k+2]}(\boldsymbol{x})\right| &= \frac{\left|[M]^t[N]^k[G]\right|}{8\pi\mu} \\ &\leq C^{(k)}\frac{U_c}{8\pi}\left(\frac{3\ell_b}{\ell_f}\right)\mathrm{e}^{3\ell_b/\ell_f}\left[\left(\frac{3\ell_b}{2\ell_d}\right)\mathrm{e}^{3\ell_b/2\ell_d}\right]^k\end{aligned} \tag{A15}$$

with $C^{(k)} \sim O(1)$, and because of it, there exists a constant $C > 0$, such that $C^{(k)} < C$ for any k. Therefore, for $k \to \infty$, the contribution given by $\boldsymbol{v}^{[2k+1]}(\boldsymbol{x}) + \boldsymbol{v}^{[2k+2]}(\boldsymbol{x})$ to the total velocity field in (4.8) vanishes only if

$$\left(\frac{3\ell_b}{2\ell_d}\right)\mathrm{e}^{3\ell_b/2\ell_d} \leq 1, \tag{A16}$$

i.e. for

$$\ell_d \gtrsim 2.65\ell_b. \tag{A17}$$

Therefore, if $\ell_d = \ell_b + \delta$, where δ is characteristic length of the gap between the surface of the particle and the walls of the confinement, the convergence of the method is ensured for

$$\delta \gtrsim 1.65\ell_b. \tag{A18}$$

The convergence analysis developed above establishes a sufficient condition $\ell_d \gg \ell_b$, regardless the geometry of the system, for the convergence of the reflection method developed in § 3. However, the convergence is not excluded even for smaller distances and (A17) suggests that it holds for $\ell_d \sim \ell_b$. Extending this argument, we can state that there exist a constant $\varGamma > 0$, depending on the geometry of the system and in principle smaller than the value 2.65 reported in (A17), such that, for

$$\ell_d > \varGamma\ell_b \tag{A19}$$

the reflection method developed in § 3 converges and the velocity field can be represented in terms of the Faxén operator of the body and the Green function of the confinement by (4.13).

Appendix B. Scaling analysis of approximate expressions

In this appendix, the approximate expressions reported in §§ 6.1 and 6.2 for forces and torques acting on a body in a bounded fluid are derived.

B.1. *Derivation of velocity fields, forces and torques for $K = 0$*

By (3.17) and (2.17), the entries of $\boldsymbol{N}_{(0,0)}$ can be expressed explicitly in terms of the geometrical moments,

$$N_{\alpha\beta}(\boldsymbol{\xi}) = \mathcal{F}_{\gamma'\beta} W_{\gamma'\alpha}(\boldsymbol{\xi}', \boldsymbol{\xi})\big|_{\boldsymbol{\xi}'=\boldsymbol{\xi}} = \sum_{n=0}^{\infty} \left. \frac{m_{\gamma'\boldsymbol{\gamma}'_n\beta}(\boldsymbol{\xi}', \boldsymbol{\xi}) \nabla_{\boldsymbol{\gamma}'_n} W_{\gamma'\alpha}(\boldsymbol{\xi}', \boldsymbol{\xi})}{n!} \right|_{\boldsymbol{\xi}'=\boldsymbol{\xi}}. \tag{B1}$$

In order to determine the terms in (B1) that can be neglected once compared with the truncation error in (6.15), a dimensional analysis of the geometrical moments should be carried out. Enforcing the linearity of the Stokes equations, the volume force $\psi_\alpha^{(n)}(\boldsymbol{x}, \boldsymbol{\xi}')$ in (2.15) can be expressed in terms of a 'geometrical' volume force $\psi_{\alpha\beta'\boldsymbol{\beta}'_n}(\boldsymbol{x}, \boldsymbol{\xi}')$ as

$$\psi_\alpha^{(n)}(\boldsymbol{x}, \boldsymbol{\xi}') = 8\pi\mu A_{\beta'\boldsymbol{\beta}'_n} \psi_{\alpha\beta'\boldsymbol{\beta}'_n}(\boldsymbol{x}, \boldsymbol{\xi}') \tag{B2}$$

by means of which the geometrical moments can be rewritten as

$$m_{\alpha\boldsymbol{\alpha}_m\beta\boldsymbol{\beta}_n}(\boldsymbol{\xi}, \boldsymbol{\xi}') = \int (\boldsymbol{x} - \boldsymbol{\xi})_{\boldsymbol{\alpha}_m} \psi_{\alpha\beta'\boldsymbol{\beta}'_n}(\boldsymbol{x}, \boldsymbol{\xi}')\, \mathrm{d}V(\boldsymbol{x}) \quad \boldsymbol{\xi}, \boldsymbol{\xi}' \in V_b. \tag{B3}$$

Considering that

$$\psi_\alpha^{(n)}(\boldsymbol{x}, \boldsymbol{\xi}') = \mu U_c O\left(\frac{1}{\ell_b^2}\right), \quad A_{\beta'\boldsymbol{\beta}'_n} = U_c O\left(\frac{1}{\ell_b^n}\right), \tag{B4}$$

we have $\psi_{\alpha\beta'\boldsymbol{\beta}'_n}(\boldsymbol{x}, \boldsymbol{\xi}') = O(\ell_b^{n-2})$ and thus, by (B3), the geometrical moments scale as

$$m_{\alpha\boldsymbol{\alpha}_m\beta\boldsymbol{\beta}_n}(\boldsymbol{\xi}, \boldsymbol{\xi}) = O(\ell_b^{m+n+1}). \tag{B5}$$

Therefore, neglecting in (B1) the terms of $\boldsymbol{N}_{(0,0)}$ of higher order than $O(\ell_b/\ell_d)$, and indicating with $R_{\alpha\beta} = -8\pi\mu\, m_{\alpha\beta}$ the resistance matrix, we obtain

$$N_{\alpha\beta}(\boldsymbol{\xi}) = -\frac{R_{\gamma\beta} W_{\gamma\alpha}(\boldsymbol{\xi}, \boldsymbol{\xi})}{8\pi\mu} + O\left(\frac{\ell_b}{\ell_d}\right)^2 \tag{B6}$$

so that (6.15) reads

$$\boldsymbol{v}(\boldsymbol{x}) = \boldsymbol{u}(\boldsymbol{x}) - \boldsymbol{F}^{[\infty]} \left(I + \frac{\boldsymbol{W}_{(0)}\boldsymbol{R}}{8\pi\mu}\right)^{-1} \frac{\boldsymbol{G}_{(0)}}{8\pi\mu} + U_c O\left(\frac{\ell_b}{\ell_f}\right)^2. \tag{B7}$$

Substituting (B6) in (6.16), and performing elementary matrix operations, we obtain the approximation provided by Brenner (1964*a*)

$$\boldsymbol{F} = \boldsymbol{F}^{[\infty]} \left(I + \frac{\boldsymbol{W}_{(0)}\boldsymbol{R}}{8\pi\mu}\right)^{-1} + F_c O\left(\frac{\ell_b}{\ell_d}\right)^2. \tag{B8}$$

Considering (6.16), the entries of $\boldsymbol{L}_{(0)}$ are, by definition (5.14),

$$\begin{aligned} L_{\alpha\beta} &= \mathcal{T}_{\gamma'\beta} W_{\gamma'\alpha}(\boldsymbol{\xi}', \boldsymbol{\xi})\big|_{\boldsymbol{\xi}'=\boldsymbol{\xi}} = \varepsilon_{\beta\delta\delta_1} \mathcal{F}_{\gamma'\delta\delta_1} W_{\gamma'\alpha}(\boldsymbol{\xi}', \boldsymbol{\xi})\big|_{\boldsymbol{\xi}'=\boldsymbol{\xi}} \\ &= \varepsilon_{\beta\delta\delta_1} \sum_{n=0}^{\infty} \left. \frac{m_{\gamma'\boldsymbol{\gamma}'_n\delta\delta_1}(\boldsymbol{\xi}', \boldsymbol{\xi}) \nabla_{\boldsymbol{\gamma}'_n} W_{\gamma'\alpha}(\boldsymbol{\xi}', \boldsymbol{\xi})}{n!} \right|_{\boldsymbol{\xi}'=\boldsymbol{\xi}}. \end{aligned} \tag{B9}$$

Following the same dimensional analysis developed in (B3)–(B6), and identifying $C_{\beta\gamma} = 8\pi\mu\, \varepsilon_{\beta\delta\delta_1} m_{\gamma\delta\delta_1}(\boldsymbol{\xi}, \boldsymbol{\xi})$ as the coupling matrix between forces and rotations of the body in the unbounded fluid (Happel & Brenner 1983; Procopio & Giona 2024)

$$L_{\alpha\beta} = \frac{C_{\beta\gamma} W_{\gamma\alpha}(\boldsymbol{\xi}, \boldsymbol{\xi})}{8\pi\mu} + O\left(\frac{\ell_b^3}{\ell_d^2}\right) \tag{B10}$$

and, therefore, considering that $\boldsymbol{W}_{(0)}$ is a symmetric matrix (Ladyzhenskaya 2014; Pozrikidis 1992), we obtain

$$\boldsymbol{T} = \boldsymbol{T}^{[\infty]} - \boldsymbol{F}^{[\infty]} \left(I + \frac{\boldsymbol{W}_{(0)} \boldsymbol{R}}{8\pi\mu} \right)^{-1} \frac{\boldsymbol{W}_{(0)} \boldsymbol{C}}{8\pi\mu} + T_c O\left(\frac{\ell_b}{\ell_d}\right)^2. \tag{B11}$$

B.2. *Derivation of extended Swan and Brady's approximations*

To begin with, let us suppose that the body translates without rotating with velocity $\boldsymbol{U}$ (therefore $\boldsymbol{u}(\boldsymbol{x}) = -\boldsymbol{U}$). By (3.9), the velocity field $\boldsymbol{v}^{[2]}(\boldsymbol{x})$, of the order of magnitude $U_c O(\ell_b/\ell_d)$ at the pole $\boldsymbol{\xi}$, where $U_c = |\boldsymbol{U}|$, can be obtained exactly by the zeroth-order Faxén operator

$$v_\alpha^{[2]}(\boldsymbol{\xi}) = -U_\beta \mathcal{F}_{\alpha'\beta} W_{\alpha\alpha'}(\boldsymbol{\xi}, \boldsymbol{\xi}')\big|_{\boldsymbol{\xi}'=\boldsymbol{\xi}} \tag{B12}$$

and, hence, the force is exactly given by

$$F_\gamma^{[3]} = -8\pi\mu \mathcal{F}_{\alpha\gamma} v_\alpha^{[2]}(\boldsymbol{\xi}) = 8\pi\mu U_\beta \mathcal{F}_{\alpha\gamma} \mathcal{F}_{\alpha'\beta} W_{\alpha\alpha'}(\boldsymbol{\xi}, \boldsymbol{\xi}')\big|_{\boldsymbol{\xi}'=\boldsymbol{\xi}} \tag{B13}$$

whereas the torque is

$$T_\gamma^{[3]} = 8\pi\mu \mathcal{T}_{\alpha\gamma} v_\alpha^{[2]}(\boldsymbol{\xi}) = -8\pi\mu U_\beta \mathcal{T}_{\alpha\gamma} \mathcal{F}_{\alpha'\beta} W_{\alpha\alpha'}(\boldsymbol{\xi}, \boldsymbol{\xi}')\big|_{\boldsymbol{\xi}'=\boldsymbol{\xi}}. \tag{B14}$$

To obtain the contributions $\boldsymbol{F}^{[5]}$ and $\boldsymbol{T}^{[5]}$ to the force and the torque, it is necessary to provide an explicit expression for the velocity field $\boldsymbol{v}^{[4]}(\boldsymbol{x})$, which, in turn, implies the knowledge of the higher-order Faxén operators. From (2.17), (B5) and (B12), we have

$$v_\alpha^{[2]}(\boldsymbol{\xi}) = U_c O\left(\frac{\ell_b}{\ell_d}\right), \quad \nabla_{\boldsymbol{\beta}_n} v_\beta^{[2]}(\boldsymbol{\xi}) = U_c O\left(\frac{\ell_b}{\ell_d^{1+n}}\right), \tag{B15}$$

hence $\nabla_{\beta_1} v_\beta^{[2]}(\boldsymbol{\xi}) \mathcal{F}_{\alpha'\beta\beta_1} W_{\alpha\alpha'}(\boldsymbol{\xi}, \boldsymbol{\xi}') = O(\ell_b/\ell_d)^3$ and, approximating the field $\boldsymbol{v}^{[4]}(\boldsymbol{\xi})$ in (3.14) to the zeroth-order Faxén operator, we get

$$v_\alpha^{[4]}(\boldsymbol{\xi}) = v_\beta^{[2]}(\boldsymbol{\xi}) \mathcal{F}_{\alpha'\beta} W_{\alpha\alpha'}(\boldsymbol{\xi}, \boldsymbol{\xi}')\Big|_{\boldsymbol{\xi}'=\boldsymbol{\xi}} + O\left(\frac{\ell_b}{\ell_d}\right)^3. \tag{B16}$$

Using (B16) we obtain for the force

$$F_\gamma^{[5]} = -8\pi\mu \mathcal{F}_{\alpha\gamma} v_\alpha^{[4]}(\boldsymbol{\xi}) = -8\pi\mu\, v_\beta^{[2]}(\boldsymbol{\xi}) \mathcal{F}_{\alpha\gamma} \mathcal{F}_{\alpha'\beta} W_{\alpha\alpha'}(\boldsymbol{\xi}, \boldsymbol{\xi}')\Big|_{\boldsymbol{\xi}'=\boldsymbol{\xi}} + O\left(\frac{\ell_b}{\ell_d}\right)^3 \tag{B17}$$

and for the torque

$$T_\gamma^{[5]} = 8\pi\mu \mathcal{T}_{\alpha\gamma} v_\alpha^{[4]}(\boldsymbol{\xi}) = 8\pi\mu\, v_\beta^{[2]}(\boldsymbol{\xi}) \mathcal{T}_{\alpha\gamma} \mathcal{F}_{\alpha'\beta} W_{\alpha\alpha'}(\boldsymbol{\xi}, \boldsymbol{\xi}')\Big|_{\boldsymbol{\xi}'=\boldsymbol{\xi}} + O\left(\frac{\ell_b}{\ell_d}\right)^3. \tag{B18}$$

By (B13), enforcing the definition of the resistance matrix $\boldsymbol{R}$

$$F_\gamma^{[3]} = R_{\gamma\alpha} v_\alpha^{[2]}(\boldsymbol{\xi}) + O\left(\frac{\ell_b}{\ell_d}\right)^2, \quad v_\alpha^{[2]}(\boldsymbol{\xi}) = (R^{-1})_{\alpha\gamma} F_\gamma^{[3]} + O\left(\frac{\ell_b}{\ell_d}\right)^2. \tag{B19}$$

Substituting (B19) into (B17) and (B18), and using the definitions (6.29)–(6.30), it follows that

$$\boldsymbol{F}^{[5]} = \boldsymbol{F}^{[3]} \boldsymbol{R}^{-1} \boldsymbol{\Phi} + O\left(\frac{\ell_b}{\ell_d}\right)^3 \tag{B20}$$

and

$$\boldsymbol{T}^{[5]} = \boldsymbol{F}^{[3]} \boldsymbol{R}^{-1} \boldsymbol{\Psi} + O\left(\frac{\ell_b}{\ell_d}\right)^3. \tag{B21}$$

Using the same approach, these results can be generalised for $k = 2, 3, \ldots$, obtaining

$$\boldsymbol{F}^{[2k+3]} = \boldsymbol{F}^{[2k+1]} \boldsymbol{R}^{-1} \boldsymbol{\Phi} + o\left(\frac{\ell_b}{\ell_d}\right)^3, \tag{B22}$$

$$\boldsymbol{T}^{[2k+3]} = \boldsymbol{F}^{[2k+1]} \boldsymbol{R}^{-1} \boldsymbol{\Psi} + o\left(\frac{\ell_b}{\ell_d}\right)^3 \tag{B23}$$

and, thus,

$$\boldsymbol{F} = \boldsymbol{F}^{[\infty]} + \sum_{k=0}^{\infty} \boldsymbol{F}^{[2k+3]} = \boldsymbol{F}^{[\infty]} + \boldsymbol{F}^{[3]} \sum_{k=0}^{\infty} (\boldsymbol{R}^{-1}\boldsymbol{\Phi})^k + O\left(\frac{\ell_b}{\ell_d}\right)^3, \tag{B24}$$

$$\boldsymbol{T} = \boldsymbol{T}^{[\infty]} + \sum_{k=0}^{\infty} \boldsymbol{T}^{[2k+3]} = \boldsymbol{T}^{[\infty]} + \boldsymbol{T}^{[3]} + \boldsymbol{F}^{[3]} \boldsymbol{R}^{-1} \sum_{k=0}^{\infty} (\boldsymbol{R}^{-1}\boldsymbol{\Phi})^k \boldsymbol{\Psi} + O\left(\frac{\ell_b}{\ell_d}\right)^3. \tag{B25}$$

Considering that $\boldsymbol{F}^{[\infty]} = -\boldsymbol{U}\boldsymbol{R}$, $\boldsymbol{T}^{[\infty]} = -\boldsymbol{U}\boldsymbol{C}$ and, from (B13)–(B14), $\boldsymbol{F}^{[3]} = -\boldsymbol{U}\boldsymbol{\Phi}$, $\boldsymbol{T}^{[3]} = -\boldsymbol{U}\boldsymbol{\Psi}$, we obtain

$$\boldsymbol{F} = -\boldsymbol{U}\left(\boldsymbol{R} + \left(\boldsymbol{I} - \boldsymbol{\Phi}\boldsymbol{R}^{-1}\right)^{-1} \boldsymbol{\Phi}\right) + O\left(\frac{\ell_b}{\ell_d}\right)^3 \tag{B26}$$

and

$$\boldsymbol{T} = -\boldsymbol{U}\left(\boldsymbol{C} + \left(\boldsymbol{I} - \boldsymbol{\Phi}\boldsymbol{R}^{-1}\right)^{-1} \boldsymbol{\Psi}\right) + O\left(\frac{\ell_b}{\ell_d}\right)^3. \tag{B27}$$

The same procedure can be applied to the case the body is rotating with angular velocity $\boldsymbol{\omega}$, obtaining

$$\boldsymbol{F} = -\boldsymbol{\omega}\left(\boldsymbol{C}^t + \boldsymbol{\Psi}^t \left(\boldsymbol{I} - \boldsymbol{\Phi}\boldsymbol{R}^{-1}\right)^{-1}\right) + O\left(\frac{\ell_b}{\ell_d}\right)^3 \tag{B28}$$

and

$$\boldsymbol{T} = -\boldsymbol{\omega}\left(\boldsymbol{\Omega} + \boldsymbol{\Theta} + \boldsymbol{\Psi}^t \boldsymbol{R}^{-1} \left(1 - \boldsymbol{\Phi}\boldsymbol{R}^{-1}\right)^{-1} \boldsymbol{\Psi}\right) + O\left(\frac{\ell_b}{\ell_d}\right)^3, \tag{B29}$$

where $\boldsymbol{\Theta}$ is defined by (6.31) and applies for bodies with generic shape in the presence of reciprocal BCs. In the case of a spherical body, the (m, n)th-order geometrical moments

$m_{\alpha\boldsymbol{\alpha}_m\beta\boldsymbol{\beta}_n}(\boldsymbol{\xi},\boldsymbol{\xi})$ vanish for $m+n$ odd (which means that m and n are neither both even or odd). More specifically, the geometrical moments providing the coupling matrix $\boldsymbol{C}$ vanish, i.e. $m_{\alpha\alpha_1\beta}(\boldsymbol{\xi},\boldsymbol{\xi}) = m_{\alpha\beta\beta_1}(\boldsymbol{\xi},\boldsymbol{\xi}) = 0$. Therefore, the first-order Faxén operator contributes to the force $\boldsymbol{F}^{[5]}$ with a term of the order of magnitude $O(\ell_b/\ell_d)^4$ smaller than the leading error term considered in (B17) and, hence, the error committed in the approximated the global force is $O(\ell_b/\ell_f)^4$ instead of $O(\ell_b/\ell_f)^3$. Furthermore, since the coupling resistance matrix vanishes, $\boldsymbol{T}^{[\infty]} = 0$. Hence, the leading-order contribution is provided by $\boldsymbol{T}^{[3]}$, which can be written in term of the resistance matrix as

$$\boldsymbol{T}^{[3]} = \boldsymbol{F}^{[\infty]}\boldsymbol{R}^{-1}\boldsymbol{\Psi}. \tag{B30}$$

The next-order contribution $\boldsymbol{T}^{[5]}$ can be evaluated as in (B18), considering that the first term in the Faxén operator for the torque vanishes, thus

$$\boldsymbol{T}^{[5]} = \boldsymbol{F}^{[3]}\boldsymbol{R}^{-1}\boldsymbol{\Psi} + O\left(\frac{\ell_b}{\ell_d}\right)^5. \tag{B31}$$

Following the same procedure adopted in (B22)–(B25), we obtain for a spherical body (or, more generally, for any body for which the unbounded coupling terms vanish)

$$\boldsymbol{F} = -U\left(\boldsymbol{R} + \left(\boldsymbol{I} - \boldsymbol{\Phi}\boldsymbol{R}^{-1}\right)^{-1}\boldsymbol{\Phi}\right) + O\left(\frac{\ell_b}{\ell_d}\right)^4 \tag{B32}$$

and

$$\boldsymbol{T} = -U\left(\boldsymbol{I} - \boldsymbol{\Phi}\boldsymbol{R}^{-1}\right)^{-1}\boldsymbol{\Psi} + O\left(\frac{\ell_b}{\ell_d}\right)^5, \tag{B33}$$

whereas for rotations

$$\boldsymbol{F} = -\omega\boldsymbol{\Psi}^t\left(\boldsymbol{I} - \boldsymbol{\Phi}\boldsymbol{R}^{-1}\right)^{-1} + O\left(\frac{\ell_b}{\ell_d}\right)^5 \tag{B34}$$

and

$$\boldsymbol{T} = -\omega\left(\boldsymbol{\Omega} + \boldsymbol{\Theta} + \boldsymbol{\Psi}^t\boldsymbol{R}^{-1}\left(1 - \boldsymbol{\Phi}\boldsymbol{R}^{-1}\right)^{-1}\boldsymbol{\Psi}\right) + O\left(\frac{\ell_b}{\ell_d}\right)^5. \tag{B35}$$

Appendix C. Scaling analysis of the entries of the [N]-matrix for a sphere near a plane wall

C.1. *Force on a translating sphere*

From (7.4), it is possible to express the force acting on the translating sphere as

$$\begin{aligned}\boldsymbol{F} &= \boldsymbol{F}^{[\infty]} - [M_{(0:3)}]^t[X_{(0:3,0)}] + O\left(\frac{R_p}{h}\right)^5 \\ &= \boldsymbol{F}^{[\infty]} - \boldsymbol{M}^t_{(0)}\boldsymbol{X}_{(0,0)} - \boldsymbol{M}^t_{(1)}\boldsymbol{X}_{(1,0)} - \boldsymbol{M}^t_{(2)}\boldsymbol{X}_{(2,0)} - \boldsymbol{M}^t_{(3)}\boldsymbol{X}_{(3,0)} + O\left(\frac{R_p}{h}\right)^5,\end{aligned} \tag{C1}$$

where the matrix $[X_{(0:3,0)}] = [\boldsymbol{X}_{(0,0)}, \boldsymbol{X}_{(1,0)}, \boldsymbol{X}_{(2,0)}, \boldsymbol{X}_{(3,0)}]^t$ is given by

$$[X_{(0:3,0)}] = \sum_{k=0}^{\infty}[N_{(0:3,0:3)}]^k[N_{(0:3,0)}] \tag{C2}$$

and, thus,

$$\boldsymbol{X}_{(m,0)} = \boldsymbol{N}_{(m,0)} + [N_{(m,0:3)}] \sum_{k=0}^{\infty} [N_{(0:3,0:3)}]^k [N_{(0:3,0)}], \quad m = 0, 1, 2, 3. \tag{C3}$$

Since in a constant unbounded flow the first- and third-order moments on a translating sphere vanish, $\boldsymbol{M}_{(1)} = 0$, $\boldsymbol{M}_{(3)} = 0$, whereas $\boldsymbol{M}^t_{(0)} = -\boldsymbol{F}^{[\infty]}$, whereas

$$\boldsymbol{F}^{[\infty]} = -6\pi\mu R_p \left(\frac{1 + 2\hat{\lambda}}{1 + 3\hat{\lambda}} \right) \boldsymbol{U}. \tag{C4}$$

Equation (C1) becomes

$$\boldsymbol{F} = \boldsymbol{F}^{[\infty]} + \boldsymbol{F}^{[\infty]} \boldsymbol{X}_{(0,0)} - \frac{\boldsymbol{M}^t_{(2)} \boldsymbol{X}_{(2,0)}}{2!} + O\left(\frac{R_p}{h} \right)^5. \tag{C5}$$

The entries of the vector $\boldsymbol{M}^t_{(2)}$ correspond to the vectorisation according to (4.2) of the tensor

$$-8\pi\mu \mathcal{F}_{\gamma\alpha\alpha_1\alpha_2} U_\gamma = -\frac{R_p^2}{3(1 + 2\hat{\lambda})} \left(F^{[\infty]}_\alpha \delta_{\alpha_1\alpha_2} + \hat{\lambda} (F^{[\infty]}_{\alpha_1} \delta_{\alpha\alpha_2} + F^{[\infty]}_{\alpha_2} \delta_{\alpha\alpha_1}) \right), \tag{C6}$$

where $\mathcal{F}_{\gamma\alpha\alpha_1\alpha_2}$, evaluated in (Procopio & Giona 2024), is reported in the supplementary material. The second term within parentheses at the right-hand side of (C6) yields a vanishing contribution to the total force since, once applied to $\boldsymbol{X}_{(2,0)}$, it provides terms $N_{\alpha\alpha_1\ldots\alpha\ldots\alpha_m\beta\boldsymbol{\beta}_n}(\boldsymbol{\xi}, \boldsymbol{\xi}) = 0$, vanishing due to the incompressibility of Stokes flows.

Therefore, the vector $\boldsymbol{M}_{(2)}$ can be expressed in matrix form as

$$\boldsymbol{M}^t_{(2)} = -\frac{R_p^2}{3(1 + 2\hat{\lambda})} \boldsymbol{F}^{[\infty]} \boldsymbol{I}_{(0,2)}, \tag{C7}$$

where $(\boldsymbol{I}_{(0,2)})_{ij}$, following the notation developed in § 3, is the matrix collecting the entries of the tensor $\delta_{\beta\alpha}\delta_{\alpha_1\alpha_2}$ by the conversion $i \equiv \beta$ and $j \leftrightarrow \alpha\alpha_1\alpha_2$ according to

$$j = \left(\sum_{h=0}^{3} \alpha_h 3^{h-3} \right) - 12, \tag{C8}$$

thus

$$\boldsymbol{I}_{(0,2)} = $$
$$\begin{pmatrix} 1&0&0&0&1&0&0&0&1&0&0&0&0&0&0&0&0&0&0&0&0&0&0&0&0&0&0 \\ 0&0&0&0&0&0&0&0&0&1&0&0&0&1&0&0&0&1&0&0&0&0&0&0&0&0&0 \\ 0&0&0&0&0&0&0&0&0&0&0&0&0&0&0&0&0&0&1&0&0&0&1&0&0&0&1 \end{pmatrix}. \tag{C9}$$

Considering (C7), the force on the sphere (C5) reads

$$\boldsymbol{F} = \boldsymbol{F}^{[\infty]} \left(\boldsymbol{I} + \boldsymbol{X}_{(0,0)} + \frac{R_p^2}{6(1 + 2\hat{\lambda})} \boldsymbol{I}_{(0,2)} \boldsymbol{X}_{(2,0)} \right) + O\left(\frac{R_p}{h} \right)^5. \tag{C10}$$

By (C3) and by the dimensional analysis of the entries of the $[N]$-matrix (see (A12))

$$\boldsymbol{X}_{(0,0)} = \boldsymbol{N}_{(0,0)} + \boldsymbol{N}^2_{(0,0)} + \boldsymbol{N}_{(0,1)}\boldsymbol{N}_{(1,0)} + \frac{1}{2}\boldsymbol{N}_{(0,2)}\boldsymbol{N}_{(2,0)} + \boldsymbol{N}^3_{(0,0)} + \boldsymbol{N}_{(0,0)}\boldsymbol{N}_{(0,1)}\boldsymbol{N}_{(1,0)} + \boldsymbol{N}_{(0,1)}\boldsymbol{N}_{(1,0)}\boldsymbol{N}_{(0,0)} + \boldsymbol{N}^4_{(0,0)} + O\left(\frac{R_p}{h}\right)^5 \tag{C11}$$

and

$$\boldsymbol{X}_{(2,0)} = \boldsymbol{N}_{(2,0)} + \boldsymbol{N}_{(2,0)}\boldsymbol{N}_{(0,0)} + O\left(\frac{R_p}{h}\right)^5. \tag{C12}$$

Equations (C10)–(C12), can be equivalently written as

$$\boldsymbol{F} = \boldsymbol{F}^{[\infty]}\left((I - \boldsymbol{N}_{(0,0)})^{-1} + \boldsymbol{N}_{(0,1)}\boldsymbol{N}_{(1,0)} + \frac{1}{2}\boldsymbol{N}_{(0,2)}\boldsymbol{N}_{(2,0)} + \boldsymbol{N}_{(0,0)}\boldsymbol{N}_{(0,1)}\boldsymbol{N}_{(1,0)} + \boldsymbol{N}_{(0,1)}\boldsymbol{N}_{(1,0)}\boldsymbol{N}_{(0,0)} + \frac{R_p^2}{6(1+2\hat{\lambda})}\boldsymbol{I}_{(0,2)}(\boldsymbol{N}_{(2,0)} + \boldsymbol{N}_{(2,0)}\boldsymbol{N}_{(0,0)})\right) + O\left(\frac{R_p}{h}\right)^5, \tag{C13}$$

where

$$(I - \boldsymbol{N}_{(0,0)})^{-1} = \begin{pmatrix} \dfrac{1}{1-N_{1,1}} & 0 & 0 \\ 0 & \dfrac{1}{1-N_{1,1}} & 0 \\ 0 & 0 & \dfrac{1}{1-N_{3,3}} \end{pmatrix}, \tag{C14}$$

with $N_{1,1}$ and $N_{3,3}$ reported in (7.2). Finally, using the entries of the matrix $\boldsymbol{N}_{(0,1)}, \boldsymbol{N}_{(1,0)}, \boldsymbol{N}_{(0,2)}, \boldsymbol{N}_{(2,0)}$, we obtain

$$\boldsymbol{F} = \boldsymbol{F}^{[\infty]}\left[\begin{pmatrix} \dfrac{1}{1-N_{1,1}} & 0 & 0 \\ 0 & \dfrac{1}{1-N_{1,1}} & 0 \\ 0 & 0 & \dfrac{1}{1-N_{3,3}} \end{pmatrix} - \begin{pmatrix} \dfrac{{R_p}^3}{16h^3(1+3\hat{\lambda})} & 0 & 0 \\ 0 & \dfrac{{R_p}^3}{16h^3(1+3\hat{\lambda})} & 0 \\ 0 & 0 & \dfrac{{R_p}^3}{4h^3(1+3\hat{\lambda})} \end{pmatrix} + \begin{pmatrix} \dfrac{27{R_p}^4\left(1+7\hat{\lambda}+20\hat{\lambda}^2+20\hat{\lambda}^3\right)}{256h^4(1+3\hat{\lambda})^2(1+5\hat{\lambda})} & 0 & 0 \\ 0 & \dfrac{27{R_p}^4\left(1+7\hat{\lambda}+20\hat{\lambda}^2+20\hat{\lambda}^3\right)}{256h^4(1+3\hat{\lambda})^2(1+5\hat{\lambda})} & 0 \\ 0 & 0 & -\dfrac{9{R_p}^4\left(1+7\hat{\lambda}-80\hat{\lambda}^2-180\hat{\lambda}^3\right)}{256h^4(1+3\hat{\lambda})^2(1+5\hat{\lambda})} \end{pmatrix}\right] + O\left(\frac{R_p}{h}\right)^5. \tag{C15}$$

After some algebra, the latter expression can be simplified as (7.7)–(7.9).

C.2. *Torque on a translating sphere*

Considering that $\boldsymbol{T}^{[\infty]} = 0$ and $\boldsymbol{M}_{(1)} = \boldsymbol{M}_{(3)} = 0$, (7.11) becomes

$$\boldsymbol{T} = [M_{(0:3)}]^t[Y_{(0:3)}] + O\left(\frac{R_p}{h}\right)^5 = \boldsymbol{M}^t_{(0)}\boldsymbol{Y}_{(0)} + \boldsymbol{M}^t_{(2)}\boldsymbol{Y}_{(2)} + O\left(\frac{R_p}{h}\right)^5, \tag{C16}$$

where $\boldsymbol{M}_{(0)}$ and $\boldsymbol{M}_{(2)}$ are given by (C4) and (C7), and

$$\boldsymbol{Y}_{(m)} = \boldsymbol{L}_{(m)} + [N_{(m,0:3)}]\sum_{k=0}^{\infty}[N_{(0:3,0:3)}]^k[L_{(0:3)}], \quad m = 0, 1, 2, 3. \tag{C17}$$

Truncating $\boldsymbol{Y}_{(0)}$ and $\boldsymbol{Y}_{(2)}$ up to the order $O(R_p/h)^5$, we have

$$\begin{aligned}\boldsymbol{Y}_{(0)} &= \boldsymbol{L}_{(0)} + \boldsymbol{N}_{(0,0)}\boldsymbol{L}_{(0)} + \boldsymbol{N}^2_{(0,0)}\boldsymbol{L}_{(0)} + \boldsymbol{N}_{(0,1)}\boldsymbol{L}_{(1)} + \frac{1}{2}\boldsymbol{N}_{(0,2)}\boldsymbol{L}_{(2)} \\ &\quad + \boldsymbol{N}_{(0,0)}\boldsymbol{N}_{(0,1)}\boldsymbol{L}_{(1)} + \boldsymbol{N}_{(0,1)}\boldsymbol{N}_{(1,0)}\boldsymbol{L}_{(0)} + O\left(\frac{R_p}{h}\right)^5\end{aligned} \tag{C18}$$

and

$$\boldsymbol{Y}_{(2)} = \boldsymbol{L}_{(2)} + \boldsymbol{N}_{(2,0)}\boldsymbol{L}_{(0)} + O\left(\frac{R_p}{h}\right)^5. \tag{C19}$$

The leading order neglected in (C18) and (C19) is smaller than that estimated for the forces, because, for the symmetries of the sphere, the first term in the first-order Faxén operator vanishes and $\boldsymbol{L}_{(m)} \sim O(R_p^2/h^{m+2})$ instead of $\boldsymbol{L}_{(m)} \sim O(R_p^2/h^{m+1})$ in the general case. Therefore, analogously to the expression for the force (C13)

$$\boldsymbol{T} = -\boldsymbol{F}^{[\infty]}\left((I - \boldsymbol{N}_{(0,0)})^{-1}\boldsymbol{L}_{(0)} + \boldsymbol{N}_{(0,1)}\boldsymbol{L}_{(1)} + \frac{1}{2}\boldsymbol{N}_{(0,2)}\boldsymbol{L}_{(2)} + \boldsymbol{N}_{(0,0)}\boldsymbol{N}_{(0,1)}\boldsymbol{L}_{(1)}\right. \tag{C20}$$

$$\left. + \boldsymbol{N}_{(0,1)}\boldsymbol{N}_{(1,0)}\boldsymbol{L}_{(0)} + \frac{R_p^2}{6(1+2\hat{\lambda})}\boldsymbol{I}_{(0,2)}(\boldsymbol{L}_{(2)} + \boldsymbol{N}_{(2,0)}\boldsymbol{L}_{(0)})\right) + O\left(\frac{R_p}{h}\right)^6. \tag{C21}$$

C.3. *Torque on a rotating sphere*

The torque on a rotating sphere with angular velocity $\boldsymbol{\omega}$ near a plane wall can be evaluated by using (6.13) with $K = 4$ and $u_a(\boldsymbol{x}) = -\varepsilon_{abc}\omega_b(\boldsymbol{x} - \boldsymbol{\xi})_c$ as ambient flow. In such ambient flow, $\boldsymbol{M}_{(2m)} = 0$ $(m = 0, 1, 2\ldots)$ due to spherical symmetry and, thus,

$$\begin{aligned}\boldsymbol{T} &= \boldsymbol{T}^{[\infty]} + [M_{(0:4)}]^t[Y_{(0:4)}] + O\left(\frac{R_p}{h}\right)^6 \\ &= \boldsymbol{T}^{[\infty]} + \boldsymbol{M}^t_{(1)}\boldsymbol{Y}_{(1)} + \boldsymbol{M}^t_{(3)}\boldsymbol{Y}_{(3)} + O\left(\frac{R_p}{h}\right)^6.\end{aligned} \tag{C22}$$

The entries of the vector $\boldsymbol{M}_{(1)}$ are given by the vectorisation of the tensor

$$M_{\alpha\alpha_1}(\boldsymbol{\xi}) = -8\pi\mu\,\mathcal{F}_{\beta'\alpha\alpha_1}\varepsilon_{\beta'\gamma'\delta'}\,\omega_{\gamma'}(\boldsymbol{\xi}' - \boldsymbol{\xi})_{\delta'}\Big|_{\boldsymbol{\xi}'=\boldsymbol{\xi}}. \tag{C23}$$

After some algebra, using the Faxén operator $\mathcal{F}_{\beta'\alpha\alpha_1}$ reported in the supplementary material,

$$M_{\alpha\alpha_1}(\boldsymbol{\xi}) = \frac{\varepsilon_{\gamma\alpha\alpha_1} T_\gamma^{[\infty]}}{2}, \tag{C24}$$

where

$$T_\gamma^{[\infty]} = -\frac{8\pi\mu R_p^3 \omega_\gamma}{1+3\hat{\lambda}}. \tag{C25}$$

Following the notation developed in § 4, (C24) reads

$$\boldsymbol{M}_{(1)} = \frac{\boldsymbol{T}^{[\infty]}\boldsymbol{\varepsilon}}{2}, \tag{C26}$$

where $\boldsymbol{\varepsilon}$ is defined in (5.16).

By (C17), enforcing the scaling error analysis addressed previously, we have

$$\begin{aligned} \boldsymbol{Y}_{(1)} = {} & \boldsymbol{L}_{(1)} + \boldsymbol{N}_{(1,0)}\boldsymbol{L}_{(0)} + \boldsymbol{N}_{(1,1)}\boldsymbol{L}_{(1)} + \frac{1}{2}\boldsymbol{N}_{(1,2)}\boldsymbol{L}_{(2)} + \boldsymbol{N}_{(1,0)}\boldsymbol{N}_{(0,0)}\boldsymbol{L}_{(0)} + \boldsymbol{N}_{(1,1)}\boldsymbol{N}_{(1,0)}\boldsymbol{L}_{(0)} \\ & + \boldsymbol{N}_{(1,1)}\boldsymbol{N}_{(1,0)}\boldsymbol{L}_{(0)} + \boldsymbol{N}_{(1,0)}\boldsymbol{N}_{(0,1)}\boldsymbol{L}_{(1)} + \boldsymbol{N}_{(1,0)}\boldsymbol{N}_{(0,0)}\boldsymbol{N}_{(0,0)}\boldsymbol{L}_{(0)} + O\left(\frac{R_p}{h}\right)^6. \end{aligned} \tag{C27}$$

Hence, (C22) reads

$$\begin{aligned} \boldsymbol{T} = {} & \boldsymbol{T}^{[\infty]} + \frac{\boldsymbol{T}^{[\infty]}\boldsymbol{\varepsilon}}{2}\Big(\boldsymbol{L}_{(1)} + \boldsymbol{N}_{(1,0)}\boldsymbol{L}_{(0)} + \boldsymbol{N}_{(1,1)}\boldsymbol{L}_{(1)} + \frac{1}{2}\boldsymbol{N}_{(1,2)}\boldsymbol{L}_{(2)} + \boldsymbol{N}_{(1,0)}\boldsymbol{N}_{(0,0)}\boldsymbol{L}_{(0)} \\ & + \boldsymbol{N}_{(1,1)}\boldsymbol{N}_{(1,0)}\boldsymbol{L}_{(0)} + \boldsymbol{N}_{(1,1)}\boldsymbol{N}_{(1,0)}\boldsymbol{L}_{(0)} + \boldsymbol{N}_{(1,0)}\boldsymbol{N}_{(0,1)}\boldsymbol{L}_{(1)} + \boldsymbol{N}_{(1,0)}\boldsymbol{N}_{(0,0)}\boldsymbol{N}_{(0,0)}\boldsymbol{L}_{(0)}\Big) \\ & + \boldsymbol{M}^t_{(3)}\boldsymbol{Y}_{(3)} + O\left(\frac{R_p}{h}\right)^6 \end{aligned} \tag{C28}$$

according to which, in order to obtain the expression for torque, the quantity $\boldsymbol{M}^t_{(3)}\boldsymbol{Y}_{(3)}$ should be estimated. The entries of the vector $\boldsymbol{M}^t_{(3)}$ are

$$M_{\alpha\alpha_1\alpha_2\alpha_3}(\boldsymbol{\xi}) = -8\pi\mu\, \mathcal{F}_{\beta'\alpha\alpha_1\alpha_2\alpha_3}\varepsilon_{\beta'\gamma'\delta'}\,\omega_{\gamma'}(\boldsymbol{\xi}'-\boldsymbol{\xi})_{\delta'}\big|_{\boldsymbol{\xi}'=\boldsymbol{\xi}} \tag{C29}$$

and they can be evaluated starting from the definition of the Faxén operators (2.17), entailing the knowledge of the geometrical moments of a sphere with Navier-slip BCs. As obtained in Procopio & Giona (2024), if $\boldsymbol{\xi}$ is the centre of the sphere, $m_{\beta\alpha\alpha_1\alpha_2\alpha_3}(\boldsymbol{\xi},\boldsymbol{\xi}) = 0$ and

$$\begin{aligned} m_{\beta\beta_1\alpha\alpha_1\alpha_2\alpha_3}(\boldsymbol{\xi},\boldsymbol{\xi}) = {} & -\frac{R_p^5}{30(1+5\hat{\lambda})(1+3\hat{\lambda})} \\ & \times\Big[\left(4+12\hat{\lambda}-15\hat{\lambda}^2\right)\delta_{\alpha\beta}\eta_{\beta_1\alpha_1\alpha_2\alpha_3} + \left(1+3\hat{\lambda}+15\hat{\lambda}^2\right)\delta_{\alpha\beta_1}\eta_{\beta\alpha_1\alpha_2\alpha_3} \\ & + 5\hat{\lambda}(1+3\hat{\lambda})(\delta_{\alpha\alpha_1}\eta_{\beta\beta_1\alpha_2\alpha_3} + \delta_{\alpha\alpha_2}\eta_{\beta\beta_1\alpha_1\alpha_3} + \delta_{\alpha\alpha_3}\eta_{\beta\beta_1\alpha_1\alpha_2})\Big] \end{aligned} \tag{C30}$$

with $\eta_{\alpha\beta\gamma\delta} = \delta_{\alpha\beta}\delta_{\gamma\delta} + \delta_{\alpha\delta}\delta_{\beta\gamma} + \delta_{\alpha\gamma}\delta_{\beta\delta}$. Therefore, since the ambient flow is linear, higher-order moments do not contribute to $\boldsymbol{M}_{(3)}$ and, thus,

$$M_{\alpha\alpha_1\alpha_2\alpha_3}(\boldsymbol{\xi}) = -8\pi\mu\,\varepsilon_{\beta\gamma\delta} m_{\beta\delta\alpha\alpha_1\alpha_2\alpha_3}(\boldsymbol{\xi},\boldsymbol{\xi})\omega_\gamma. \tag{C31}$$

Substituting (C30) into (C31), we have

$$M_{\alpha\alpha_1\alpha_2\alpha_3}(\boldsymbol{\xi}) = \frac{R_p^2 T_\gamma^{[\infty]}}{10}(1-2\hat{\lambda})\left(\varepsilon_{\gamma\alpha\alpha_1}\delta_{\alpha_2\alpha_3} + \varepsilon_{\gamma\alpha\alpha_2}\delta_{\alpha_1\alpha_3} + \varepsilon_{\gamma\alpha\alpha_3}\delta_{\alpha_1\alpha_2}\right). \tag{C32}$$

As regards $\boldsymbol{Y}_{(3)}$, from (C17), performing the scaling error analysis discussed previously, we obtain

$$\boldsymbol{Y}_{(3)} = \boldsymbol{L}_{(3)} + \boldsymbol{N}_{(3,0)}\boldsymbol{L}_{(0)} + O\left(\frac{R_p}{h}\right)^6 \tag{C33}$$

hence, by definition of $\boldsymbol{L}_{(m)}$ (5.15), the entries of $\boldsymbol{Y}_{(3)}$ are given by

$$Y_{\beta\alpha\alpha_1\alpha_2\alpha_3} = \varepsilon_{\beta\delta\delta_1}(N_{\alpha\alpha_1\alpha_2\alpha_3\delta\delta_1}(\boldsymbol{\xi}) + N_{\alpha\alpha_1\alpha_2\alpha_3\gamma}(\boldsymbol{\xi})N_{\gamma\delta\delta_1}(\boldsymbol{\xi})) + O\left(\frac{R_p}{h}\right)^6. \tag{C34}$$

Due to the harmonicity of the vorticity of Stokes flows and the reciprocal symmetry of the Green function $W_{\theta'\alpha}(\boldsymbol{\xi}', \boldsymbol{\xi}) = W_{\alpha\theta'}(\boldsymbol{\xi}, \boldsymbol{\xi}')$ (Pozrikidis 1992)

$$\varepsilon_{\gamma\alpha\alpha_1}\delta_{\alpha_2\alpha_3}N_{\alpha\alpha_1\alpha_2\alpha_3\delta\delta_1}(\boldsymbol{\xi}) = \mathcal{F}_{\theta'\delta\delta_1}\,\Delta_\xi\,\varepsilon_{\gamma\alpha\alpha_1}\nabla_{\alpha_1}W_{\theta'\alpha}(\boldsymbol{\xi}', \boldsymbol{\xi})\big|_{\boldsymbol{\xi}'=\boldsymbol{\xi}} = 0. \tag{C35}$$

Therefore, the entries of $\boldsymbol{M}^t_{(3)}\boldsymbol{Y}_{(3)}$ are vanishing

$$\varepsilon_{\beta\delta\delta_1} M_{\alpha\alpha_1\alpha_2\alpha_3}(\boldsymbol{\xi})(N_{\alpha\alpha_1\alpha_2\alpha_3\delta\delta_1}(\boldsymbol{\xi}) + N_{\alpha\alpha_1\alpha_2\alpha_3\gamma}(\boldsymbol{\xi})N_{\gamma\delta\delta_1}(\boldsymbol{\xi})) = 0 \tag{C36}$$

and (C28) becomes

$$\begin{aligned}\boldsymbol{T} = \boldsymbol{T}^{[\infty]} + \frac{\boldsymbol{T}^{[\infty]}\boldsymbol{\varepsilon}}{2}\Big(&\boldsymbol{L}_{(1)} + \boldsymbol{N}_{(1,0)}\boldsymbol{L}_{(0)} + \boldsymbol{N}_{(1,1)}\boldsymbol{L}_{(1)} + \frac{1}{2}\boldsymbol{N}_{(1,2)}\boldsymbol{L}_{(2)} + \boldsymbol{N}_{(1,0)}\boldsymbol{N}_{(0,0)}\boldsymbol{L}_{(0)} \\ &+ \boldsymbol{N}_{(1,1)}\boldsymbol{N}_{(1,0)}\boldsymbol{L}_{(0)} + \boldsymbol{N}_{(1,1)}\boldsymbol{N}_{(1,0)}\boldsymbol{L}_{(0)} + \boldsymbol{N}_{(1,0)}\boldsymbol{N}_{(0,1)}\boldsymbol{L}_{(1)} + \boldsymbol{N}_{(1,0)}\boldsymbol{N}_{(0,0)}\boldsymbol{N}_{(0,0)}\boldsymbol{L}_{(0)}\Big) \\ &+ O\left(\frac{R_p}{h}\right)^6.\end{aligned} \tag{C37}$$

Substituting the entries of the $[N]$-matrix, $\boldsymbol{L}_{(1)}$ is the only term within the parentheses in (C37) contributing to the torque on the sphere. Therefore, (C37) attains the simpler form

$$\boldsymbol{T} = \boldsymbol{T}^{[\infty]} + \frac{\boldsymbol{T}^{[\infty]}\boldsymbol{\varepsilon}\boldsymbol{L}_{(1)}}{2} + O\left(\frac{R_p}{h}\right)^6, \tag{C38}$$

which provide (7.17).

References

BEENAKKER, C.W.J. & MAZUR, P. 1985 Is sedimentation container-shape dependent? *Phys. Fluids* **28** (11), 3203–3206.

BHATIA, R. 1997 *Matrix Analysis*. Springer.

BLAKE, J.R. 1971 A note on the image system for a Stokeslet in a no-slip boundary. *Math. Proc. Camb. Phil.* **70** (2), 303–310.

BLAKE, J.R. & CHWANG, A.T. 1974 Fundamental singularities of viscous flow. Part I. The image systems in the vicinity of a stationary no-slip boundary. *J. Engng Maths* **8** (1), 23–29.

BRADY, J.F. & BOSSIS, G. 1988 Stokesian dynamics. *Annu. Rev. Fluid Mech.* **20**, 111–157.

BRENNER, H. 1961 The slow motion of a sphere through a viscous fluid towards a plane surface. *Chem. Engng Sci.* **16** (3–4), 242–251.

BRENNER, H. 1962 Effect of finite boundaries on the Stokes resistance of an arbitrary particle. *J. Fluid Mech.* **12** (1), 35–48.

BRENNER, H. 1964*a* Effect of finite boundaries on the Stokes resistance of an arbitrary particle. Part 2. Asymmetrical orientations. *J. Fluid Mech.* **18** (1), 144–158.

BRENNER, H. 1964*b* The Stokes resistance of an arbitrary particle—II: an extension. *Chem. Engng Sci.* **19** (9), 599–629.

CERBELLI, S., GIONA, M. & GAROFALO, F. 2013 Quantifying dispersion of finite-sized particles in deterministic lateral displacement microflow separators through Brenner's macrotransport paradigm. *Microfluid. Nanofluid.* **15**, 431–449.

COOKE, R.G. 1950 *Infinite Matrices and Sequence Spaces*. Macmillan and Co.

COX, R.G. 1974 The motion of suspended particles almost in contact. *Intl J. Multiphase Flow* **1** (2), 343–371.

COX, R.G. & BRENNER, H. 1967*a* Effect of finite boundaries on the Stokes resistance of an arbitrary particle. Part 3. Translation and rotation. *J. Fluid Mech.* **28** (2), 391–411.

COX, R.G. & BRENNER, H. 1967*b* The slow motion of a sphere through a viscous fluid towards a plane surface—II. Small gap widths, including inertial effects. *Chem. Engng Sci.* **22** (12), 1753–1777.

COX, R.G. & BRENNER, H. 1968 The lateral migration of solid particles in Poiseuille flow—I. Theory. *Chem. Engng Sci.* **23** (2), 147–173.

DE CORATO, M., GRECO, F., D'AVINO, G. & MAFFETTONE, P.L. 2015 Hydrodynamics and Brownian motions of a spheroid near a rigid wall. *J. Chem. Phys.* **142** (19), 194901.

DEAN, W.R. & O'NEILL, M.E. 1963 A slow motion of viscous liquid caused by the rotation of a solid sphere. *Mathematika* **10** (1), 13–24.

DESAI, N. & MICHELIN, S. 2021 Instability and self-propulsion of active droplets along a wall. *Phys. Rev. Fluids* **6** (11), 114103.

DI CARLO, D. 2009 Inertial microfluidics. *Lab on a Chip* **9** (21), 3038–3046.

DURLOFSKY, L., BRADY, J.F. & BOSSIS, G. 1987 Dynamic simulation of hydrodynamically interacting particles. *J. Fluid Mech.* **180**, 21–49.

GOLDMAN, A.J., COX, R.G. & BRENNER, H. 1967 Slow viscous motion of a sphere parallel to a plane wall—I. Motion through a quiescent fluid. *Chem. Engng Sci.* **22** (4), 637–651.

GOLDSMITH, H.L. & MASON, S.G. 1962 The flow of suspensions through tubes. I. Single spheres, rods, and discs. *J. Colloid Interface Sci.* **17** (5), 448–476.

GOLDSMITH, H.L. & SKALAK, R. 1975 Hemodynamics. *Annu. Rev. Fluid Mech.* **7** (1), 213–247.

GOREN, S.L. 1979 The hydrodynamic force resisting the approach of a sphere to a plane permeable wall. *J. Colloid Interface Sci.* **69** (1), 78–85.

GUAZZELLI, E. & MORRIS, J.F. 2012 *A Physical Introduction to Suspension Dynamics*. Cambridge University Press.

HABERMAN, W.L. & SAYRE, R.M. 1958 Motion of rigid and fluid spheres in stationary and moving liquids inside cylindrical tubes. *Tech. Rep.* David Taylor Model Basin Washington DC.

HAPPEL, J. & BRENNER, H. 1983 *Low Reynolds Number Hydrodynamics: With Special Applications to Particulate Media*. Martinus Nijhoff.

HASIMOTO, H. 1976 Slow motion of a small sphere in a cylindrical domain. *J. Phys. Soc. Japan* **41** (6), 2143–2144.

HASIMOTO, H. 1983 An extension of Faxen's law te the ellipsoid of revolution. *J. Phys. Soc. Japan* **52** (10), 3294–3296.

HILL, R. & POWER, G. 1956 Extremum principles for slow viscous flow and the approximate calculation of drag. *Q. J. Mech. Appl. Maths* **9** (3), 313–319.

HO, B.P. & LEAL, L.G. 1974 Inertial migration of rigid spheres in two-dimensional unidirectional flows. *J. Fluid Mech.* **65** (2), 365–400.

HOCKING, L.M. 1973 The effect of slip on the motion of a sphere close to a wall and of two adjacent spheres. *J. Engng Maths* **7** (3), 207–221.

HÖFER, R.M. & VELÁZQUEZ, J.J.L. 2018 The method of reflections, homogenization and screening for Poisson and Stokes equations in perforated domains. *Arch. Ration. Mech. Anal.* **227** (3), 1165–1221.

HUANG, L.R., COX, E.C., AUSTIN, R.H. & STURM, J.C. 2004 Continuous particle separation through deterministic lateral displacement. *Science* **304** (5673), 987–990.

ICHIKI, K. & BRADY, J.F. 2001 Many-body effects and matrix inversion in low-Reynolds-number hydrodynamics. *Phys. Fluids* **13** (1), 350–353.

JEFFERY, G.B. 1915 On the steady rotation of a solid of revolution in a viscous fluid. *Proc. Lond. Math. Soc.* **2** (1), 327–338.

JEFFREY, D.J. & ONISHI, Y. 1984 Calculation of the resistance and mobility functions for two unequal rigid spheres in low-Reynolds-number flow. *J. Fluid Mech.* **139**, 261–290.

KIM, S. 1985 A note on Faxen laws for nonspherical particles. *Intl J. Multiphase Flow* **11** (5), 713–719.

KIM, S. & KARRILA, S.J. 2005 *Microhydrodynamics: Principles and Selected Applications*. Dover Publications.

KLIMCHITSKAYA, G.L., MOHIDEEN, U. & MOSTEPANENKO, V.M. 2009 The Casimir force between real materials: experiment and theory. *Rev. Mod. Phys.* **81** (4), 1827–1885.

LADYZHENSKAYA, O.A. 2014 *The Mathematical Theory of Viscous Incompressible Flow*. Martino Publishing.

LAUGA, E. 2020 *The Fluid Dynamics of Cell Motility*. Cambridge University Press.

LIRON, N. & MOCHON, S. 1976 Stokes flow for a stokeslet between two parallel flat plates. *J. Engng Maths* **10** (4), 287–303.

LUKE, J.H.C. 1989 Convergence of a multiple reflection method for calculating Stokes flow in a suspension. *SIAM J. Appl. Maths* **49** (6), 1635–1651.

MICHELIN, S. 2023 Self-propulsion of chemically active droplets. *Annu. Rev. Fluid Mech.* **55**, 77–101.

MITCHELL, W.H. & SPAGNOLIE, S.E. 2015 Sedimentation of spheroidal bodies near walls in viscous fluids: glancing, reversing, tumbling and sliding. *J. Fluid Mech.* **772**, 600–629.

O'NEILL, M.E. 1964 A slow motion of viscous liquid caused by a slowly moving solid sphere. *Mathematika* **11** (1), 67–74.

O'NEILL, M.E. & MAJUMDAR, R. 1970 Asymmetrical slow viscous fluid motions caused by the translation or rotation of two spheres. Part I. The determination of exact solutions for any values of the ratio of radii and separation parameters. *Z. Angew. Math. Phys.* **21**, 164–179.

PASOL, L., CHAOUI, M., YAHIAOUI, S. & FEUILLEBOIS, F. 2005 Analytical solutions for a spherical particle near a wall in axisymmetrical polynomial creeping flows. *Phys. Fluids* **17** (7), 073602.

POISSON, E., POUND, A. & VEGA, I. 2011 The motion of point particles in curved space–time. *Living Rev. Relativ.* **14** (1), 1–190.

POPEL, A.S. & JOHNSON, P.C. 2005 Microcirculation and hemorheology. *Annu. Rev. Fluid Mech.* **37**, 43–69.

POZRIKIDIS, C. 1992 *Boundary Integral and Singularity Methods for Linearized Viscous Flow*. Cambridge University Press.

PROCOPIO, G. & GIONA, M. 2022 Stochastic modeling of particle transport in confined geometries: problems and peculiarities. *Fluids* **7** (3), 105.

PROCOPIO, G. & GIONA, M. 2023 Bitensorial formulation of the singularity method for Stokes flows. *Maths Engng* **5** (2), 1–34.

PROCOPIO, G. & GIONA, M. 2024 On the Hinch–Kim dualism between singularity and Faxén operators in the hydromechanics of arbitrary bodies in Stokes flows. *Phys. Fluids* **36** (3), 032016.

SEGRE, G. & SILBERBERG, A. 1961 Radial particle displacements in poiseuille flow of suspensions. *Nature* **189** (4760), 209–210.

SMOLUCHOWSKI, M. 1911 Über die wechselwirkung von kugeln die sich in einer zähen flüssigkeit bewegen. *Bull. Intl Acad. Sci.* **1A**, 28–39.

SONSHINE, R.M., COX, R.G. & BRENNER, H. 1966 The Stokes translation of a particle of arbitrary shape along the axis of a circular cylinder: filled to a finite depth with viscous liquid i. *Appl. Sci. Res.* **16**, 273–300.

SPAGNOLIE, S.E. & LAUGA, E. 2012 Hydrodynamics of self-propulsion near a boundary: predictions and accuracy of far-field approximations. *J. Fluid Mech.* **700**, 105–147.

STRIEGEL, A.M. & BREWER, A.K. 2012 Hydrodynamic chromatography. *Annu. Rev. Anal. Chem.* **5**, 15–34.

SWAN, J.W. & BRADY, J.F. 2007 Simulation of hydrodynamically interacting particles near a no-slip boundary. *Phys. Fluids* **19** (11), 113306.

SWAN, J.W. & BRADY, J.F. 2010 Particle motion between parallel walls: hydrodynamics and simulation. *Phys. Fluids* **22** (10), 103301.

UNDVALL, E., GAROFALO, F., PROCOPIO, G., QIU, W., LENSHOF, A., LAURELL, T. & BAASCH, T. 2022 Inertia-induced breakdown of acoustic sorting efficiency at high flow rates. *Phys. Rev. Appl.* **17** (3), 034014.

VENDITTI, C., CERBELLI, S., PROCOPIO, G. & ADROVER, A. 2022 Comparison between one-and two-way coupling approaches for estimating effective transport properties of suspended particles undergoing Brownian sieving hydrodynamic chromatography. *Phys. Fluids* **34** (4), 042010.

ZHANG, J., YAN, S., YUAN, D., ALICI, G., NGUYEN, N.-T., WARKIANI, M.E. & LI, W. 2016 Fundamentals and applications of inertial microfluidics: a review. *Lab on a Chip* **16** (1), 10–34.